

Score-based Causal Representation Learning: Linear and General Transformations

Burak Varıcı*

*Machine Learning Department
Carnegie Mellon University
Pittsburgh, PA 15213, USA*

BVARICI@ANDREW.CMU.EDU

Emre Acartürk*

*Electrical, Computer, and Systems Engineering
Rensselaer Polytechnic Institute
Troy, NY 12180, USA*

ACARTE@RPI.EDU

Karthikeyan Shanmugam

*Google DeepMind India
Bengaluru 560043, India*

KARTHIKEYANVS@GOOGLE.COM

Abhishek Kumar

Amazon AGI, USA

ABHISHEK.MLWORK@GMAIL.COM

Ali Tajer

*Electrical, Computer, and Systems Engineering
Rensselaer Polytechnic Institute
Troy, NY 12180, USA*

TAJER@ECSE.RPI.EDU

Abstract

This paper addresses intervention-based causal representation learning (CRL) under a general nonparametric latent causal model and an unknown transformation that maps the latent variables to the observed variables. Linear and general transformations are investigated. The paper addresses both the *identifiability* and *achievability* aspects. Identifiability refers to determining algorithm-agnostic conditions that ensure recovering the true latent causal variables and the latent causal graph underlying them. Achievability refers to the algorithmic aspects and addresses designing algorithms that achieve identifiability guarantees. By drawing novel connections between *score functions* (i.e., the gradients of the logarithm of density functions) and CRL, this paper designs a *score-based class of algorithms* that ensures both identifiability and achievability. First, the paper focuses on *linear* transformations and shows that one stochastic hard intervention per node suffices to guarantee identifiability. It also provides partial identifiability guarantees for soft interventions, including identifiability up to ancestors for general causal models and perfect latent graph recovery for sufficiently non-linear causal models. Secondly, it focuses on *general* transformations and shows that two stochastic hard interventions per node suffice for identifiability. Notably, one does *not* need to know which pair of interventional environments have the same node intervened. Finally, the theoretical results are empirically validated via experiments on structured synthetic data and image data.

Keywords: causal representation learning, causality, interventions

*. Equal contribution

1. Overview

Causal representation learning (CRL) aims to form a causal understanding of the world by learning appropriate representations that support causal interventions, reasoning, and planning (Schölkopf et al., 2021). Specifically, CRL considers a data-generating process in which high-level latent causally-related variables are mapped to low-level, generally high-dimensional observed data through an *unknown* transformation. Formally, consider a causal Bayesian network (Pearl, 2009) encoded by a directed acyclic graph (DAG) \mathcal{G} with n nodes and generating *causal* random variables $Z \triangleq [Z_1, \dots, Z_n]^\top$. These random variables are transformed by an *unknown* function $g : \mathbb{R}^n \rightarrow \mathbb{R}^d$ to generate the d -dimensional *observed* random variables $X \triangleq [X_1, \dots, X_d]^\top$ according to:

$$X = g(Z). \quad (1)$$

CRL is the process of using the observed data X and recovering (i) **the causal structure \mathcal{G}** and (ii) **the latent causal variables Z** . Achieving these implicitly involves another objective of recovering the unknown transformation g as well. Addressing CRL consists of two central questions:

- **Identifiability**, which refers to determining the necessary and sufficient conditions under which \mathcal{G} and Z can be recovered. The scope of identifiability (e.g., perfect or partial) critically depends on the extent of information available about the data, the underlying causal structure, and the transformation. The nature of the identifiability results can be algorithm-agnostic and non-constructive without specifying how to recover \mathcal{G} and Z . In particular, this is the case when considering CRL under a general transform g without parametric assumptions. Furthermore, the study of identifiability also covers investigating necessary conditions, e.g., which type of data is required for identifiability, regardless of the algorithmic approach.
- **Achievability**, which complements identifiability and pertains to designing algorithms that can recover \mathcal{G} and Z while maintaining identifiability guarantees. Achievability hinges on forming reliable estimates for the transformation g .

CRL from Interventions. Identifiability is known to be impossible without additional supervision or sufficient statistical diversity among the samples of the observed data X . As shown in (Hyvärinen and Pajunen, 1999; Locatello et al., 2019), this is the case even for the simpler settings in which the latent variables are statistically independent (i.e., graph \mathcal{G} has no edges). On the other hand, using data generated under interventions in addition to the observational data generated by the underlying latent model creates useful statistical diversity. Specifically, an intervention on a set of causal variables alters the causal mechanisms that generate those variables. Note that these causal mechanisms capture the effect of parents on the child variable. Such interventions, even when imposing sparse changes in the statistical models, create variations in the observed data sufficient for learning latent causal representations. This has led to CRL via intervention as an important class of CRL problems, which in its general form has remained an open problem (Schölkopf et al., 2021). This paper addresses this open problem by drawing a novel connection to score functions, i.e., the gradients of the logarithm of density functions.

We note that we use the interventions as a weak form of supervision via having access to *only* the pair of distributions before and after an intervention. Such supervision can be quite flexible and bodes well for practical applications in genomics (Tejada-Lapuerta et al., 2023) and robotics (Lee et al., 2021). For instance, genomics experiments often involve interventions, which can be modeled

as deterministic or stochastic interventions, depending on the experimental mechanism. In robotics, let us consider the causal variables to be joint angles of a robotic arm. A stochastic intervention would correspond to setting the joint angle to take values in some suitable support. We note that the interventions here can be soft since the feasible support for the joint may still depend on the other joint angles after the intervention. In this setting, the observations are simply images of the entire arm from a camera positioned at a certain place.

Contributions. This paper provides both identifiability and achievability results for CRL from interventions under general latent causal models and general transformations. We establish these results by uncovering hitherto unknown connections between *score functions* (i.e., the gradients of the logarithm of density functions) and CRL. We leverage these connections to design CRL algorithms that serve as constructive proofs for the identifiability and achievability results. We do not make any parametric assumption on the latent causal model, i.e., the relationships among elements of Z take any arbitrary form. For the transformation g , we consider a diffeomorphism (i.e., bijective such that both g and g^{-1} are continuously differentiable) onto its image. Our results are categorized into two main groups based on the form of g : (i) **linear** transformation, and (ii) **general** (nonparametric) transformation. We consider both stochastic hard and soft interventions, and our contributions are summarized below.

Linear transformations. We first focus on linear transformations and investigate various extents of identifiability and achievability (perfect and partial) given *one* intervention per node. In this setting, we consider both hard and soft interventions.

- ✓ On **identifiability from hard interventions**, we show that *one* hard intervention per node suffices to guarantee perfect identifiability (Theorem 3).
- ✓ On **identifiability from soft interventions**, we show that *one* soft intervention per node suffices to guarantee identifiability up to ancestors – transitive closure of the latent DAG is recovered and latent variables are recovered up to a linear function of their ancestors (Theorem 1). Importantly, these results are tight since identifying the latent linear models beyond ancestors using soft interventions is known to be impossible.
- ✓ We further tighten the previous result and show that when the latent causal model is sufficiently non-linear, perfect DAG recovery becomes possible using soft interventions. Furthermore, we recover a latent representation that is Markov with respect to the latent DAG, preserving the true conditional independence relationships (Theorem 2).
- ✓ On **achievability**, we design an algorithm referred to as **Linear Score-based Causal Latent Estimation via Interventions (LSCALE-I)**. This algorithm achieves the identifiability guarantees under both soft and hard interventions. LSCALE-I consists of modules (i) for achieving identifiability up to ancestors, and (ii) in the case of hard interventions, refines the output of module (i) without requiring any conditional independence test.

General transformations. In this setting, we do not have any restriction on the transformation from the latent space to the observed space. In this general setting, our contributions are as follows.

- ✓ On **identifiability**, we show that observational data and *two* distinct hard interventions per node suffice to guarantee perfect identifiability (Theorem 6). This result generalizes the recent

results in the literature in two ways. First, we do not require the commonly adopted *faithfulness* assumption on latent causal models. Secondly, we assume the learner does not know which pair of environments intervene on the same node.

- ✓ More importantly, on **achievability**, we design the first provably correct algorithm that recovers \mathcal{G} and Z perfectly. This algorithm is referred to as **Generalized Score-based Causal Latent Estimation via Interventions (GSCALE-I)**. We note that GSCALE-I requires only the score functions of observed variables as its inputs and computes those of the latent variables by leveraging the Jacobian of the decoders.
- ✓ We also establish new results that shed light on the role of observational data. Specifically, when two interventional environments per node are given in pairs, observational data is only needed for recovering the latent DAG (Theorem 4). Furthermore, we show that observational data can be dispensed with under a weak faithfulness condition on the latent causal model (Theorem 5). Remarkably, our results are tight in terms of the identifiability objectives, which we will discuss in Section 3.4.
- ✓ Finally, we show that extrapolation to unseen combinations of single-node interventions can be achieved *without performing CRL*, just by using score functions of the *observed* space (Section 6.5).

Before describing our novel methodology, we recall the general approach to solving CRL. Recovering the latent causal variables hinges on finding the inverse of g based on the observed data X , which facilitates recovering Z via $Z = g^{-1}(X)$. In other words, referring to (g^{-1}, g) as the *true* encoder-decoder pair, we search for an encoder that takes observed variables back to the true latent space. A valid encoder should necessarily have an associated decoder to ensure a perfect reconstruction of observed variables from estimated latent variables. However, there are infinitely many valid encoder-decoder pairs that satisfy the reconstruction property. The purpose of using interventions is to inject variations into the observed data, which can help us distinguish among these solutions.

Score-based methodology. We start by showing that an intervention on a latent node induces changes only in the score function's coordinates corresponding to the intervened node and its parents. This is because the intervention changes only the causal mechanism (i.e., conditional distribution) of the intervened node, which is a function of the latent node and its parents. Furthermore, when we consider two hard interventions on the same node, such changes will be limited only to the intervened node (parents intact). This implies that score changes of the latent variables Z are generally sparse across different environments. Furthermore, these score changes contain all the information about the latent causal structure. Motivated by these key properties, we formalize a score-based CRL framework based on which we design provably correct distinct algorithms LSCALE-I and GCALE-I for linear and general transformations, respectively, presented in Sections 5 and 6. We briefly describe the key technique in GSCALE-I for general transformation via two interventions. LSCALE-I involves more finesse to achieve identifiability using only one intervention per node by exploiting the linearity of the transformation.

Algorithm sketch for general transformations. Consider two interventional environments in which the same node is intervened. As described in the preceding paragraph, we show that the score functions of the latent variables under these two environments differ only at the coordinate of the

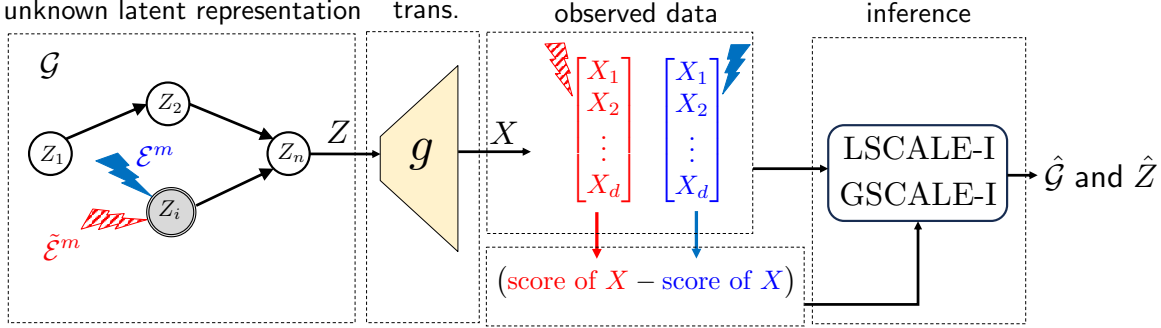


Figure 1: **An overview of LSCALE-I and GSCALE-I algorithms.** For each latent variable Z_i , there are two interventional mechanisms, denoted by red and blue. For each pair of environments, the score functions of observed variables are fed into GSCALE-I algorithm. Then, GSCALE-I uses this input to compute *latent score differences* for a given encoder and returns the encoder that minimizes these latent score differences. This encoder is used to compute estimates $\hat{\mathcal{G}}$ and \hat{Z} .

intervened node. Subsequently, the key idea of the score-based framework is that tracing these sparse changes in the score functions of the latent variables can guide finding reliable estimates for the inverse of transformation g , which in turn facilitates estimating Z . In particular, we will look for the encoders such that, the score variations among the estimated latent variables will also be sparse, matching the properties of the true latent variables. To this end, we consider a pair of interventional environments for each node and find an encoder that minimizes the variations in the score functions across all pairs. We show that the encoder obtained via this procedure perfectly recovers \mathcal{G} and Z . An important process in this methodology is projecting the score changes in observed data to the latent space so that we do not need to estimate latent scores for each possible encoder. We show that this can be done by multiplying the observed score difference by the Jacobian of the decoder associated with the encoder. Therefore, recovering \mathcal{G} and Z is facilitated by solving the following problem:

$$\min_{\substack{\text{encoder-decoder} \\ \text{pairs}}} \sum_{\substack{\text{int. env.} \\ \text{pairs}}} \left\| \text{Jac. of decoder} \times (\text{score difference of } X) \right\|_0, \quad (2)$$

in which score differences of observed variables are computed across two environments with the same intervened node. The minimization is performed over the set of valid encoder-decoder pairs that ensure perfect reconstruction of X .

Organization. The rest of the paper is organized as follows. Section 2 provides an overview of the literature with the main focus on CRL via interventions. Section 3 provides the preliminaries for formulating the problem and specifies the notations and definitions used throughout the paper. Section 4 establishes the properties of score functions under interventions and presents the key lemmas and their implications which will be used in our CRL framework. We present our CRL algorithms and results for linear transformations in Section 5, and general transformations in Section 6. Overviews of the proofs are presented in the main body of the paper, and the rest of the proofs are provided in the appendices. In Section 7, we empirically assess the performance of the proposed CRL algorithms for recovering the latent causal variables and the latent causal graph on both structured synthetic data and image data. Section 8 concludes the paper with a discussion of the results and the future directions.

Table 1: Parametric Settings. Comparison of the results to prior studies in *parametric* settings. Only the main results of the most closely related studies are listed and standard shared assumptions are omitted. Formal definitions of identifiability measures are provided in Section 3.

Work	Transform	Latent Model	Int. Data (one env. per node)	Identifiability result
Squires et al. (2023)	Linear	Lin. Gaussian	Hard	perfect
	Linear	Lin. Gaussian	Soft	up to ancestors
Ahuja et al. (2023)	Polynomial	General	<i>do</i>	perfect
	Polynomial	Bounded RV	Soft	perfect
Buchholz et al. (2023)	General	Lin. Gaussian	Hard	perfect
	General	Lin. Gaussian	Soft	up to ancestors
Zhang et al. (2023)	Polynomial	Non-linear	Soft	up to ancestors
	Polynomial	Non-linear (polytree)	Soft	perfect
Jin and Syrgkanis (2023)	Linear	Non-linear	Soft	perfect DAG and
	Linear	Lin. non-Gaussian	Soft	mixing w. surrounding
Theorem 3	Linear	General	Hard	perfect
Theorem 1	Linear	General	Soft	up to ancestors
Theorem 2	Linear	Non-linear	Soft	perfect DAG and mixing w. surrounding

2. Related Work

In this paper, we address identifiability and achievability in CRL given different interventional environments in which the interventions act on the latent space. We first provide an overview of the literature that investigates CRL from interventional data, with the main results of the most closely related work summarized in Tables 1 and 2. Then, we discuss the other relevant lines of work.

Interventional causal representation learning. The majority of the rapidly growing literature on CRL from interventions focuses on *parametric* settings, i.e., a parametric form is assumed for the latent model, the transformation, or both of them. Among the related studies, that in (Ahuja et al., 2023) mainly considers polynomial transformations without restrictions on the latent causal model and shows identifiability under deterministic *do* interventions. It also establishes identifiability under general transformations albeit requiring a combinatorial number of *do* interventions. Finally, it shows identifiability under soft interventions with independent support assumptions on latent variables. The study in (Squires et al., 2023) considers a linear latent model with a linear mapping to observations and proves identifiability under hard interventions. It also shows the impossibility of perfect identifiability under soft interventions and proves identifiability up to ancestors. The study in (Buchholz et al., 2023) focuses on linear Gaussian latent models and extends the results in (Squires et al., 2023) to prove identifiability for general transformations. Zhang et al. (2023) consider polynomial transformations under nonlinearity assumptions on latent models and prove identifiability up to ancestors under soft interventions. If the latent graph is restricted to polytrees, they further prove perfect identifiability. Identifying the non-intervened variables from the intervened variables by using single-node and multi-node soft interventions is studied in (Ahuja et al., 2024). It also considers a new setting in which the latent DAG can change across data points and rely on the support invariance of non-intervened variables to identify them from the rest. The study in (Bing et al., 2024) considers a non-linear latent model under linear transformation and uses multi-target *do* interventions to prove identifiability under certain sparsity assumptions. Linear transformation and

sufficiently non-linear latent models under a linear transform are studied in (Jin and Syrgkanis, 2023), establish identifiability up to surrounding parents using soft interventions. It also establishes sufficient conditions for multi-target soft interventions to ensure identifiability. The study in (Saengkyongam et al., 2024) takes a different approach and considers the task of intervention extrapolation. In this formulation, interventions are applied to exogenous action variables (e.g., instrumental variables) which affect the latent variables linearly.

On the fully *nonparametric* setting, von Kügelgen et al. (2023) provide the most closely related identifiability results to ours. Specifically, they show that two *coupled* hard interventions per node suffice for identifiability under faithfulness assumption on latent causal models. Our results have two major differences: 1) We address achievability via a provably correct algorithm whereas von Kügelgen et al. (2023) focus mainly on identifiability (e.g., no algorithm for recovery of the latent variables), 2) we dispense with the restrictive assumptions on identifiability results, namely, we do not require to know which two environments share the same intervention target (hence, *uncoupled* interventions), and do not require faithfulness on the latent models. While for single-node interventions the importance of this relaxation is not fully apparent, being able to work without knowing intervention targets is critical for investigating CRL under more realistic cases of multi-node interventions. Among the other studies on the nonparametric setting, Jin and Syrgkanis (2023) provide analogous results to (von Kügelgen et al., 2023) by considering two coupled soft interventions and identifying latent variables up to mixing with surrounding variables. Jiang and Aragam (2023) consider identifying the latent DAG without recovering latent variables, where it is shown that a restricted class of DAGs can be recovered. Finally, some studies use stronger supervision signals such as the annotations of the ground truth causal variables (Shen et al., 2022), or the knowledge of causal graph to recover the latent variables under hard interventions (Liang et al., 2023).

Multi-view causal representation learning. A commonly used form of weak supervision in CRL involves multi-view data, non-i.i.d. samples (or views) are observed, typically generated by the same or closely related realizations of underlying latent variables. Multi-view scenarios can involve various data settings. The earlier studies mostly consider paired data, in which pre- and post-intervention observations are generated from the same set of latent variables (Locatello et al., 2020; von Kügelgen et al., 2021; Brehmer et al., 2022). The more generalized and relaxed formulation usually involves partial observability, in which multiple views are concurrently generated by an overlapping subset of latent variables, such as observing different camera angles of the same scene (Sturma et al., 2023). Yao et al. (2024b) generalizes the multi-view approach via a unified framework, which also allows partial observability with non-linear transforms. We also note that Yao et al. (2024a) presents an even more general unifying view to interpret different CRL approaches, including interventional and multi-view, as special ways of aligning the representations to known data symmetries via leveraging the invariance principle.

Temporal causal representation learning. Temporal CRL is particularly motivated by applications in domains where time-series data is readily available, such as robotics and control systems, which has led to a growing interest in this area. Some studies in this category assume that the latent causal variables are mutually independent, meaning there are no instantaneous causal effects between variables at the same time step (Lippe et al., 2022; Yao et al., 2022; Lachapelle et al., 2024). However, more recent works have relaxed this assumption, allowing for instantaneous causal effects when sufficient diversity is present in the observed or interventional data (Lippe et al., 2023a,b; Li et al., 2024).

Table 2: General (Non-parametric) Settings. Comparison of the results to prior studies in the *general* setting. Formal definitions of identifiability measures are provided in Section 3. The shared assumptions (interventional discrepancy) and additional assumptions (faithfulness) are discussed in Section 6.4.

Work	Transform and Latent Model	Obs. Data	Int. Data (env. per node)	Faithfulness	Identifiability result	Provable algorithm
von Kügelgen et al. (2023)	General	No	2 coupled hard	Yes	perfect	✗
Jin and Syrgkanis (2023)	General	No	2 coupled soft	No	perfect DAG and mixing w. surrounding	✗
Theorem 4	General	Yes	2 coupled hard	No	perfect	✓
Theorem 5	General	No	2 coupled hard	Yes	perfect	✓
Theorem 6	General	Yes	2 uncoupled hard	No	perfect	✓

Identifiable representation learning. As a special case of CRL, where the latent variables are independent, there is extensive literature on identifying latent representations. Some representative approaches include leveraging the knowledge of the mechanisms that govern the evolution of the system (Ahuja et al., 2022) and using weak supervision with auxiliary information (Shu et al., 2020). Non-linear independent component analysis (ICA) also uses side information, in the form of structured time series to exploit temporal information (Hyvärinen and Morioka, 2017; Hälvä and Hyvärinen, 2020) or knowledge of auxiliary variables that renders latent variables conditionally independent (Khemakhem et al., 2020a,b; Hyvärinen et al., 2019). Morioka and Hyvärinen (2023) impose additional constraints on observational mixing and causal model to prove identifiability. Kivva et al. (2022) studies the identifiability of deep generative models without auxiliary information.

Score functions for causal discovery within observed variables. Score matching has recently gained attraction in the causal discovery of observed variables. Rolland et al. (2022) use score matching to recover non-linear additive Gaussian noise models. Montagna et al. (2023b) focus on the same setting, recover the full graph from Jacobian scores, and dispense with the computationally expensive pruning stage of the algorithm in (Rolland et al., 2022). Montagna et al. (2023a) empirically demonstrate the robustness of score-matching-based approaches against the assumption violations in causal discovery. Zhu et al. (2023) establish bounds on the error rate of score matching-based causal discovery methods. All of these studies are limited to observed causal variables, whereas in our case, we have a causal model in the latent space.

3. Preliminaries and Definitions

Notations. For a vector $a \in \mathbb{R}^m$, the i -th entry is denoted by a_i . Matrices are denoted by bold upper-case letters, e.g., \mathbf{A} , where \mathbf{A}_i denotes the i -th row of \mathbf{A} and $\mathbf{A}_{i,j}$ denotes the entry at row i and column j . For matrices \mathbf{A} and \mathbf{B} with the same shapes, $\mathbf{A} \preceq \mathbf{B}$ denotes component-wise inequality. We denote the indicator function by $\mathbb{1}$, and for a matrix $\mathbf{A} \in \mathbb{R}^{m \times n}$, we use the convention that $\mathbb{1}\{\mathbf{A}\} \in \{0, 1\}^{m \times n}$, where the entries are specified by $[\mathbb{1}\{\mathbf{A}\}]_{i,j} = \mathbb{1}\{\mathbf{A}_{i,j} \neq 0\}$. For a positive integer $n \in \mathbb{N}$, we define $[n] \triangleq \{1, \dots, n\}$. The permutation matrix associated with any permutation π of $[n]$ is denoted by \mathbf{P}_π , i.e., $[\pi_1 \ \pi_2 \ \dots \ \pi_n]^\top = \mathbf{P}_\pi \cdot [1 \ 2 \ \dots \ n]^\top$. The n -dimensional identity matrix is denoted by $\mathbf{I}_{n \times n}$, and the Hadamard product is denoted by \odot . Given a function $f : \mathbb{R}^r \rightarrow \mathbb{R}^s$ that has first-order partial derivatives on \mathbb{R}^r , we denote the Jacobian of f at $z \in \mathbb{R}^s$ by $J_f(z)$. We use $\text{im}(f)$ to denote the image of f and define *rank* of f as the number of linearly

independent vectors in its image and denote it by $\mathcal{R}(f) \triangleq \dim(\text{im}(f))$. Accordingly, for a set of functions $\mathcal{F} \triangleq \{f_i : i \in [k], f_i : \mathbb{R}^r \rightarrow \mathbb{R}^s\}$ we define $\text{im}(\mathcal{F}) \triangleq \bigcup_{i=1}^k \text{im}(f_i)$, and denote the rank of \mathcal{F} by $\mathcal{R}(\mathcal{F}) \triangleq \dim(\text{im}(\mathcal{F}))$.

3.1 Latent Causal Structure

Consider latent causal random variables $Z \triangleq [Z_1, \dots, Z_n]^\top$. An *unknown* transformation $g : \mathbb{R}^n \rightarrow \mathbb{R}^d$ generates the observable random variables $X \triangleq [X_1, \dots, X_d]^\top$ from the latent variables Z according to:

$$X = g(Z). \quad (3)$$

We assume that $d \geq n$, and transformation g is continuously differentiable and a diffeomorphism onto its image (otherwise, identifiability is ill-posed). We denote the image of g by $\mathcal{X} \triangleq \text{im}(g) \subseteq \mathbb{R}^d$. The probability density functions (pdfs) of Z and X are denoted by p and p_X , respectively. We assume that p is absolutely continuous with respect to the n -dimensional Lebesgue measure. Subsequently, p_X , which is defined on the image manifold $\text{im}(g)$, is absolutely continuous with respect to the n -dimensional Hausdorff measure rather than d -dimensional Lebesgue measure¹. The distribution of latent variables Z factorizes with respect to a DAG that consists of n nodes and is denoted by \mathcal{G} . Node $i \in [n]$ of \mathcal{G} represents Z_i and p factorizes according to:

$$p(z) = \prod_{i=1}^n p_i(z_i | z_{\text{pa}(i)}), \quad (4)$$

where $\text{pa}(i)$ denotes the set of parents of node i and $p_i(z_i | z_{\text{pa}(i)})$ is the conditional pdf of z_i given the variables of its parents. We use $\text{ch}(i)$, $\text{an}(i)$, and $\text{de}(i)$ to denote the children, ancestors, and descendants of node i , respectively. Accordingly, for each node $i \in [n]$ we also define

$$\overline{\text{pa}}(i) \triangleq \text{pa}(i) \cup \{i\}, \quad \overline{\text{ch}}(i) \triangleq \text{ch}(i) \cup \{i\}, \quad \overline{\text{an}}(i) \triangleq \text{an}(i) \cup \{i\}, \quad \text{and} \quad \overline{\text{de}}(i) \triangleq \text{de}(i) \cup \{i\}. \quad (5)$$

We denote the transitive closure and transitive reduction of \mathcal{G} by \mathcal{G}_{tc} and \mathcal{G}_{tr} , respectively². The parental relationships in these graphs are denoted by pa_{tc} and pa_{tr} , and other graphical relationships are denoted similarly. Based on the modularity property, a change in the causal mechanism of node i does not affect those of the other nodes. We also assume that all conditional pdfs $\{p_i(z_i | z_{\text{pa}(i)}) : i \in [n]\}$ are continuously differentiable with respect to all z variables and $p(z) \neq 0$ for all $z \in \mathbb{R}^n$. We consider the general structural causal models (SCMs) based on which for each $i \in [n]$,

$$Z_i = f_i(Z_{\text{pa}(i)}, N_i), \quad (6)$$

where $\{f_i : i \in [n]\}$ are general functions that capture the dependence of node i on its parents and $\{N_i : i \in [n]\}$ account for the exogenous noise terms that we assume to have pdfs with full support. We specialize some of the results to additive noise SCMs, in which (6) becomes

$$Z_i = f_i(Z_{\text{pa}(i)}) + N_i. \quad (7)$$

Next, we provide a number of definitions that we will use frequently throughout the paper for formalizing the framework and analyzing it.

1. For details of where this has been used, see Appendix A.2.
 2. Transitive closure of a DAG \mathcal{G} , denoted by \mathcal{G}_{tr} , is a DAG with parents denoted by $\text{pa}_{\text{tr}}(i) = \text{an}(i)$ for each node i . The transitive reduction of a DAG \mathcal{G} is the DAG with the fewest edges preserves the same reachability relation as \mathcal{G} .



Figure 2: Sample latent DAGs \mathcal{G} . **(Left)** The valid causal orders are $(1, 2, 3, 4)$ and $(1, 3, 2, 4)$, and only surrounded node is 4 with $\text{sur}(4) = \{2, 3\}$. **(Right)** The only valid causal order is $(1, 2, 3)$, and the surrounded nodes are $\mathcal{S} = \{2, 3\}$ with $\text{sur}(2) = \{1\}$, $\text{sur}(3) = \{1, 2\}$.

Definition 1 (Valid Causal Order) We refer to a permutation (π_1, \dots, π_n) of $[n]$ as a valid causal order³ if $\pi_i \in \text{pa}(\pi_j)$ indicates that $i < j$.

In this paper, without loss of generality, we assume that $(1, \dots, n)$ is a valid causal order. We also define a graphical notion that will be useful for presenting our results and analysis on CRL under a linear transformation.

Definition 2 (Surrounded Node) Node $i \in [n]$ in DAG \mathcal{G} is said to be surrounded if there exists another node $j \in [n]$ such that $\overline{\text{ch}}(i) \subseteq \text{ch}(j)$. We denote the set of nodes that surround $i \in [n]$ by $\text{sur}(i)$, and the set of all nodes that are surrounded by \mathcal{S} , i.e.,

$$\text{sur}(i) \triangleq \{j \in [n] : j \neq i, \overline{\text{ch}}(i) \subseteq \text{ch}(j)\}, \quad \text{and} \quad \mathcal{S} \triangleq \{i \in [n] : \text{sur}(i) \neq \emptyset\}. \quad (8)$$

The intuition behind surrounded nodes is that, the effect of i on its children $\text{ch}(i)$ can be dominated by the effect of its surrounding node j .⁴ Specifically, any effect of i on a node $k \in \text{ch}(i)$ can also be interpreted as the effect of node j since $k \in \text{ch}(j)$ as well. This effect causes ambiguities in the recovery of Z_i in the case of soft interventions.

3.2 Score Functions

The *score function* associated with a pdf is defined as the gradient of its logarithm. The score function associated with p is denoted by

$$s(z) \triangleq \nabla_z \log p(z). \quad (9)$$

Noting the connection $X = g(Z)$, the density of X under \mathcal{E}^0 , denoted by p_X , is supported on an n -dimensional manifold \mathcal{X} embedded in \mathbb{R}^d . Hence, specifying the score function of X requires notions from differential geometry. For this purpose, we denote the tangent space of manifold \mathcal{X} at point $x \in \mathcal{X}$ by $T_x \mathcal{X}$. Tangent vectors $v \in T_x \mathcal{X}$ are equivalence classes of continuously differentiable curves $\gamma: (-1, 1) \rightarrow \mathcal{X} \subseteq \mathbb{R}^d$ with $\gamma(0) = x$ and $\gamma'(0) = v$. Furthermore, given a function $f: \mathcal{X} \rightarrow \mathbb{R}$, denote its directional derivative at point $x \in \mathcal{X}$ along a tangent vector $v \in T_x \mathcal{X}$ by $D_v f(x)$, which is defined as

$$D_v f(x) \triangleq \left. \frac{d}{dt} (f \circ \gamma)(t) \right|_{t=0}, \quad (10)$$

3. It is also called *topological ordering* or *topological sort* in the literature.

4. Surrounded node concept is first defined by (Varıcı et al., 2023), and later adopted by Jin and Syrgkanis (2023) when considering soft interventions.

for any curve γ in equivalence class v . The differential of f at point $x \in \mathcal{X}$, denoted by df_x , is the linear operator mapping tangent vector $v \in T_x \mathcal{X}$ to $D_v f(x)$ (Simon, 2014, p. 57), i.e.,

$$df_x : T_x \mathcal{X} \ni v \mapsto D_v f(x) \in \mathbb{R}. \quad (11)$$

Let $\mathbf{B} \in \mathbb{R}^{d \times n}$ be a matrix for which the columns of \mathbf{B} form an orthonormal basis for $T_x \mathcal{X}$. Denote the directional derivative of f along the i -th column of \mathbf{B} by $D_i f$ for all $i \in [n]$. Then, the differential operator can be expressed by the vector

$$Df(x) \triangleq \mathbf{B} \cdot [D_1 f(x) \dots D_n f(x)]^\top \in \mathbb{R}^d, \quad (12)$$

such that

$$df_x(v) = v^\top \cdot Df(x), \quad \forall x \in \mathcal{X}, \quad \forall v \in T_x \mathcal{X}. \quad (13)$$

Note that the differential operator df is a generalization of the gradient. Hence, we can generalize the definition of the score function using the differential operator by setting f to the logarithm of pdf. Therefore, the score function of X under \mathcal{E}^0 is specified as follows:

$$s_X(x) \triangleq D \log p_X(x), \quad \forall x \in \mathcal{X}. \quad (14)$$

3.3 Intervention Mechanisms

We consider two types of interventions. A *soft* intervention on node i (also referred to as *imperfect* intervention in literature), changes the conditional distribution $p_i(z_i | z_{\text{pa}(i)})$ to a distinct conditional distribution, which we denote by $q_i(z_i | z_{\text{pa}(i)})$. A soft intervention does not necessarily remove the functional dependence of an intervened node on its parents and rather alters it to a different mechanism. A stochastic *hard* intervention on node i (also referred to as *perfect* intervention) is stricter than a soft intervention and removes the edges incident on i . A hard intervention on node i changes $p_i(z_i | z_{\text{pa}(i)})$ to $q_i(z_i)$ that emphasizes the lack of dependence of z_i on $z_{\text{pa}(i)}$. Finally, we note that in some settings, we assume two hard interventions per node, in which case the two hard interventional mechanisms for node i are denoted by two distinct pdfs $q_i(z_i)$ and $\tilde{q}_i(z_i)$.

Interventional environments. We consider atomic *interventional* environments in which each environment one node is intervened in, as it is customary to the closely related CRL literature (Squires et al., 2023; Ahuja et al., 2023; Buchholz et al., 2023). In some settings (linear transformation), we will have *one* interventional environment per node and denote the interventional environments by $\mathcal{E} \triangleq \{\mathcal{E}^1, \dots, \mathcal{E}^n\}$, where we call \mathcal{E} the *atomic* environment set. We denote the node intervened in environment \mathcal{E}^m by $I^m \in [n]$. For other settings (general transformation), we will have *two* interventional environments per node and denote the second atomic environment set by $\tilde{\mathcal{E}} = \{\tilde{\mathcal{E}}^1, \dots, \tilde{\mathcal{E}}^n\}$. Similarly, we denote the intervened node in $\tilde{\mathcal{E}}^m$ by \tilde{I}^m for each $m \in [n]$. We assume that node-environment pairs are *unspecified*, i.e., the ordered intervention sets $\mathcal{I} \triangleq (I^1, \dots, I^n)$ and $\tilde{\mathcal{I}} \triangleq (\tilde{I}^1, \dots, \tilde{I}^n)$ are two *unknown* permutations of $[n]$. We also adopt the convention that \mathcal{E}^0 is the *observational* environment and $I^0 \triangleq \emptyset$. Next, we define the notion of coupling between the environment sets \mathcal{E} and $\tilde{\mathcal{E}}$.

Definition 3 (Coupled/Uncoupled Environments) *The two environment sets \mathcal{E} and $\tilde{\mathcal{E}}$ are said to be **coupled** if for the unknown permutations \mathcal{I} and $\tilde{\mathcal{I}}$ we know that $\mathcal{I} = \tilde{\mathcal{I}}$, i.e., the same node is intervened in environments \mathcal{E}^i and $\tilde{\mathcal{E}}^i$. The two environment sets are said to be **uncoupled** if $\tilde{\mathcal{I}}$ is an unknown permutation of \mathcal{I} .*

Next, we define p^m as the pdf of Z in environment \mathcal{E}^m . Hence, under soft and hard intervention for each $m \in [n]$, p^m can be factorized as follows.

$$\text{soft intervention in } \mathcal{E}^m : \quad p^m(z) = q_\ell(z_\ell \mid z_{\text{pa}(\ell)}) \prod_{i \neq \ell} p_i(z_i \mid z_{\text{pa}(i)}) , \quad \text{where } \ell = I^m , \quad (15)$$

$$\text{hard intervention in } \mathcal{E}^m : \quad p^m(z) = q_\ell(z_\ell) \prod_{i \neq \ell} p_i(z_i \mid z_{\text{pa}(i)}) , \quad \text{where } \ell = I^m . \quad (16)$$

Similarly, we define \tilde{p}^m as the pdf of Z in $\tilde{\mathcal{E}}^m$, which can be factorized similarly to (16) with \tilde{q}_ℓ replaced with q_ℓ . Hence, the score functions associated with p^m and \tilde{p}^m are specified as follows.

$$s^m(z) \triangleq \nabla_z \log p^m(z) , \quad \text{and} \quad \tilde{s}^m(z) \triangleq \nabla_z \log \tilde{p}^m(z) . \quad (17)$$

We denote the score functions of the observed variables X under \mathcal{E}^m and $\tilde{\mathcal{E}}^m$ by s_X^m and \tilde{s}_X^m , respectively. Note that the score functions change across different environments, which is induced by the changes in the distribution of Z . Specifically, following (4) and (15), the latent scores $s(z)$ and $s^m(z)$ are decomposed as

$$s(z) = \nabla_z \log p_\ell(z_\ell \mid z_{\text{pa}(\ell)}) + \sum_{i \neq \ell} \nabla_z \log p_i(z_i \mid z_{\text{pa}(i)}) , \quad (18)$$

$$\text{and} \quad s^m(z) = \nabla_z \log q_\ell(z_\ell \mid z_{\text{pa}(\ell)}) + \sum_{i \neq \ell} \nabla_z \log p_i(z_i \mid z_{\text{pa}(i)}) . \quad (19)$$

where $\ell = I^m$. Hence, $s(z)$ and $s^m(z)$ differ in only the causal mechanism of the intervened node in environment \mathcal{E}^m . In Section 4, we investigate these discrepancies between s and s^m (or \tilde{s}^m) and characterize the relationship between the scores in the observational and interventional environments. Finally, we use Z^m and X^m to denote the latent variables Z and observed variables X in environment \mathcal{E}^m , respectively.

3.4 Identifiability and Achievability Objectives

The objective of CRL is to use observations X generated by the observational and interventional environments and estimate the true latent variables Z and causal relations among them captured by \mathcal{G} . The first objective is *identifiability*, which pertains to determining algorithm-agnostic sufficient conditions under which Z and \mathcal{G} can be recovered uniquely up to a permutation and element-wise transform which is the strongest form of recovery in CRL from interventions as shown in (von Kügelgen et al., 2023). The second objective is *achievability*, which refers to designing algorithms that are amenable to practical implementation and generate provably correct estimates for Z and \mathcal{G} , foreseen by the identifiability guarantees. In this subsection, we provide the definitions needed for formalizing identifiability and achievability objectives.

We denote a generic estimator of Z given X by $\hat{Z}(X) : \mathbb{R}^d \rightarrow \mathbb{R}^n$. We also consider a generic estimate of \mathcal{G} denoted by $\hat{\mathcal{G}}$. In order to assess the fidelity of the estimates $\hat{Z}(X)$ and $\hat{\mathcal{G}}$ with respect to the ground truth Z and \mathcal{G} , we provide the following identifiability measures. We start with specifying *perfect* identifiability, which is relevant for assessing the identifiability and achievability results under hard interventions.

Definition 4 (Perfect Identifiability) *To formalize perfect identifiability in CRL we define:*

1. **Perfect DAG recovery:** *DAG recovery is said to be perfect if $\hat{\mathcal{G}}$ is isomorphic to \mathcal{G} .*
2. **Perfect latent recovery**⁵: *Given the estimator $\hat{Z}(X)$, latent recovery is said to be perfect if $\hat{Z}(X)$ is an element-wise diffeomorphism of a permutation of Z , i.e., there exists a permutation π of $[n]$ and a set diffeomorphisms $\{\phi_i : \mathbb{R} \rightarrow \mathbb{R} : i \in [n]\}$ such that we have*

$$\hat{Z}(X) = (\pi \circ \phi)(Z), \quad \forall Z \in \mathbb{R}^n, \quad (20)$$

where $\phi(Z) \triangleq (\phi_1(Z_1), \dots, \phi_n(Z_n))$.

3. **Scaling consistency:** *The estimator $\hat{Z}(X)$ is said to maintain scaling consistency if there exists a permutation π of $[n]$ and a constant diagonal matrix $\mathbf{C}_s \in \mathbb{R}^{n \times n}$ such that*

$$\hat{Z}(X) = \mathbf{P}_\pi \cdot \mathbf{C}_s \cdot Z, \quad \forall Z \in \mathbb{R}^n. \quad (21)$$

We note that scaling consistency is a special case of perfect latent recovery in which the diffeomorphism in the perfect latent recovery is restricted to an element-wise scaling. Next, we provide *partial identifiability* measures which will be useful to assess the identifiability and achievability results under soft interventions.

Definition 5 (Partial Identifiability) *To formalize partial identifiability in CRL we define:*

1. **Transitive closure recovery:** *DAG recovery is said to maintain transitive closure if $\hat{\mathcal{G}}$ and \mathcal{G} have the same ancestral relationships, i.e., $\hat{\mathcal{G}}_{\text{tr}}$ is isomorphic to \mathcal{G}_{tr} .*
2. **Mixing consistency up to ancestors:** *The estimator $\hat{Z}(X)$ is said to maintain mixing consistency up to ancestors if there exists a permutation π of $[n]$ and a constant matrix $\mathbf{C}_{\text{an}} \in \mathbb{R}^{n \times n}$ such that*

$$\hat{Z}(X) = \mathbf{P}_\pi \cdot \mathbf{C}_{\text{an}} \cdot Z, \quad \forall Z \in \mathbb{R}^n, \quad (22)$$

where \mathbf{C}_{an} has non-zero diagonal entries and for all $j \notin \overline{\text{an}}(i)$, \mathbf{C}_{an} satisfies $[\mathbf{C}_{\text{an}}]_{i,j} = 0$. Equivalently, \hat{Z}_{π_i} is a linear function of $\{Z_j : j \in \overline{\text{an}}(i)\}$ for all $i \in [n]$.

3. **Mixing consistency up to surrounding parents:** *The estimator $\hat{Z}(X)$ is said to maintain mixing consistency up to surrounding parents if there exists a permutation π of $[n]$ and a constant matrix $\mathbf{C}_{\text{sur}} \in \mathbb{R}^{n \times n}$ such that*

$$\hat{Z}(X) = \mathbf{P}_\pi \cdot \mathbf{C}_{\text{sur}} \cdot Z, \quad \forall Z \in \mathbb{R}^n, \quad (23)$$

where \mathbf{C}_{sur} has non-zero diagonal entries and for all $i \neq j$ and $j \notin \text{sur}(i)$, \mathbf{C}_{sur} satisfies $[\mathbf{C}_{\text{sur}}]_{i,j} = 0$. Equivalently, \hat{Z}_{π_i} is a linear function of $\{Z_j : j \in \overline{\text{sur}}(i)\}$ for all $i \in [n]$.

5. We note that identifiability up to element-wise transforms is a standard definition in related literature, including nonlinear ICA (Khemakhem et al., 2020b). Therefore, we use the term *perfect* to distinguish this complete identifiability from the subsequent partial identifiability definitions.

Tightness of the identifiability definitions. For general transformations, von Kügelgen et al. (2023, Proposition 3.1) show that identifiability up to element-wise diffeomorphisms is the best possible result under interventions, without additional assumptions. For linear transformations, Squires et al. (2023, Proposition 2) and Buchholz et al. (2023, Remark 2) show that under hard interventions, identifiability up to scaling consistency and permutation ambiguity is the best achievable outcome without further information on Z . Furthermore, for soft interventions, identifiability up to ancestors is shown to be the best possible result without additional assumptions on the causal model (Squires et al., 2023, Appendix J). Finally, Jin and Syrgkanis (2023, Theorem 6) show that, under some non-degeneracy assumptions, mixing consistency up to surrounding parents is the optimal result. Therefore, given a complete set of atomic interventions, the perfect and partial identifiability definitions presented in this section represent the ultimate objectives when using hard and soft interventions, respectively.

3.5 Algorithm-related Definitions

For formalizing the achievability results and designing the associated algorithms, generating the estimates $\hat{Z}(X)$ and $\hat{\mathcal{G}}$ is facilitated by estimating the inverse of g based on the observed data X . Specifically, an estimate of g^{-1} , where g^{-1} denotes the inverse of g , facilitates recovering Z via $Z = g^{-1}(X)$. Throughout the rest of this paper, we refer to g^{-1} as the *true encoder*. To formalize the procedures of estimating g^{-1} , we define \mathcal{H} as the set of possible valid encoders, i.e., candidates for g^{-1} . A function $h \in \mathcal{H}$ can be such a candidate if it is invertible, that is, there exists an associated decoder h^{-1} such that $(h^{-1} \circ h)(X) = X$. Hence, the set of valid encoders is specified by

$$\mathcal{H} \triangleq \{h : \mathcal{X} \rightarrow \mathbb{R}^n : \exists h^{-1} : \mathbb{R}^n \rightarrow \mathbb{R}^d \text{ such that } (h^{-1} \circ h)(X) = X, \forall X \in \mathcal{X}\}. \quad (24)$$

Next, corresponding to any pair of observation X and valid encoder $h \in \mathcal{H}$, we define $\hat{Z}(X; h)$ as an *auxiliary* estimate of Z generated by applying the valid encoder h on X , i.e.,

$$\hat{Z}(X; h) \triangleq h(X) = (h \circ g)(Z), \quad \forall h \in \mathcal{H}, X \in \mathcal{X}. \quad (25)$$

The estimate $\hat{Z}(X; h)$ inherits its randomness from X , and its statistical model is governed by that of X and the choice of h . To emphasize the dependence on h , we denote the score functions associated with the pdfs of $\hat{Z}(X; h)$ under environments $\mathcal{E}^0, \mathcal{E}^m$, and $\tilde{\mathcal{E}}^m$, respectively, by

$$s_{\hat{Z}}(\cdot; h), \quad s_{\hat{Z}}^m(\cdot; h), \quad \text{and} \quad \tilde{s}_{\hat{Z}}^m(\cdot; h). \quad (26)$$

We will be addressing both general and linear transformations g . In the linear transformation setting, the true linear transformation g is denoted by matrix $\mathbf{G} \in \mathbb{R}^{d \times n}$. Accordingly, we denote a valid linear encoder by $\mathbf{H} \in \mathbb{R}^{n \times d}$. For a given valid encoder \mathbf{H} , the associated valid decoder is given by its Moore-Penrose inverse, i.e., $\mathbf{H}^\dagger \triangleq \mathbf{H}^\top \cdot (\mathbf{H} \cdot \mathbf{H}^\top)^{-1}$.

4. Properties of Score Functions under Interventions

Score functions and their variations across different interventional environments play pivotal roles in our approach to identifying latent representations. In this section, we present the key properties of the score functions that will be leveraged in Sections 5 and 6 to construct identifiability results along with algorithms.

We first investigate score variations across pairs of environments such as the observational environment and an interventional one (under both soft and hard atomic interventions) or two

interventional environments, either coupled or uncoupled. The following lemma delineates the set of coordinates of the score function that are affected by the interventions in all relevant cases. The key insight is that an intervention causes changes in only certain coordinates of the score function, as indicated by the sparse changes in the decompositions of the score functions in (18) and (19).

Lemma 1 (Score Changes under Interventions) *Consider the observational environment \mathcal{E}^0 and an interventional environment \mathcal{E}^m with unknown intervention target I^m . Then, for any causal model and intervention type, $\mathbb{E}\left[\left| [s(Z) - s^m(Z)]_i \right| \right] \neq 0$ implies that $i \in \overline{\text{pa}}(I^m)$. For the reverse direction, we have the following results specified for each relevant case.*

(i) **Hard interventions:** *If the intervention in \mathcal{E}^m (or $\tilde{\mathcal{E}}^m$) is hard, then score functions s and s^m (or \tilde{s}^m) differ in their i -th coordinate if and only if node i or one of its children is intervened in \mathcal{E}^m (or in $\tilde{\mathcal{E}}^m$).*

$$\mathbb{E}\left[\left| [s(Z) - s^m(Z)]_i \right| \right] \neq 0 \iff i \in \overline{\text{pa}}(I^m), \quad (27)$$

$$\text{and } \mathbb{E}\left[\left| [s(Z) - \tilde{s}^m(Z)]_i \right| \right] \neq 0 \iff i \in \overline{\text{pa}}(\tilde{I}^m). \quad (28)$$

(ii) **Soft interventions:** *If the intervention in \mathcal{E}^m is soft and the latent causal model is an additive noise model, then score functions s and s^m differ in their i -th coordinate if and only if node i or one of its children is intervened in \mathcal{E}^m .*

$$\mathbb{E}\left[\left| [s(Z) - s^m(Z)]_i \right| \right] \neq 0 \iff i \in \overline{\text{pa}}(I^m). \quad (29)$$

(iii) **Coupled environments $I^m = \tilde{I}^m$:** *In the coupled environment setting, s^m and \tilde{s}^m differ in their i -th coordinate if and only if i is intervened.*

$$\mathbb{E}\left[\left| [s^m(Z) - \tilde{s}^m(Z)]_i \right| \right] \neq 0 \iff i = I^m. \quad (30)$$

(iv) **Uncoupled environments $I^m \neq \tilde{I}^m$:** *Consider two interventional environments \mathcal{E}^m and $\tilde{\mathcal{E}}^m$ with different intervention targets $I^m \neq \tilde{I}^m$, and consider additive noise models specified in (7). Given that $p(Z)$ is twice differentiable, the score functions s^m and \tilde{s}^m differ in their i -th coordinate if and only if node i or one of its children is intervened.*

$$\mathbb{E}\left[\left| [s^m(Z) - \tilde{s}^m(Z)]_i \right| \right] \neq 0 \iff i \in \overline{\text{pa}}(I^m, \tilde{I}^m). \quad (31)$$

Proof: See Appendix A.1.

Lemma 1 provides the necessary and sufficient conditions for the invariance of the coordinates of the score functions of latent variables. The core idea of the score-based framework is that tracing these sparse changes in the score functions of the latent variables guides finding reliable estimates for the inverse of transformation g , which in turn facilitates estimating Z . Intuitively, we will look for the encoders $h \in \mathcal{H}$ such that the variations between the score estimates $s_{\hat{Z}}(\hat{z}; h)$, $s_{\hat{Z}}^m(\hat{z}; h)$, and $\tilde{s}_{\hat{Z}}^m(\hat{z}; h)$ will be similar to the true score variations given by Lemma 1. However, the scores of the latent variables are not directly accessible. To circumvent this, we need to understand the connection between score functions of X and Z . In the next lemma, we establish this relationship for any injective mapping f from latent to observed space.

Lemma 2 (Score Difference Transformation) Consider random vectors $Y_1, Y_2 \in \mathbb{R}^r$ and $W_1, W_2 \in \mathbb{R}^s$ that are related through

$$Y_1 = f(W_1), \quad \text{and} \quad Y_2 = f(W_2), \quad (32)$$

such that $r \geq s$, probability measures of W_1, W_2 are absolutely continuous with respect to the s -dimensional Lebesgue measure, and $f : \mathbb{R}^s \rightarrow \mathbb{R}^r$ is an injective and continuously differentiable function. The difference of the score functions of Y_1 and Y_2 , and that of W_1 and W_2 are related as

$$s_{W_1}(w) - s_{W_2}(w) = [J_f(w)]^\top \cdot [s_{Y_1}(y) - s_{Y_2}(y)], \quad \text{where } y = f(w). \quad (33)$$

Proof: See Appendix A.2.

Throughout the paper, we customize Lemma 2 to two special cases. First, we consider score differences of $\hat{Z}(X; h)$ and X . Recall that $\hat{Z}(X; h) = h(X)$. By setting $f = h^{-1}$, Lemma 2 gives

$$\text{between } \mathcal{E}^0 \text{ and } \mathcal{E}^m : \quad s_{\hat{Z}}(\hat{z}; h) - s_{\hat{Z}}^m(\hat{z}; h) = [J_{h^{-1}}(\hat{z})]^\top \cdot [s_X(x) - s_X^m(x)], \quad (34)$$

$$\text{between } \mathcal{E}^0 \text{ and } \tilde{\mathcal{E}}^m : \quad s_{\hat{Z}}(\hat{z}; h) - \tilde{s}_{\hat{Z}}^m(\hat{z}; h) = [J_{h^{-1}}(\hat{z})]^\top \cdot [s_X(x) - \tilde{s}_X^m(x)], \quad (35)$$

$$\text{between } \mathcal{E}^m \text{ and } \tilde{\mathcal{E}}^m : \quad s_{\hat{Z}}^m(\hat{z}; h) - \tilde{s}_{\hat{Z}}^m(\hat{z}; h) = [J_{h^{-1}}(\hat{z})]^\top \cdot [s_X^m(x) - \tilde{s}_X^m(x)]. \quad (36)$$

Next, recall that $\hat{Z}(X; h) = h(X) = (h \circ g)(Z)$. Then, by defining $\phi_h = h \circ g$ and setting $f = \phi_h^{-1}$, Lemma 2 gives

$$\text{between } \mathcal{E}^0 \text{ and } \mathcal{E}^m : \quad s_{\hat{Z}}(\hat{z}; h) - s_{\hat{Z}}^m(\hat{z}; h) = [J_{\phi_h}(z)]^{-\top} \cdot [s(z) - s^m(z)], \quad (37)$$

$$\text{between } \mathcal{E}^0 \text{ and } \tilde{\mathcal{E}}^m : \quad s_{\hat{Z}}(\hat{z}; h) - \tilde{s}_{\hat{Z}}^m(\hat{z}; h) = [J_{\phi_h}(z)]^{-\top} \cdot [s(z) - \tilde{s}^m(z)], \quad (38)$$

$$\text{between } \mathcal{E}^m \text{ and } \tilde{\mathcal{E}}^m : \quad s_{\hat{Z}}^m(\hat{z}; h) - \tilde{s}_{\hat{Z}}^m(\hat{z}; h) = [J_{\phi_h}(z)]^{-\top} \cdot [s^m(z) - \tilde{s}^m(z)], \quad (39)$$

in which $J_{\phi_h}(z)$ denotes the Jacobian of ϕ_h at point $z \in \mathbb{R}^n$. Finally, for the reverse direction of Lemma 2, i.e., going from score functions in latent space to observed space, we have the following result, which will be critical for intervention extrapolation discussion in Section 6.5.

Corollary 1 Under the same setting and the assumptions as Lemma 2, we have

$$s_{Y_1}(y) - s_{Y_2}(y) = \left[[J_f(w)]^\dagger \right]^\top \cdot [s_{W_1}(w) - s_{W_2}(w)], \quad \text{where } y = f(w). \quad (40)$$

5. CRL under Linear Transformations

In this section, we consider CRL under linear transformation, in which, the general transformation model in (3) becomes:

$$X = \mathbf{G} \cdot Z, \quad (41)$$

where $\mathbf{G} \in \mathbb{R}^{d \times n}$ is an *unknown* full-rank matrix mapping the latent variables to the observed ones. We will present steps of leveraging the properties of the score functions presented in Section 4 to design an algorithm to identify the true encoder and recover the true causal representations. The algorithm is referred to as **Linear Score-based Causal Latent Estimation via Interventions (LSCALE-I)**. The theoretical guarantees associated with the algorithm steps will also be presented, serving as steps of constructive proof of identifiability. Hence, we address both identifiability and achievability aspects laid out in Section 1.

Inputs. The inputs of LSCALE-I are the observed data from the observational environment, the data from one interventional environment per node, and $\text{im}(\mathbf{G})$. We can estimate $\text{im}(\mathbf{G})$ correctly from n random samples of X using singular value decomposition with probability 1.

Statistical diversity. Similarly to the existing identifiability results, it is necessary to have some regularity conditions⁶ on the probability distributions of observational and interventional environments. To ensure that the intervention sufficiently differentiates the target variable and its parents in the score function, we adopt the following assumption for the case of linear transformations.

Assumption 1 *For any environment $\mathcal{E}^m \in \mathcal{E}$, and for all $k \in \text{pa}(I^m)$, we have*

$$\mathcal{R} \left(\begin{bmatrix} [s - s^m]_k \\ [s - s^m]_\ell \end{bmatrix} \right) = 2, \quad \text{where } \ell = I_m. \quad (42)$$

This assumption holds for a wide range of models (including additive noise models under hard interventions) and is discussed in more detail in Section 5.7.

We recall that the main benefit of using interventions for CRL is that interventions inject proper statistical variations into the observed data, i.e., introduce non-i.i.d. data. Subsequently, our approach to CRL is built on using such statistical variations via tracking the variations of the score functions associated with the interventional data. Specifically, we will learn a decoder \mathbf{H} , row by row, where each row is an estimate of a row of the true decoder \mathbf{G}^\dagger . At each step, Lemma 1 will guide us for which properties to seek for in a desired decoder, e.g., sparsity structure. Meanwhile, Lemma 2 will ensure access to *latent* score differences via score differences in observed space.

Our algorithmic approach to identifiability consists of three stages outlined in LSCALE-I (Algorithm 1). In the first stage, we will learn a causal order of the interventional environments with respect to their intervened nodes. This causal order and the initial estimate of the true encoder \mathbf{G}^\dagger will serve as an intermediate step toward more accurate identifiability. In the second stage, we will refine the outcome of the first stage to learn a DAG $\hat{\mathcal{G}}$ consistent with the causal order and update our encoder estimate \mathbf{H}^* . We will show that the outputs of this stage satisfy *identifiability up to ancestors* for soft interventions. Finally, as an optional third stage for *hard* interventions, we will enforce the independence statements implied by the hard interventions to update the encoder learned in the previous step. We will show that this refinement recovers the true latent DAG and the latent variables, hence, achieves *perfect identifiability*. Before we explain the details of each stage and establish identifiability results in the following subsections, we first present the common rationale shared between the stages and the key lemmas that make everything work.

5.1 Rationale of LSCALE-I

Sparsity structure. First, recall that the structure of the latent DAG determines the number and sites of the changes in score functions across environments. Specifically, using Lemma 1 for all $i, m \in [n]$ we have

$$\mathbb{E} \left[\left| [s(Z) - s^m(Z)]_i \right| \right] \neq 0 \iff i \in \overline{\text{pa}}(I^m). \quad (43)$$

6. Some examples include *generic interventions* in Squires et al. (2023), *no pure shift interventions* condition in Buchholz et al. (2023), and the *genericity condition* in von Kügelgen et al. (2023).

Algorithm 1 Linear Score-based Causal Latent Estimation via Interventions (LSCALE-I)

- 1: **Input:** Samples of X from environment \mathcal{E}^0 and environment set \mathcal{E}
- 2: Compute score differences: $(s_X - s_X^m)$ for all $m \in [n]$
- 3: **Stage L1:** Apply Algorithm 2 (Identifiability up to causal order)
- 4: **Stage L2:** Apply Algorithm 3 (Identifiability up to ancestors)
- 5: **if** the interventions are hard **then**
- 6: **Stage L3:** Apply Algorithm 4 (Perfect identifiability)
- 7: **end if**
- 8: **Return** $\hat{\mathcal{G}}$ and \hat{Z}

Hence, the expected value $\mathbb{E}[\|s(Z) - s^m(Z)\|]$ is zero for all environments in which neither node i or a child of node i is intervened. Then, taking the summation of this expected value over all these environments, we obtain

$$\sum_{\{m \in [n] : i \notin \text{pa}(I^m)\}} \mathbb{E}\left[\|s(Z) - s^m(Z)\|\right] = 0. \quad (44)$$

This indicates that, for instance, if i is a leaf node in \mathcal{G} , then the sum of $\mathbb{E}[\|s(Z) - s^m(Z)\|]$ over all environments except \mathcal{E}^{I^i} is zero. Subsequently, the key idea for identifying the true encoder is enforcing the estimated latent score differences $(s_{\hat{Z}} - s_{\hat{Z}}^m)$ to have similar structures as the true score differences $(s - s^m)$, e.g., sufficiently many zero entries at appropriate coordinates.

Score differences for linear transformation. For a linear transformation matrix \mathbf{F} , Jacobian $J_{\mathbf{F}}(z)$ is independent of z and equal to matrix \mathbf{F} . Hence, for linear transformation $X = \mathbf{G} \cdot Z$, using Lemma 2 we have

$$s(z) - s^m(z) = \mathbf{G}^\top \cdot [s_X(x) - s_X^m(x)]. \quad (45)$$

Similarly, for a valid encoder \mathbf{H} and $\hat{Z}(X; \mathbf{H}) = \mathbf{H} \cdot X = (\mathbf{H} \cdot \mathbf{G}) \cdot Z$, we have

$$s_{\hat{Z}}(\hat{z}; \mathbf{H}) - s_{\hat{Z}}^m(\hat{z}; \mathbf{H}) = (\mathbf{H}^\dagger)^\top \cdot [s_X(x) - s_X^m(x)] = (\mathbf{H} \cdot \mathbf{G})^{-\top} \cdot [s(z) - s^m(z)]. \quad (46)$$

Then, for a valid encoder \mathbf{H} and set $\mathcal{A} \subseteq [n]$, the latent score difference under \mathbf{H} becomes

$$\sum_{m \in \mathcal{A}} \mathbb{E}\left[\|s_{\hat{Z}}(\hat{Z}; \mathbf{H}) - s_{\hat{Z}}^m(\hat{Z}; \mathbf{H})\|\right] = \sum_{m \in \mathcal{A}} \mathbb{E}\left[\|[(\mathbf{H}^\dagger)^\top]_i \cdot [s_X(x) - s_X^m(x)]\|\right] \quad (47)$$

$$= \sum_{m \in \mathcal{A}} \mathbb{E}\left[\|[\mathbf{H} \cdot \mathbf{G}]_i^{-\top} \cdot [s(z) - s^m(z)]\|\right]. \quad (48)$$

Subsequently, to find an encoder \mathbf{H} that makes the estimated latent scores conform to a causal structure as in (44), we investigate finding the associated decoder \mathbf{H}^\dagger by analyzing equation (48).

Observation. Consider the following question: by choosing a non-zero vector $b \in \mathbb{R}^n$, for how many environments \mathcal{E}^m we can make $\mathbb{E}[b^\top \cdot [s(Z) - s^m(Z)]] = 0$? The answer lies in the following observation, which is an immediate result of Lemma 1. To formalize the answer, for set $\mathcal{A} \subseteq [n]$, we define $I^{\mathcal{A}} \triangleq \{I^m : m \in \mathcal{A}\}$ as the set of nodes intervened environments $\{\mathcal{E}^m : m \in \mathcal{A}\}$.

Lemma 3 (Score Difference Rank) *For any set $\mathcal{A} \subseteq [n]$, we have*

$$|\mathcal{A}| \leq \mathcal{R}(\{s - s^m : m \in \mathcal{A}\}) \leq |\overline{\text{pa}}(I^{\mathcal{A}})|. \quad (49)$$

Furthermore, if $I^{\mathcal{A}}$ is ancestrally closed, i.e., $\text{an}(I^{\mathcal{A}}) \subseteq I^{\mathcal{A}}$, the inequalities become equalities, i.e.,

$$|\mathcal{A}| = \mathcal{R}(\{s - s^m : m \in \mathcal{A}\}) = |\overline{\text{pa}}(I^{\mathcal{A}})|. \quad (50)$$

Proof: See Appendix B.1.

Lemma 3 implies that a non-zero vector b can make $\mathbb{E}[b^T \cdot [s(Z) - s^m(Z)]] = 0$ for at most $(n-1)$ values of $m \in [n]$, since rank of the set of score differences should be less than n for existence of such vector b . Also note that if i is a leaf node in \mathcal{G} , then $\mathbb{E}[[s(Z) - s^m(Z)]_i]$ is zero for all $m \in [n]$ except $m = I^i$. Hence, by finding a vector $b \in \mathbb{R}^n$ that makes $\mathbb{E}[b^T \cdot [s(Z) - s^m(Z)]] = 0$ for all except one environment $m \in [n]$, we can effectively identify an environment in which a leaf node is intervened. We start from this simple observation to establish the following result.

Lemma 4 (Score Difference Rank under Ancestral Closedness) *Consider set $\mathcal{A} \subseteq [n]$ such that $I^{\mathcal{A}} \triangleq \{I^m : m \in \mathcal{A}\}$ is ancestrally closed, i.e., $\text{an}(I^{\mathcal{A}}) \subseteq I^{\mathcal{A}}$. Then, under Assumption 1 we have*

$$\mathcal{R}(\{s - s^m : m \in \mathcal{A} \setminus \{k\}\}) = \begin{cases} |\mathcal{A}|, & \text{if } \exists j \in \mathcal{A} \setminus \{k\} \text{ such that } I^k \in \text{pa}(I^j) \\ |\mathcal{A}| - 1, & \text{otherwise} \end{cases}. \quad (51)$$

Proof: See Appendix B.2.

The importance of this result is that, given an ancestrally closed set, it guides us to identify the *youngest* nodes that do not have any children within the set. We leverage this key property in the subsequent algorithm steps, starting with obtaining a causal order.

5.2 Identifiability up to Causal Order

In our analysis, finding a valid causal order among the environments is crucial for recovering the latent variables and the latent graph. First, note that since the set $\mathcal{I}^{[n]} = [n]$ is ancestrally closed, Lemma 4 gives

$$\mathcal{R}(\{s - s^m : m \in [n]\}) = n. \quad (53)$$

Consequently, an encoder cannot simultaneously make the estimated latent score differences equal to zero for all environments. However, this becomes possible if an environment with an intervened leaf node I^k is excluded since Lemma 4 implies

$$\mathcal{R}(\{s - s^m : m \in [n] \setminus \{k\}\}) = n - 1. \quad (54)$$

Otherwise, if I^k is not a leaf node, i.e., it has a descendant among $[n] \setminus \{k\}$, then Lemma 4 implies

$$\mathcal{R}(\{s - s^m : m \in [n] \setminus \{k\}\}) = n. \quad (55)$$

Subsequently, the key idea is sequentially searching for an environment \mathcal{E}^k for which the intervened node I^k has no descendant among the intervened nodes in the remaining environments. Specifically, when considering an ancestrally closed set $\mathcal{V} \subseteq [n]$, we look for an environment \mathcal{E}^k such that the rank of the remaining score differences, $\{s - s^m : m \in \mathcal{V} \setminus \{k\}\}$ will be $|\mathcal{V}| - 1$. As such we can form a causal order in reverse order, i.e., starting from the *youngest* nodes to the *eldest* (root) nodes.

Algorithm 2 Obtain Causal Order

```

1: Input: Samples of  $X$  from environment  $\mathcal{E}^0$  and environment set  $\mathcal{E}$ 
2: Initialize  $\mathbf{A} = \mathbf{0}_{n \times d}$                                       $\triangleright \mathbf{A}$  holds for the estimate of  $(\mathbf{H}^\dagger)^\top$ 
3:  $\mathcal{V}_n = \{1, \dots, n\}$                                           $\triangleright$  remaining unordered set
4: for  $t \in (n, \dots, 1)$  do
5:    $\mathcal{F}_t = \text{im}(\mathbf{G}) \setminus \text{span}(\mathbf{A}_{\pi_{t+1}}^\top, \dots, \mathbf{A}_{\pi_n}^\top)$             $\triangleright$  define the feasible set
6:   for  $k \in \mathcal{V}_t$  do
7:      $c = \min_{a \in \mathcal{F}_t} \sum_{m \in \mathcal{V}_t \setminus \{k\}} \mathbb{E} \left[ \left| a^\top \cdot [s_X(X) - s_X^m(X)] \right| \right]$       (52)
8:     if  $c = 0$  then
9:       Denote a minimizer by  $a^*$  and set  $\mathbf{A}_k^\top = a^*$             $\triangleright$  the intermediate estimate
10:       $\pi_t = k$                                           $\triangleright I^k$  has no ancestors in  $I^{\mathcal{V}_t}$ 
11:       $\mathcal{V}_{t-1} = \mathcal{V}_t \setminus \{\pi_t\}$             $\triangleright$  remove the identified node from unordered set
12:      break
13:    end if
14:  end for
15: end for
16: Return  $\pi$  and  $\mathbf{A}$ 

```

This idea is realized by minimizing the estimated latent score differences as specified in (52). By following this routine, Algorithm 2 finds the *youngest* node among the remaining ones at each step and forms a causal order, denoted by permutation π of $[n]$. The following result shows that this procedure returns a valid causal order.

Lemma 5 (Causal Order) *Under Assumption 1, for permutation π determined by Algorithm 2, the ordered set $I^\pi \triangleq (I^{\pi_1}, \dots, I^{\pi_n})$ is a valid causal order.*

Proof: See Appendix B.3.

Lemma 5 ensures that we can order environments as $(\mathcal{E}^{\pi_1}, \dots, \mathcal{E}^{\pi_n})$ such that the intervened nodes $(I^{\pi_1}, \dots, I^{\pi_n})$ form a valid causal order. This property guides estimating the rows of the encoder sequentially, starting with the leaf and sequentially advancing to the root node(s).

5.3 Identifiability up to Ancestors

After obtaining a valid causal order for the intervened nodes in the environments via Algorithm 2, our next goal is to find ancestors of each node and construct our encoder estimate \mathbf{H}^* that will satisfy mixing consistency up to ancestors. We achieve this objective via Algorithm 3 as follows.

First, we form the ancestrally closed set $\mathcal{V}_i = \{\pi_1, \dots, \pi_i\}$ for each node $i \in [n]$. Note that \mathcal{V}_i contains all ancestors of i and does not contain any descendant of i . Then, for each pair of $(t, j) \in (n-1, \dots, 1) \times (t+1, \dots, n)$, we will check whether t is an ancestor of j in the latent graph by leveraging the results of Lemma 4 for ancestral closedness implications. Algorithm 3 realizes this idea in a similar fashion to obtaining a causal order. Specifically, it minimizes the estimated latent score differences over a set rank of which is determined by whether t is an ancestor of node j , specified in (56). Minimizers of the optimization problem are also used to construct the rows of the encoder estimate \mathbf{H}^* .

Algorithm 3 Minimize Score Variations

1: **Input:** Samples of X from environment \mathcal{E}^0 and environment set \mathcal{E} , and $\{\pi, \mathbf{A}\}$ generated by Algorithm 2

2: Initialize $\hat{\mathcal{G}}$ with empty graph over nodes $\{\pi_1, \dots, \pi_n\}$

3: **for** $t \in (n-1, \dots, 1)$ **do**

4: $\mathcal{V}_t = \{\pi_1, \dots, \pi_t\}$ ▷ form the ancestrally closed set

5: $\mathcal{F}_t = \text{im}(\mathbf{G}) \setminus \text{span}(\mathbf{A}_{\pi_{t+1}}^\top, \dots, \mathbf{A}_{\pi_n}^\top)$ ▷ update the feasible set

6: **for** $j \in (t+1, \dots, n)$ **do**

7: **if** Assumption 2 holds **then** ▷ set for determining whether $\pi_t \rightarrow \pi_j$

8: $\mathcal{M}_{t,j} = \mathcal{V}_j \setminus \{\hat{\text{ch}}(\pi_t) \cup \{\pi_t\}\}$

9: **else**

10: $\mathcal{M}_{t,j} = \mathcal{V}_j \setminus \{\hat{\text{de}}(\pi_t) \cup \{\pi_t\}\}$

11: **end if**

12: $c = \min_{a \in \mathcal{F}_t} \sum_{m \in \mathcal{M}_{t,j}} \mathbb{E} \left[\left| a^\top \cdot [s_X(X) - s_X^m(X)] \right| \right]$ (56)

13: **if** $c = 0$ **then** ▷ update the estimate

14: Denote a minimizer by a^* and set $\mathbf{A}_{\pi_t}^\top = a^*$

15: **else**

16: Add $\pi_t \rightarrow \pi_j$ to $\hat{\mathcal{G}}$

17: **end if**

18: **end for**

19: **end for**

20: Encoder estimate: $\mathbf{H}^* = (\mathbf{A}^\top)^\dagger$

21: **Return** $\hat{\mathcal{G}}$ and \mathbf{H}^*

In our most general result, we show that *for any latent causal model* under Assumption 1, Algorithm 3 achieves the objective of recovering ancestral relationships and satisfies mixing consistency up to ancestors.

Lemma 6 (Identifiability up to Ancestors) *Under Assumption 1, the outputs of Algorithm 1 for soft interventions achieve identifiability up to ancestors. Specifically,*

(C1) *Transitive closures of $\hat{\mathcal{G}}$ and \mathcal{G} are related through a graph isomorphism.*

(C2) *\mathbf{H}^* satisfies mixing consistency up to ancestors. Specifically, $\hat{Z}(X; \mathbf{H}^*) = \mathbf{P}_{\mathcal{I}} \cdot \mathbf{C}_{\text{an}} \cdot Z$ such that diagonal entries of \mathbf{C}_{an} are non-zero and $j \notin \text{an}(i)$ implies $[\mathbf{C}_{\text{an}}]_{i,j} = 0$.*

Proof: See Appendix B.3.

Note that both Lemma 5 and Lemma 6 are valid for soft interventions. Hence, we achieve *identifiability up to ancestors* for soft interventions. We note that these results are tight in the sense that they cannot be improved without making additional assumptions. Specifically, it is shown that Squires et al. (2023, Appendix J) shows that for linear Gaussian models under linear transformations, identifiability beyond mixing up to ancestors is impossible under soft interventions. In the next section, we investigate identifiability via hard interventions.

Algorithm 4 Unmixing Procedure

```

1: Input: Samples of  $X$  from environment  $\mathcal{E}^0$  and environment set  $\mathcal{E}, \pi$  from Algorithm 2 and
    $\mathbf{H}^*$  from Algorithm 3
2: Initialize  $\mathbf{V} = \mathbf{I}_{n \times n}$ 
3: for  $k \in (1, \dots, n)$  do
4:   Initialize  $\mathbf{A} = \mathbf{0}_{(k-1) \times (k-1)}$ 
5:    $\tilde{Z}^{\pi_k} = \mathbf{H}^* \cdot X^{\pi_k}$ 
6:   for  $j \in \{1, \dots, k-1\}$  do
7:      $\tilde{Z}_{\pi_j} = \mathbf{V}_{\pi_j} \cdot \tilde{Z}^{\pi_k}$ 
8:   end for
9:   for  $j, \ell \in \{1, \dots, k-1\}$  do
10:     $\mathbf{A}_{j,\ell} = \text{Cov}(\tilde{Z}_{\pi_j}^{\pi_k}, \tilde{Z}_{\pi_\ell})$ 
11:   end for
12:    $b = \text{Cov}(\tilde{Z}_{\pi_k}^{\pi_k}, [\tilde{Z}_{\pi_1}, \dots, \tilde{Z}_{\pi_{k-1}}])$ 
13:   for  $j \in \{1, \dots, k-1\}$  do
14:      $\mathbf{V}_{\pi_k, \pi_j} = -[\mathbf{A}^{-1} \cdot b]_j$ 
15:   end for
16: end for
17: Update the encoder estimate:  $\mathbf{H}^* = \mathbf{V} \cdot \mathbf{H}^*$ 
18: Latent DAG recovery: Construct  $\hat{\mathcal{G}}$  according to (58).
19: return  $\hat{\mathcal{G}}$  and  $\mathbf{H}^*$ 

```

5.4 Perfect Identifiability via Hard Interventions

Hard interventions (i.e., perfect interventions) are special cases of soft interventions and can be leveraged to establish stronger identifiability guarantees. Specifically, when a hard intervention is applied, node ℓ loses its functional dependence on $\text{pa}(\ell)$. The following statement is a direct result of this additional property exclusive to hard interventions.

Proposition 1 *For the environment \mathcal{E}^m in which node $\ell = I^m$ is hard intervened, we have*

$$Z_\ell^m \perp\!\!\!\perp Z_j^m, \quad \forall j \in \text{nd}(\ell), \quad (57)$$

where $\text{nd}(\ell)$ is the set of non-descendants of ℓ in \mathcal{G} .

This property can be readily verified by noting that based on the Markov property, each variable in a DAG is independent of its non-descendants, given its parents. When node ℓ is hard-intervened, it has no parents, and the statement follows directly.

Motivated by this property of hard interventions, the main idea of Algorithm 4 is to ensure that the estimated latent variables conform to Proposition 1. To this end, we consider \mathbf{H}^* , the encoder estimate of Algorithm 3, and aim to learn an *unmixing* matrix $\mathbf{V} \in \mathbb{R}^{n \times n}$ such that $\mathbf{V} \cdot \mathbf{H}^*$ would satisfy scaling consistency. We achieve this objective as follows.

Note that Proposition 1 provides us with random variable pairs that are supposed to be independent, and the covariance of two independent random variables is necessarily zero. Therefore, in Algorithm 4, we use covariance as a surrogate of independence and estimate the rows of the unmixing matrix \mathbf{V} by making covariances of those random variables pairs zero. Then, we update

the encoder estimate as $\mathbf{H}^* = \mathbf{V} \cdot \mathbf{H}^*$. Finally, for the perfect DAG recovery, we compute the latent score differences under the final encoder estimate and construct the graph $\hat{\mathcal{G}}$ according to Lemma 1 as

$$i \in \{\hat{\text{pa}}(m) \cup \{m\}\} \iff \mathbb{E} \left[\left[[s_{\hat{Z}}(\hat{Z}; \mathbf{H}^*) - s_{\hat{Z}}^m(\hat{Z}; \mathbf{H}^*)]_i \right] \right] \neq 0, \quad (58)$$

In Lemma 7, we show that $\hat{\mathcal{G}}$ is isomorphic to \mathcal{G} and $\hat{Z}(X; \mathbf{H}^*)$ satisfies scaling consistency.

Lemma 7 (Unmixing) *Under Assumption 1, the outputs of Algorithm 1 for hard interventions satisfy*

- (C5) $\hat{\mathcal{G}}$ and \mathcal{G} are related through a graph isomorphism.
- (C6) \mathbf{H}^* satisfies scaling consistency. Specifically, $\hat{Z}(X; \mathbf{H}^*) = \mathbf{P}_{\mathcal{I}} \cdot \mathbf{C}_s \cdot Z$ such that \mathbf{C}_s is a constant diagonal matrix.

Proof: See Appendix B.5.

5.5 Identifiability up to Surrounding Parents

For linear transformations, finally, we consider a class of nonlinear latent causal models so that we can achieve stronger results than transitive closure and mixing up to ancestors while still using soft interventions in Algorithm 3. In particular, we specify one condition on the rank of the score function differences ($s - s^m$), formalized next.

Assumption 2 (Full-rank Score Difference) *For all interventional environments $\mathcal{E}^m \in \mathcal{E}$ we have*

$$\mathcal{R}(s - s^m) = |\overline{\text{pa}}(I^m)|. \quad (59)$$

For insight into this assumption, it can be readily verified that for linear Gaussian latent models $\mathcal{R}(s - s^m) \leq 2$ and on the other hand, for sufficiently nonlinear causal models, $\mathcal{R}(s - s^m)$ is $\overline{\text{pa}}(I^m)$. This assumption is stronger than Assumption 1 since it implies that the effects of an intervention on *all* parents of the target variable are different. We will provide more discussions on this assumption in Section 5.7.

Similarly to the discussion in Section 5.3, Algorithm 3 considers each pair $(t, j) \in (n-1, \dots, 1) \times (t+1, \dots, n)$. However, instead of checking whether t is an ancestor of j , under Assumption 2, we directly check whether t is a parent of j . This is realized by a minor change in the algorithm – minimizing the score variations over the environment set with indices $\mathcal{M}_{t,j} = \mathcal{V}_j \setminus \{\hat{\text{ch}}(\pi_t) \cup \{\pi_t\}\}$. Subsequently, we show that Algorithm 3 recovers the true latent DAG up to an isomorphism and identifies the latent variables up to mixing with only surrounding variables. Hence, we achieve stronger identifiability guarantees for sufficiently nonlinear causal models under soft interventions, summarized next.

Lemma 8 (Identifiability up to Surrounding Parents) *Under Assumption 2, the outputs of Algorithm 1 for soft interventions satisfy*

- (C3) $\hat{\mathcal{G}}$ and \mathcal{G} are related through a graph isomorphism.
- (C4) \mathbf{H}^* satisfies mixing consistency up to surrounding parents. Specifically, $\hat{Z}(X; \mathbf{H}^*) = \mathbf{P}_{\mathcal{I}} \cdot \mathbf{C}_{\text{sur}} \cdot Z$ such that diagonal entries of \mathbf{C}_{sur} are non-zero and $j \notin \text{sur}(i)$ implies $[\mathbf{C}_{\text{sur}}]_{i,j} = 0$. Furthermore, $\hat{Z}(X; \mathbf{H}^*)$ is Markov with respect to $\hat{\mathcal{G}}$.

Proof: See Appendix B.4.

5.6 Summarizing Identifiability and Achievability Results

In this section, we summarize the results derived alongside the algorithms in the previous subsections. We will also discuss the relevance and distinctions of our results vis-à-vis the results in the existing literature. Our first result for the linear transformation setting establishes that identifiability up to ancestors, defined in Definition 5, is possible by using one soft intervention per node under the general latent causal models.

Theorem 1 (Linear – Soft Interventions for General SCMs) *Under Assumption 1 for linear transformations, using observational data and interventional data from one soft intervention per node suffice to identify (i) the transitive closure of the latent DAG \mathcal{G} and (ii) the latent variables Z with mixing consistency up to ancestors. Specifically, Algorithm 1 achieves these identifiability guarantees.*

Proof: Under Assumption 1, Lemma 5 shows that Algorithm 2 returns a permutation π such that I^π is a causal order. Given such π , Lemma 6 shows that Algorithm 3 outputs satisfy transitive closure recovery and mixing consistency up to ancestors. Hence, Algorithm 1 achieves the identifiability guarantees for soft interventions stated in Theorem 1. \square

We note that the existing literature on CRL with linear transformations and one soft intervention requires the latent causal model to be either linear Gaussian (Squires et al., 2023; Buchholz et al., 2023) or satisfy nonlinearity conditions (Zhang et al., 2023)⁷. In contrast, Theorem 1 achieves transitive closure recovery and mixing consistency up to ancestors without imposing any restrictions on the latent causal model.

Next, we investigate the conditions under which soft interventions are guaranteed to achieve identifiability results stronger than transitive closure and mixing up to ancestors. The next theorem tightens the identifiability and achievability guarantees of Theorem 1 under Assumption 2.

Theorem 2 (Linear – Soft Interventions for Nonlinear SCMs) *Under Assumption 2 for linear transformations, using observational data and interventional data from one soft intervention per node suffice to identify (i) the latent DAG \mathcal{G} and (ii) the latent variables Z with mixing consistency up to surrounding parents. Specifically, Algorithm 1 achieves these identifiability guarantees.*

Proof: Assumption 2 is strictly stronger than Assumption 1. Hence, Lemma 5 is valid and Algorithm 2 returns a permutation π such that I^π is a causal order. Given such π and Assumption 2, Lemma 8 shows that Algorithm 3 outputs satisfy perfect DAG recovery and mixing consistency up to surrounding parents. Hence, Algorithm 1 achieves the identifiability guarantees for soft interventions stated in Theorem 2. \square

Theorem 2 has two important implications. First, the latent DAG can be identified using *only* soft interventions under mild nonlinearity assumptions on the latent causal model. To our knowledge, this is the first result in the literature for fully recovering latent DAG with soft interventions without restricting the graphical structure, e.g., Zhang et al. (2023) require *linear faithfulness* assumption to achieve similar results, which is only shown to hold for nonlinear latent models with polytree structure. Secondly, the estimated latent variables reveal the true conditional independence relationships since they satisfy the Markov property with respect to the estimated latent DAG, which is isomorphic to the true DAG. Recalling that the motivation of CRL is learning useful representations that preserve causal relationships, our result shows that it can be achieved without perfect identifiability for a

7. The “linear interventional faithfulness” (Zhang et al., 2023, Assumption 2) implies nonlinearity, which we elaborate in Appendix D.3.

large class of models. Furthermore, Jin and Syrgkanis (2023, Theorem 6) establish that under some non-degeneracy assumptions that are similar to our Assumption 2, mixing consistency up to surrounding parents is the best possible result when using single-node soft interventions. Hence, Theorem 2 results are tight for the considered setting.

Finally, we investigate hard interventions for general latent causal models. The major consequence of applying hard versus soft interventions is that the variations in the latent distributions caused by hard interventions are, in general, stronger than those caused by soft interventions. The reason is that the intervention target is not necessarily isolated from its parents under a soft intervention. Consequently, the identifiability guarantees for hard interventions are usually stronger. The final theorem for the linear transformations establishes that scaling consistency and perfect DAG recovery are possible by using one hard intervention per node. Furthermore, the score-based algorithms presented in this section guarantee achieving these perfect recovery objectives specified in Definition 4.

Theorem 3 (Linear – Hard Interventions) *Under Assumption 1 for linear transformations, using observational data and interventional data from one hard intervention per node suffice to identify (i) the latent DAG \mathcal{G} and (ii) the latent variables Z with scaling consistency. Specifically, Algorithm 1 achieves these identifiability guarantees.*

Proof: Note that under Assumption 1, Lemmas 5 and 6 hold for both soft and hard interventions. Therefore, by Theorem 1, inputs of Algorithm 4 satisfy identifiability up to ancestors. Subsequently, Lemma 7 shows that outputs of Algorithm 4, i.e., Stage L3 of Algorithm 1 satisfy perfect DAG recovery and scaling consistency. \square

Similar to the restrictions in the existing results for soft interventions, the identifiability results for hard interventions in the existing literature restrict the latent causal model, e.g., to linear Gaussian models (Squires et al., 2023; Buchholz et al., 2023). In contrast, Theorem 3 does not impose any restriction on the latent causal model and shows that one stochastic hard intervention per node is sufficient for the identifiability of general latent causal models.

5.7 Discussion on Assumptions 1 and 2

In this subsection, we elaborate on Assumptions 1 and 2, which are relevant to Theorems 1 and 2, respectively. Assumption 1 essentially states that score changes in the coordinates of the intervened node and a parent of the intervened node are linearly independent. This property holds for (but is not limited to) the widely adopted additive noise models specified in (7) when we apply hard interventions.

Lemma 9 *Assumption 1 is satisfied for additive noise models under hard interventions.*

Proof: See Appendix D.1.

When soft interventions are applied, we note that even partial identifiability is shown to be impossible without making assumptions about the effect of the interventions. Specifically, for linear latent causal models, Buchholz et al. (2023) prove impossibility results for pure shift interventions and Squires et al. (2023) show that a *genericity condition* is necessary for identifying the transitive closure of the latent DAG. Therefore, Assumption 1 can be interpreted as the counterpart of the commonly adopted assumptions in the literature on soft interventions adapted to the setting of general latent causal models. Finally, the next example demonstrates the working of Assumption 1 on a linear Gaussian latent model.

Example 1 Consider a linear Gaussian latent model with $Z \sim \mathcal{N}(0, \Sigma)$. Score function of Z is given by $s(z) = -\Sigma^{-1} \cdot z$. Let $Z_i = \mathbf{w} \cdot Z_{\text{pa}(i)} + N_i$ where $N_i \sim \mathcal{N}(0, \sigma_i^2)$ for the node i . Consider an intervention on node i on environment \mathcal{E}^m such that $Z_i^m = \bar{\mathbf{w}} \cdot Z_{\text{pa}(i)}^m + \bar{N}_i$, where $Z_m \sim \mathcal{N}(0, \bar{\Sigma})$, and $\bar{N}_i \sim \mathcal{N}(0, \bar{\sigma}_i^2)$, which yields $s(z) - s^m(z) = -(\Sigma^{-1} - \bar{\Sigma}^{-1}) \cdot z$. Then, for a node $k \in \text{pa}(i)$, we obtain

$$[s(z) - s^m(z)]_i = \left(\frac{1}{\sigma_i^2} - \frac{1}{\bar{\sigma}_i^2} \right) z_i - \left(\frac{\mathbf{w}}{\sigma_i^2} - \frac{\bar{\mathbf{w}}}{\bar{\sigma}_i^2} \right) z_{\text{pa}(i)}, \quad (60)$$

$$[s(z) - s^m(z)]_k = - \left(\frac{w_k}{\sigma_i^2} - \frac{\bar{w}_k}{\bar{\sigma}_i^2} \right) z_i + \left(w_k \frac{\mathbf{w}}{\sigma_i^2} - \bar{w}_k \frac{\bar{\mathbf{w}}}{\bar{\sigma}_i^2} \right) z_{\text{pa}(i)}, \quad (61)$$

where w_k and \bar{w}_k correspond to weights of the parent Z_k in observational and interventional models, respectively. Note that, for Assumption 1 to be violated, there must exist a constant $\kappa \in \mathbb{R}$ such that

$$\kappa \cdot [s(z) - s^m(z)]_i = [s(z) - s^m(z)]_k, \quad \forall z \in \mathbb{R}^n. \quad (62)$$

However, using (60) and (61), this is possible if and only if $w_k = \bar{w}_k$. Therefore, if the weight of the node $k \in \text{pa}(i)$ changes, Assumption 1 is satisfied for the node pair (i, k) .

Given the known result that perfect identifiability is impossible for linear Gaussian models given soft interventions (Squires et al., 2023), the purpose of Assumption 2 is to get more insight into the extent of identifiability guarantees under soft interventions. Intuitively, the mentioned impossibility results for linear Gaussian models are due to the rank deficiency of score differences for linear models – specifically, we know that $\mathcal{R}(s - s^m) \leq 2$ for linear Gaussian models. In contrast, for sufficiently nonlinear causal models, $\mathcal{R}(s - s^m)$ can be as high as $\overline{\text{pa}}(I^m)$. Assumption 2 ensures that this upper bound is satisfied with equality for all nodes. This condition holds for the class of sufficiently nonlinear models, such as quadratic causal models. In particular, we show that this condition holds for the two-layer neural networks (NNs) as a function class that can effectively approximate any continuous function. This result is formalized in the next lemma.

Lemma 10 Consider the additive model in (7) where f_i is a two-layer NN with sigmoid activation function, and weight matrices \mathbf{W}^i and $\bar{\mathbf{W}}^i$ for observational and interventional mechanisms, respectively. If $\max\{\text{rank}(\mathbf{W}^i), \text{rank}(\bar{\mathbf{W}}^i)\} = |\text{pa}(i)|$ for all $i \in [n]$, then Assumption 2 holds.

We discuss the nonlinearity and the proof of Lemma 10 in Appendix D.2.

6. CRL under General Transformations

In this setting, we consider general transformations without any parametric assumption for transformation g . In the previous section, we exploited the transformation's linearity and recovered the true encoder's parameters sequentially using *one* intervention per node. For general transformations (parametric or non-parametric), however, we cannot use the same parametric approach and rely on the properties of linear transforms. To rectify these and design the general CRL algorithm, we use more information in the form of *two* interventions per node. Specifically, we will present the steps of leveraging the score functions under two interventions and build an algorithm that will identify the true encoder and recover the true causal representations. The algorithm is referred to as **General Score-based Causal Latent Estimation via Interventions (GSCALE-I)**, which will be summarized in Algorithm 5.

Inputs. The inputs of GSCALE-I are the observed data from the observational environment, the data from two interventional environments per node, whether environments are coupled/uncoupled, and a set of valid encoders \mathcal{H} . Two sets of interventional environments are denoted by $\mathcal{E} = \{\mathcal{E}^1, \dots, \mathcal{E}^n\}$ and $\tilde{\mathcal{E}} = \{\tilde{\mathcal{E}}^1, \dots, \tilde{\mathcal{E}}^n\}$, as defined in Section 3.3. For these inputs, we compute the score functions $s_X, \{s_X^1, \dots, s_X^n\}$ and $\{\tilde{s}_X^1, \dots, \tilde{s}_X^n\}$. Note that we will use Lemma 2 again to ensure access to the latent score differences by using these observed score functions.

Statistical diversity. For being more informative than a single intervention mechanism, we assume that the two intervention mechanisms per node are sufficiently distinct. This is formalized by defining *interventional discrepancy* (Liang et al., 2023) among the causal mechanisms of a latent variable.

Definition 6 (Interventional Discrepancy) *Two intervention mechanisms with pdfs $p, q : \mathbb{R} \rightarrow \mathbb{R}$ are said to satisfy interventional discrepancy if*

$$\frac{\partial}{\partial u} \frac{p(u)}{q(u)} \neq 0, \quad \forall u \in \mathbb{R} \setminus \mathcal{T}, \quad (63)$$

where \mathcal{T} is a null set (i.e., has a zero Lebesgue measure).

This condition ensures that the two distributions are sufficiently distinct, formally expressed as the partial derivative of their ratio with respect to the intervened variable is nonzero almost everywhere. For instance, two univariate distinct Gaussians trivially satisfy this discrepancy condition. As shown by Liang et al. (2023), even when the latent graph \mathcal{G} is known, for identifiability via one intervention per node, it is necessary to have interventional discrepancy between observational distribution p_i and interventional distribution q_i , for all $z_{\text{pa}(i)} \in \mathbb{R}^{|\text{pa}(i)|}$.

6.1 Rationale of GSCALE-I

The core tool for identifiability via the GSCALE-I algorithm is that among all valid encoders $h \in \mathcal{H}$, the true encoder g^{-1} results in the minimum number of variations between the score estimates $s_{\hat{Z}}^m(\hat{z}; h)$ and $\tilde{s}_{\hat{Z}}^m(\hat{z}; h)$, as we will show in Lemma 11 shortly. To formalize these, corresponding to each valid encoder $h \in \mathcal{H}$, we define score change matrices $\mathbf{D}_t(h)$, $\mathbf{D}(h)$, and $\tilde{\mathbf{D}}(h)$ as follows. For all $i, m \in [n]$:

$$[\mathbf{D}_t(h)]_{i,m} \triangleq \mathbb{E} \left[\left| [s_{\hat{Z}}^m(\hat{Z}; h) - \tilde{s}_{\hat{Z}}^m(\hat{Z}; h)]_i \right| \right], \quad (64)$$

$$[\mathbf{D}(h)]_{i,m} \triangleq \mathbb{E} \left[\left| [s_{\hat{Z}}(\hat{Z}; h) - s_{\hat{Z}}^m(\hat{Z}; h)]_i \right| \right], \quad (65)$$

$$[\tilde{\mathbf{D}}(h)]_{i,m} \triangleq \mathbb{E} \left[\left| [s_{\hat{Z}}(\hat{Z}; h) - \tilde{s}_{\hat{Z}}^m(\hat{Z}; h)]_i \right| \right], \quad (66)$$

where expectations are under the measures of latent score functions induced by the probability measure of observational data. The entry $[\mathbf{D}_t(h)]_{i,m}$ will be strictly positive only when there is a set of samples X with a strictly positive measure that renders non-identical scores $s_{\hat{Z}}^m(\hat{z}; h)$ and $\tilde{s}_{\hat{Z}}^m(\hat{z}; h)$. Similar properties hold for the entries of $\mathbf{D}(h)$ and $\tilde{\mathbf{D}}(h)$ for the respective score functions.

Sparsity structure. Similarly to LSCALE-I, analyzing GSCALE-I involves minimizing score differences. However, in contrast to linear transformations, estimated and true latent score differences are not always related by a constant matrix for general transformations. To circumvent this issue,

we rely on Lemma 1(iii), i.e., the score difference between coupled interventional environments is one-sparse. Subsequently, the key idea for identifying the encoder is that the number of variances between the score estimates $s_{\hat{Z}}^m(\hat{z}; h)$ and $\tilde{s}_{\hat{Z}}^m(\hat{z}; h)$ is minimized under the true encoder $h = g^{-1}$. To show that, first, we denote the *true* score change matrix by \mathbf{D}_t , which is specified as

$$[\mathbf{D}_t]_{i,m} \triangleq \mathbb{E} \left[\left| [s^m(Z) - \tilde{s}^m(Z)]_i \right| \right], \quad \forall i, m \in [n]. \quad (67)$$

For clarity in the exposition of the ideas, we consider coupled environments here, i.e., $I^m = \tilde{I}^m$ for all $m \in [n]$. Since the only varying causal mechanism across \mathcal{E}^m and $\tilde{\mathcal{E}}^m$ is the intervened node $I^m = \tilde{I}^m$, based on (30) in Lemma 1 we have

$$\mathbb{E} \left[\left| [s^m(Z) - \tilde{s}^m(Z)]_i \right| \right] \neq 0 \iff i = I^m, \quad (68)$$

which implies that $\mathbf{1}\{\mathbf{D}_t\}$ is a permutation matrix, specifically, $\mathbf{1}\{\mathbf{D}_t\} = \mathbf{P}_{\mathcal{I}}^\top$. We show that the number of variations between the score estimates $s_{\hat{Z}}^m(\hat{z}; h)$ and $\tilde{s}_{\hat{Z}}^m(\hat{z}; h)$, i.e., ℓ_0 norm of $\mathbf{D}_t(h)$, cannot be less than the number of variations under the true encoder g^{-1} , that is $n = \|\mathbf{D}_t\|_0$.

Lemma 11 (Score Change Matrix Density) *For every $h \in \mathcal{H}$, the score change matrix $\mathbf{D}_t(h)$ is at least as dense as the score change matrix \mathbf{D}_t associated with the true latent variables,*

$$\|\mathbf{D}_t(h)\|_0 \geq \|\mathbf{D}_t\|_0 = n. \quad (69)$$

Proof: See Appendix C.1.

6.2 Identifying the Encoder

At the first stage of GSCALE-I, we leverage the intermediate result Lemma 11 and identify the encoder via minimizing latent score differences. Depending on the available information about the two intervention sets \mathcal{E} and $\tilde{\mathcal{E}}$, we perform this step in two slightly different ways.

6.2.1 COUPLED ENVIRONMENTS

First, we consider the case of coupled environments, i.e., we are given the information that which two environments share the same intervention target. In this setting, we directly leverage Lemma 11 and solve the following optimization problem

$$\mathcal{P}_1 \triangleq \begin{cases} \min_{h \in \mathcal{H}} & \|\mathbf{D}_t(h)\|_0 \\ \text{s.t.} & \mathbf{D}_t(h) \text{ is a diagonal matrix.} \end{cases} \quad (70)$$

Constraining $\mathbf{D}_t(h)$ to be diagonal enforces that the final estimate \hat{Z} and Z will be related by permutation \mathcal{I} (the intervention order). We select a solution of \mathcal{P}_1 in (70) as our encoder estimate and denote it by h^* .

Algorithm 5 Generalized Score-based Causal Latent Estimation via Interventions (GSCALE-I)

1: **Input:** \mathcal{H} , samples of X from environment \mathcal{E}^0 and environment sets \mathcal{E} and $\tilde{\mathcal{E}}$, `is_coupled`.
 2: Compute score functions: s_X, s_X^m , and \tilde{s}_X^m for all $m \in [n]$.

3: **Stage G1: Identifying the encoder**

4: **if** `is_coupled` **then** ▷ coupled environments
 5: Solve the following and select a solution h^* .

$$\mathcal{P}_1 \triangleq \begin{cases} \min_{h \in \mathcal{H}} \|\mathbf{D}_t(h)\|_0 \\ \text{s.t. } \mathbf{D}_t(h) \text{ is a diagonal matrix} \end{cases}.$$

6: **else** ▷ search for the correct coupling
 7: **for all** permutations π of $[n]$ **do**
 8: Temporarily relabel $\tilde{\mathcal{E}}^m$ to $\tilde{\mathcal{E}}^{\pi_m}$ for all $m \in [n]$, and solve

$$\mathcal{P}_2 \triangleq \begin{cases} \min_{h \in \mathcal{H}} \|\mathbf{D}_t(h)\|_0 \\ \text{s.t. } \mathbf{D}_t(h) \text{ is a diagonal matrix} \\ \mathbf{1}\{\mathbf{D}(h)\} = \mathbf{1}\{\tilde{\mathbf{D}}(h)\} \\ \mathbf{1}\{\mathbf{D}(h)\} \odot \mathbf{1}\{\mathbf{D}^\top(h)\} = \mathbf{I}_{n \times n} \end{cases}.$$

9: If \mathcal{P}_2 is feasible, select a solution h^* and break from the loop.
 10: **end for**
 11: **end if**
 12: Latent estimates: $\hat{Z} = h^*(X)$.
 13: Construct score difference matrix $\mathbf{D}(h^*)$ with entries defined in (64).

14: **Stage G2: Latent DAG recovery**
 15: Construct latent DAG $\hat{\mathcal{G}}$ according to $\hat{\text{pa}}(i) \triangleq \{j \neq i : [\mathbf{D}(h^*)]_{j,i} \neq 0\}, \forall i \in [n]$.
 16: **return** \hat{Z} and $\hat{\mathcal{G}}$.

6.2.2 UNCOUPLED ENVIRONMENTS

In this setting, additionally, we need to determine the correct coupling between the interventional environment sets \mathcal{E} and $\tilde{\mathcal{E}}$. However, this is not a straightforward objective since we cannot readily determine the intervention target in an environment. To circumvent this issue, we solve the problems of finding the correct coupling and minimizing score variations together. Specifically, we iterate through permutations π of $[n]$, and temporarily relabel $\tilde{\mathcal{E}}^m$ to $\tilde{\mathcal{E}}^{\pi_m}$ for all $m \in [n]$ within each iteration. Subsequently, we solve the following optimization problem:

$$\mathcal{P}_2 \triangleq \begin{cases} \min_{h \in \mathcal{H}} \|\mathbf{D}_t(h)\|_0 \\ \text{s.t. } \mathbf{D}_t(h) \text{ is a diagonal matrix} \\ \mathbf{1}\{\mathbf{D}(h)\} = \mathbf{1}\{\tilde{\mathbf{D}}(h)\} \\ \mathbf{1}\{\mathbf{D}(h)\} \odot \mathbf{1}\{\mathbf{D}^\top(h)\} = \mathbf{I}_{n \times n} \end{cases} \quad (71)$$

The constraint $\mathbf{1}\{\mathbf{D}(h)\} = \mathbf{1}\{\tilde{\mathbf{D}}(h)\}$ ensures that a permutation of the correct encoder is a solution to \mathcal{P}_2 if the coupling is correct, and the last constraint ensures that $\mathbf{D}(h)$ does not contain 2-cycles. To prove that solving this problem iteratively for all permutations leads to identifiability, we first show that \mathcal{P}_2 does not admit a solution under an incorrect coupling.

Lemma 12 (Feasibility) *If the coupling is incorrect, i.e., $\pi \neq \mathcal{I}$, the optimization problem \mathcal{P}_2 specified in (71) does not have a feasible solution.*

Proof sketch: See Appendix C.4 for the complete proof. The main intuition is that the constraints of \mathcal{P}_2 cannot be satisfied simultaneously under an incorrect coupling. We prove it by contradiction. We assume that h^* is a solution, hence, $\mathbf{D}_t(h^*)$ is diagonal and $\mathbf{1}\{\mathbf{D}(h)\} = \mathbf{1}\{\tilde{\mathbf{D}}(h)\}$. Then, by scrutinizing the *eldest* mismatched node, we show that $\mathbf{D}(h^*) \cdot \mathbf{D}^\top(h^*)$ cannot be a diagonal matrix, which contradicts the premise that h^* is a feasible solution. Next, we show that the \mathcal{P}_2 admits a solution when the coupling is correct.

Lemma 13 (Existence) *If the coupling is correct, i.e., $\pi = \mathcal{I}$, $h = \pi^{-1} \circ g^{-1}$ is a solution to \mathcal{P}_2 specified in (71), and yields $\|\mathbf{D}_t(h)\|_0 = n$.*

Proof sketch: The proof follows by using Lemma 1(i) and (iii) to show that $h = \pi^{-1} \circ g^{-1}$ satisfies the constraints in \mathcal{P}_2 and minimizes $\|\mathbf{D}_t(h)\|_0$ according to Lemma 11. See Appendix C.5 for the complete proof.

Therefore, combining Lemma 12 and Lemma 13, \mathcal{P}_2 admits a solution if and only if π is the correct coupling, in which case, we select a solution as our encoder estimate and denote it by h^* .

Remark 1 *For the nonparametric identifiability results, having an oracle that solves the functional optimization problems \mathcal{P}_1 and \mathcal{P}_2 in (70) and (71), respectively, is sufficient. Solving these two problems in their most general form requires calculus of variations. These two problems, however, for any desired parameterized family of functions \mathcal{H} (e.g., linear, polynomial, and neural networks), reduce to parametric optimization problems.*

6.3 Latent DAG Recovery

The latent graph recovery for general transformations is similar to that for linear transformations under hard interventions. In particular, we recall that using Lemma 1 for all $i, m \in [n]$ we have

$$\mathbb{E}\left[\left| [s(Z) - s^m(Z)]_i \right| \right] \neq 0 \iff i \in \overline{\text{pa}}(I^m), \quad (72)$$

or, equivalently,

$$\text{pa}(i) \triangleq \{j \neq i : [\mathbf{D}(g^{-1})]_{j,i} \neq 0\}, \quad \forall i \in [n]. \quad (73)$$

Therefore, after solving either of \mathcal{P}_1 or \mathcal{P}_2 , we use the learned encoder to estimate latent variables as $\hat{Z} = h^*(X)$ and construct the score difference matrix $\mathbf{D}(h^*)$ with entries defined in (64). Subsequently, we construct $\hat{\mathcal{G}}$ via the parent sets as follows

$$\hat{\text{pa}}(i) \triangleq \{j \neq i : [\mathbf{D}(h^*)]_{j,i} \neq 0\}, \quad \forall i \in [n]. \quad (74)$$

6.4 Summarizing Identifiability and Achievability Results

In this section, we establish the identifiability guarantees associated with the GSCALE-I algorithm. We also present additional results and discuss the role of various inputs and the distinction of our results compared to the existing literature. Our first result for general transformations establishes that perfect identifiability is possible given two coupled atomic intervention sets.

Theorem 4 (General – Coupled Environments) *Using observational data and interventional data from two uncoupled hard environments for which the pair (q_i, \tilde{q}_i) satisfies interventional discrepancy for all $i \in [n]$, suffice to identify (i) the latent DAG \mathcal{G} and (ii) the latent variables Z in the sense of perfect recovery in Definition 4. Specifically, Algorithm 5 achieves these identifiability guarantees.*

Proof Sketch: The complete proof is given in Appendix C.2. In short, Lemma 11 establishes the lower bound for ℓ_0 norm of $\mathbf{D}_t(h)$ for any encoder h . Building on this result, we show that any solution h^* to \mathcal{P}_1 specified in (70) satisfies $\mathbf{1}\{J_{\phi_{h^*}}^{-1}(z)\} = \mathbf{P}_{\mathcal{I}}^\top$ for all $z \in \mathbb{R}^n$. This will imply that each entry of $\hat{Z}(X; h^*)$ is a function of a single latent variable Z_i , i.e., perfect latent recovery specified in (20). Finally, using Lemma 1(i) we show that DAG $\hat{\mathcal{G}}$ constructed using $\mathbf{D}(h^*)$ is isomorphic to the true latent DAG \mathcal{G} . For the complete proof, see .

Next, we shed light on the role of observational data. In the proof of Theorem 4, we also show that the advantage of environment coupling is that it renders interventional data sufficient for perfect latent recovery, and the observational data is only used for recovering the graph. We further tighten this result by showing that for DAG recovery, the observational data becomes unnecessary when we have additive noise models and a weak faithfulness condition holds.

Theorem 5 (No Observational Data) *Using interventional data from two coupled hard environments for which the pair (q_i, \tilde{q}_i) satisfies interventional discrepancy for all $i \in [n]$, suffices to perfectly recover the latent variables. Specifically, Stage G1 of Algorithm 5 achieves this objective. Furthermore, if the latent causal model has additive noise, $p(Z)$ is twice differentiable and satisfies the adjacency-faithfulness, the latent DAG is also identifiable.*

Proof sketch: The recovery of latent variables follow similarly to that in Theorem 4. For the recovery of latent DAG, we leverage Lemma 1(iv) under the additive noise assumption. Specifically, using the score difference between environments \mathcal{E}^i and $\tilde{\mathcal{E}}^j$, we obtain $\bar{p}(i, j)$ for all $i, j \in [n], i \neq j$. Then, we perform at most n conditional independence tests to identify $p(i)$ for all $i \in [n]$. For the complete proof, see Appendix C.3.

Finally, we present our strongest result for general transformations. We show that Algorithm 5 achieves perfect identifiability given two atomic environment sets, even when the environments corresponding to the same node are not specified in pairs. That is, not only is it unknown what node is intervened in an environment, additionally the learner also does not know which two environments intervene on the same node.

Theorem 6 (General – Uncoupled Environments) *Using observational data and interventional data from two uncoupled hard environments for which each pair in $\{p_i, q_i, \tilde{q}_i\}$ satisfies interventional discrepancy, suffice to identify (i) the latent DAG \mathcal{G} and (ii) the latent variables Z in the sense of perfect recovery in Definition 4. Specifically, Algorithm 5 achieves these identifiability guarantees.*

Proof sketch: Lemmas 12 and 13 collectively prove Theorem 6 identifiability as follows. We search over the permutations of $[n]$ until \mathcal{P}_2 admits a solution h^* . By Lemma 12, the existence of this

solution means that coupling is correct. Note that when the coupling is correct, the constraint set of \mathcal{P}_1 is a subset of the constraints in \mathcal{P}_2 . Furthermore, the minimum value of $\|\mathbf{D}_t(h)\|_0$ is lower bounded by n (Lemma 11), which is achieved by the solution h^* (Lemma 13). Hence, h^* is also a solution to \mathcal{P}_1 , and by Theorem 4, it satisfies perfect recovery of the latent DAG and the latent variables. See Appendix C.6 for the detailed proof.

Theorem 6 shows that using observational data enables us to resolve any mismatch between the uncoupled environment sets and shows identifiability in the setting of uncoupled environments. This generalizes the identifiability result of von Kügelgen et al. (2023), which requires coupled environments. Importantly, Theorem 6 does not require faithfulness whereas the study in (von Kügelgen et al., 2023) requires that the estimated latent distribution is faithful to the associated candidate graph for all $h \in \mathcal{H}$. Even though a faithfulness assumption does not compromise the identifiability result, it is a strong requirement to verify and poses challenges to devising recovery algorithms. In contrast, we only require observational data, which is generally accessible in practice.

Finally, we note that Theorem 6 requires slightly stronger interventional discrepancy conditions than Theorem 4. In particular, when environments are coupled, we only need (q_i, \tilde{q}_i) to satisfy the interventional discrepancy. On the other hand, to find the correct coupling while performing CRL, Theorem 6 requires each of the pairs $\{(q_i, \tilde{q}_i), (p_i, q_i), (p_i, \tilde{q}_i)\}$ satisfy interventional discrepancy.

6.5 Intervention Extrapolation without CRL

So far, we have studied learning the latent causal representations using the data from single-node interventional environments. A related research problem is extrapolating to unseen combinations of interventions. Namely, given a set of interventions $\mathcal{I} = \{I^1, \dots, I^k\}$, it is desired to emulate the data from an unseen combination of these interventions, e.g., accessing multi-node interventional data using only the single-node interventional data. This is especially important in domains where interventions can be costly or not viable, e.g., not all combinations of different drugs can be clinically tested. Causal representation learning literature has also taken an interest in this problem. Specifically, Zhang et al. (2023, Theorem 3) show for polynomial transformations that given interventions $\mathcal{I} = \{I^1, \dots, I^k\}$, one can sample from any intervention $I \subseteq \mathcal{I}$ after learning the latent representations. We argue that extrapolation to unseen combinations of interventions can be achieved on the observed space *without performing CRL* for the general transformations.

Consider two single-node interventional environments, \mathcal{E}^1 and \mathcal{E}^2 . Without loss of generality, suppose that $I^1 = \{1\}$ and $I^2 = \{2\}$. Also consider the observational environment \mathcal{E}^0 with $I^0 = \emptyset$ and the *unseen* double-node interventional environment \mathcal{E}^m with $I^m = \{1, 2\}$. First, using the score function decompositions in (18) and (19), we have

$$s(z) = \nabla_z \log p_1(z_1 | z_{\text{pa}(1)}) + \nabla_z \log p_2(z_2 | z_{\text{pa}(2)}) + \sum_{k=3}^n \nabla_z \log p_k(z_k | z_{\text{pa}(k)}) , \quad (75)$$

$$s^1(z) = \nabla_z \log q_1(z_1 | z_{\text{pa}(1)}) + \nabla_z \log p_2(z_2 | z_{\text{pa}(2)}) + \sum_{k=3}^n \nabla_z \log p_k(z_k | z_{\text{pa}(k)}) , \quad (76)$$

$$s^2(z) = \nabla_z \log p_1(z_1 | z_{\text{pa}(1)}) + \nabla_z \log q_2(z_2 | z_{\text{pa}(2)}) + \sum_{k=3}^n \nabla_z \log p_k(z_k | z_{\text{pa}(k)}) , \quad (77)$$

$$s^m(z) = \nabla_z \log q_1(z_1 | z_{\text{pa}(1)}) + \nabla_z \log q_2(z_2 | z_{\text{pa}(2)}) + \sum_{k=3}^n \nabla_z \log p_k(z_k | z_{\text{pa}(k)}) . \quad (78)$$

Then, we have

$$(s^1(z) - s(z)) + (s^2(z) - s(z)) = s^m(z) - s(z). \quad (79)$$

Next, recall that Corollary 1 gives us the relationship for going from the latent score differences to observed score differences. Applying it to observed X in environment pairs $(\mathcal{E}^1, \mathcal{E}^0)$, $(\mathcal{E}^2, \mathcal{E}^0)$, and $(\mathcal{E}^m, \mathcal{E}^0)$, and using (79) we obtain

$$(s_X^1(x) - s_X(x)) + (s_X^2(x) - s_X(x)) = \left[[J_g(z)]^\dagger \right]^\top \cdot \left[(s^1(z) - s(z)) + (s^2(z) - s(z)) \right] \quad (80)$$

$$= \left[[J_g(z)]^\dagger \right]^\top (s^m(z) - s(z)) \quad (81)$$

$$\stackrel{\text{Cor. 1}}{=} s_X^m(x) - s_X(x). \quad (82)$$

This means that, given score functions of observed data from environments \mathcal{E}^0 , \mathcal{E}^1 , and \mathcal{E}^2 , we can obtain the score function of the unseen interventional environment with $I^m = \{I^1, I^2\}$, and subsequently generate data from this synthetic environment (using techniques like Langevin Sampling (Welling and Teh, 2011) that uses score function as the drift vector field). Note that this process does not require learning the latent causal representations, and can be applied to obtain the observed score function s_X^m for any intervention $I^m \subset \mathcal{I}$.

7. Empirical Evaluations

In this section, we provide empirical assessments of the achievability guarantees. Specifically, we empirically evaluate the performance of the LSCALE-I (Section 7.1) and GSCALE-I (Section 7.2) algorithms for recovering the latent causal variables Z and the latent DAG \mathcal{G} on synthetic data. We also apply GSCALE-I on image data to demonstrate the potential of our approach in realistic datasets (Section 7.3). Finally, we note that any desired score estimators can be modularly incorporated into our algorithms. In Section 7.4, we assess the sensitivity of our performance to the quality of the estimators.⁸ Additional results and further implementation details are deferred to Appendix E.

Evaluation metrics. The objectives are recovering the graph \mathcal{G} and the latent variables Z . We use the following metrics to evaluate the accuracy of LSCALE-I and GSCALE-I for recovering these (depending on the specifics of the transformations and interventions, we will have more specific metrics as well). For each metric, we will report the mean and standard error over multiple runs.

- **Structural Hamming distance:** For assessing the recovery of the latent DAG, we report structural Hamming distance (SHD) between the estimate $\hat{\mathcal{G}}$ and true DAG \mathcal{G} . This captures the number of edge operations (add, delete, flip) needed to transform $\hat{\mathcal{G}}$ to \mathcal{G} .
- **Mean correlation coefficient:** For the recovery of the latent variables, we use mean correlation coefficient (MCC), which was introduced in (Khemakhem et al., 2020b) and commonly used as a standard metric in CRL. Specifically, MCC measures linear correlations between the estimated and ground truth latent variables. Since the recovery of latent variables is up to permutations, it

8. The codebase for the algorithms and simulations are available at:
<https://github.com/acarturk-e/score-based-crl>.

is reported for the best matching permutation between the components of \hat{Z} and Z , i.e.,

$$\text{MCC}(Z, \hat{Z}) \triangleq \max_{\pi} \frac{1}{n} \sum_{i \in [n]} \text{corr}(Z_i, \hat{Z}_{\pi(i)}) . \quad (83)$$

Score functions. LSCALE-I and GSCALE-I algorithms, in their first steps, compute estimates of the score differences in the observational environment. The designs of our algorithms are agnostic to how this is performed, i.e., any reliable method for estimating the score differences can be adopted and incorporated into our algorithms in a modular way. In our experiments, we adopt two score estimators necessary for describing the different aspects of the identifiability and achievability results.

- **Perfect score oracle for identifiability:** Identifiability, by definition, refers to the possibility of recovering the causal graph and latent variables under all idealized assumptions for the data. Assessing the identifiability guarantees formalized in Theorems 1–6 requires using *perfect* estimates for the score differences. Hence, we adopt a perfect score oracle for evaluating identifiability. Specifically, We use a perfect score oracle that computes the score differences in Step L1 of LSCALE-I and Step G1 of GSCALE-I by leveraging Lemma 2 and using the ground truth score functions s, s^m and \tilde{s}^m (see Appendix E.1 for details).
- **Data-driven score estimates for achievability:** For evaluating the accuracy of our algorithms in practice, we need real score estimates, which are inevitably noisy. For this purpose, when the pdf p_X has a parametric form and score function s_X has a closed-form expression, then we can estimate the parameters to form an estimated score function. For instance, when X follows a linear Gaussian distribution, then we have $s_X(x) = -\Theta \cdot x$ in which Θ is the precision matrix of X and can be estimated from samples of X . In other cases in which s_X does not have a known closed-form, we adopt non-parametric score estimators. In particular, we use sliced score matching with variance reduction (SSM-VR) for score estimation due to its efficiency and accuracy for downstream tasks (Song et al., 2020). We also introduce a classification-based score difference estimation method, inspired by Gutmann and Hyvärinen (2012, Section 2.1). The key observation is that given two distributions p and q , the optimal minimum cross-entropy classifier for distinguishing the samples from two distributions is the log density ratio function $\log p/q$. The difference between the score functions of these distributions, $\nabla \log p - \nabla \log q = \nabla \log p/q$ is exactly the gradient of the learned function, which enables us to directly estimate score differences using a classifier.

7.1 LSCALE-I Algorithm for Linear Transformations

Data generation. To generate \mathcal{G} , we use Erdős-Rényi model with density 0.5 and $n = 5$ nodes, which is generally the size of the latent graphs considered in CRL literature. We consider target dimension values $d \in \{5, 25, 100\}$ and generate 100 latent graphs for each d value. For the causal mechanisms, we adopt both linear and nonlinear models:

1. **Linear causal model:** We adopt the linear Gaussian model with

$$Z_i = \mathbf{A}_i \cdot Z + N_i , \quad \forall i \in [n] , \quad (84)$$

where $\mathbf{A}_i \in \mathbb{R}^{1 \times n}$ are the rows of the weight matrix \mathbf{A} in which $\mathbf{A}_{i,j} \neq 0$ if and only $j \in \text{pa}(i)$. The non-zero edge weights are sampled from $\text{Unif}(\pm[0.5, 1.5])$, and the noise terms

are zero-mean Gaussian variables with variances σ_i^2 sampled from $\text{Unif}([0.5, 1.5])$. For node i , a hard intervention is given by $Z_i = \bar{N}_i$ where $\mathcal{N}(0, \frac{\sigma_i^2}{4})$, and a soft intervention is given by $Z_i = \frac{\bar{\mathbf{A}}_i}{2} \cdot Z + N_i$.

2. **Quadratic causal model:** We adopt an additive noise model with

$$Z_i = \sqrt{Z_{\text{pa}(i)}^\top \cdot \mathbf{Q}_i \cdot Z_{\text{pa}(i)}} + N_i, \quad (85)$$

where $\{\mathbf{Q}_i : i \in [n]\}$ are positive-definite matrices, and the noise terms are zero-mean Gaussian variables with variances σ_i^2 sampled randomly from $\text{Unif}([0.5, 1.5])$. For node i , a hard intervention is given by $Z_i = \bar{N}_i$ where $\mathcal{N}(0, \frac{\sigma_i^2}{4})$, and a soft intervention is given by $Z_i = \frac{1}{2} \sqrt{Z_{\text{pa}(i)}^\top \cdot \mathbf{Q}_i \cdot Z_{\text{pa}(i)}} + N_i$.

For each graph, we sample n_s independent and identically distributed (i.i.d.) samples of Z from each environment. We consider $n_s \in \{5000, 10000, 50000\}$ to investigate the effect of the number of samples on the performance of LSCALE-I. The observed variables X are generated according to $X = \mathbf{G} \cdot Z$, in which $\mathbf{G} \in \mathbb{R}^{d \times n}$ is randomly sampled full-rank matrix.

Implementation of the algorithm steps. We solve the optimization problems (52) of Algorithm 2 and (56) of Algorithm 3 by finding null spaces of the covariance matrices of the observed score difference functions. The details of this implementation are provided in Appendix E.1.

7.1.1 HARD INTERVENTIONS

Theorem 3 ensures scaling consistency and perfect DAG recovery under hard interventions for linear transformations. As such, we assess the recovery of the latent DAG by the SHD between the estimate $\hat{\mathcal{G}}$ and true graph \mathcal{G} . For the recovery of the latent variables, we report MCC between \hat{Z} and Z . Note that, scaling consistency for linear transformations also allows us to directly measure the closeness of \hat{Z} to Z . To this end, we also report the normalized ℓ_2 loss,

$$\ell(Z, \hat{Z}) \triangleq \frac{\|Z - \hat{Z}\|_2}{\|Z\|_2}. \quad (86)$$

Table 3 shows the performance of the LSCALE-I algorithm using perfect scores and noisy scores under hard interventions on linear causal models. The first observation is that we have excellent performance at latent variable recovery, demonstrated by perfect MCC and nearly perfect normalized ℓ_2 loss, even when using noisy score estimates. For graph recovery, SHD between the estimated and true latent graphs reduces to approximately 0.1 even when using noisy scores given enough samples, e.g., $n_s = 50000$ in Table 3. Another key observation is that the results remain consistent while the dimension of observed variables increases from $d = 5$ to $d = 100$. This confirms our analysis that the performance of LSCALE-I is agnostic to the dimension of the observations. We defer the additional results on hard interventions, e.g. for $n = 8$ latent variables and using quadratic latent models, to Appendix E.2.

7.1.2 SOFT INTERVENTIONS

For evaluating soft interventions, we first consider linear causal models. In this setting, Theorem 1 ensures the recovery of the latent variables and the latent DAG up to ancestors when using soft

Table 3: LSCALE-I for a linear causal model with **one hard** intervention per node ($n = 5$).

n	d	n_s	perfect scores			noisy scores		
			MCC	$\ell(Z, \hat{Z})$	$\text{SHD}(\mathcal{G}, \hat{\mathcal{G}})$	MCC	$\ell(Z, \hat{Z})$	$\text{SHD}(\mathcal{G}, \hat{\mathcal{G}})$
5	5	5000	1.00 ± 0.00	0.01 ± 0.00	0.23 ± 0.05	1.00 ± 0.00	0.02 ± 0.00	1.55 ± 0.13
5	25	5000	1.00 ± 0.00	0.01 ± 0.00	0.33 ± 0.06	1.00 ± 0.00	0.02 ± 0.00	1.58 ± 0.12
5	100	5000	1.00 ± 0.00	0.01 ± 0.00	0.42 ± 0.06	1.00 ± 0.00	0.02 ± 0.00	1.61 ± 0.12
5	5	10000	1.00 ± 0.00	0.01 ± 0.00	0.28 ± 0.05	1.00 ± 0.00	0.02 ± 0.00	0.74 ± 0.10
5	25	10000	1.00 ± 0.00	0.01 ± 0.00	0.12 ± 0.03	1.00 ± 0.00	0.02 ± 0.00	1.02 ± 0.11
5	100	10000	1.00 ± 0.00	0.01 ± 0.00	0.30 ± 0.06	1.00 ± 0.00	0.02 ± 0.00	0.74 ± 0.10
5	5	50000	1.00 ± 0.00	0.01 ± 0.00	0.05 ± 0.02	1.00 ± 0.00	0.01 ± 0.00	0.11 ± 0.03
5	25	50000	1.00 ± 0.00	0.01 ± 0.00	0.02 ± 0.01	1.00 ± 0.00	0.01 ± 0.00	0.08 ± 0.03
5	100	50000	1.00 ± 0.00	0.01 ± 0.00	0.07 ± 0.03	1.00 ± 0.00	0.01 ± 0.00	0.23 ± 0.05

Table 4: LSCALE-I for a linear causal model with **one soft** intervention per node ($n = 5$).

n	d	n_s	perfect scores			noisy scores		
			MCC	$\ell_{\text{an}}(Z, \hat{Z})$	$\text{SHD}(\mathcal{G}_{\text{tc}}, \hat{\mathcal{G}}_{\text{tc}})$	MCC	$\ell_{\text{an}}(Z, \hat{Z})$	$\text{SHD}(\mathcal{G}_{\text{tc}}, \hat{\mathcal{G}}_{\text{tc}})$
5	5	5000	0.90 ± 0.01	0.00 ± 0.00	0.00 ± 0.00	0.82 ± 0.01	1.58 ± 0.15	2.16 ± 0.18
5	25	5000	0.90 ± 0.01	0.00 ± 0.00	0.00 ± 0.00	0.82 ± 0.01	1.41 ± 0.16	1.90 ± 0.18
5	100	5000	0.89 ± 0.01	0.00 ± 0.00	0.00 ± 0.00	0.80 ± 0.01	1.57 ± 0.15	2.09 ± 0.17
5	5	10000	0.90 ± 0.01	0.00 ± 0.00	0.00 ± 0.00	0.82 ± 0.01	1.14 ± 0.12	1.51 ± 0.15
5	25	10000	0.92 ± 0.01	0.00 ± 0.00	0.00 ± 0.00	0.82 ± 0.01	0.96 ± 0.13	1.30 ± 0.14
5	100	10000	0.92 ± 0.01	0.00 ± 0.00	0.00 ± 0.00	0.81 ± 0.01	1.14 ± 0.13	1.70 ± 0.17
5	5	50000	0.91 ± 0.01	0.00 ± 0.00	0.00 ± 0.00	0.88 ± 0.01	0.13 ± 0.05	0.15 ± 0.06
5	25	50000	0.92 ± 0.01	0.00 ± 0.00	0.00 ± 0.00	0.88 ± 0.01	0.19 ± 0.06	0.22 ± 0.08
5	100	50000	0.90 ± 0.01	0.00 ± 0.00	0.00 ± 0.00	0.90 ± 0.01	0.09 ± 0.06	0.10 ± 0.06

interventions. So, we report the SHD between the transitive closure of the estimate $\hat{\mathcal{G}}_{\text{tc}}$ and that of the true graph \mathcal{G}_{tc} . For assessing the recovery of latent variables, we note that Z_i can be recovered up to mixing with all its ancestors. Specifically, $\hat{Z} = (\mathbf{H} \cdot \mathbf{G}) \cdot Z$, in which $[\mathbf{H} \cdot \mathbf{G}]_{I^i, j} = 0$ for all $j \notin \overline{\text{an}}(i)$. In this case, MCC is not guaranteed to be 1 even if the partial recovery guarantees are perfectly met. Therefore, in addition to MCC, we also report the average number of *incorrect mixing components*, i.e., the number of (i, j) pairs such that $j \notin \overline{\text{an}}(i)$ and $[\mathbf{H} \cdot \mathbf{G}]_{I^i, j} \geq \eta$ for some small threshold η , which we set to 0.1.

$$\ell_{\text{an}}(Z, \hat{Z}) \triangleq \sum_{j \notin \overline{\text{an}}(i)} \mathbf{1}([\mathbf{H} \cdot \mathbf{G}]_{i, j} \geq \eta) \quad (87)$$

Table 4 shows that by using perfect scores from as few as $n_s = 5000$ samples, we meet the partial identifiability guarantees, implied by zero values of SHD and incorrect mixing metrics. Similar to the case of hard interventions, we observe that increasing the number of samples significantly improves the performance under noisy scores. For instance, given $n_s = 50000$ samples, the average SHD between the transitive closures $\hat{\mathcal{G}}_{\text{tc}}$ and \mathcal{G}_{tc} is approximately 0.2, and the average number of incorrect mixing components is approximately 0.2. Furthermore, MCC under perfect and noisy score settings become almost equal at approximately 0.90.

Table 5: LSCALE-I for a quadratic causal model with **one soft** intervention per node ($n = 5$).

n	d	n_s	perfect scores			noisy scores		
			MCC	$\ell_{\text{sur}}(Z, \hat{Z})$	$\text{SHD}(\mathcal{G}, \hat{\mathcal{G}})$	MCC	$\ell_{\text{sur}}(Z, \hat{Z})$	$\text{SHD}(\mathcal{G}, \hat{\mathcal{G}})$
5	5	5000	0.94 ± 0.01	0.06 ± 0.04	0.13 ± 0.04	0.85 ± 0.01	7.48 ± 0.24	7.56 ± 0.19
5	25	5000	0.93 ± 0.01	0.04 ± 0.02	0.09 ± 0.03	0.86 ± 0.01	7.10 ± 0.21	7.41 ± 0.20
5	100	5000	0.93 ± 0.01	0.09 ± 0.05	0.11 ± 0.04	0.86 ± 0.01	6.55 ± 0.18	7.14 ± 0.22
5	5	10000	0.93 ± 0.01	0.03 ± 0.02	0.12 ± 0.04	0.86 ± 0.01	5.62 ± 0.27	6.78 ± 0.29
5	25	10000	0.93 ± 0.01	0.06 ± 0.03	0.14 ± 0.04	0.85 ± 0.01	5.32 ± 0.28	6.32 ± 0.34
5	100	10000	0.93 ± 0.01	0.01 ± 0.01	0.08 ± 0.03	0.85 ± 0.01	5.72 ± 0.26	6.64 ± 0.29
5	5	50000	0.93 ± 0.01	0.02 ± 0.02	0.09 ± 0.03	0.85 ± 0.01	5.40 ± 0.16	5.87 ± 0.19
5	25	50000	0.94 ± 0.01	0.05 ± 0.03	0.12 ± 0.03	0.86 ± 0.01	5.52 ± 0.15	6.43 ± 0.16
5	100	50000	0.93 ± 0.01	0.06 ± 0.04	0.11 ± 0.04	0.87 ± 0.01	5.07 ± 0.17	6.28 ± 0.19

Next, we consider quadratic causal models specified in (85). In this case, Assumption 2 is satisfied, and Theorem 2 ensures the perfect recovery of the latent DAG, and the recovery of the latent variables up to surrounding variables. Hence, we report SHD between true \mathcal{G} and estimate $\hat{\mathcal{G}}$, and the incorrect mixing components for this setting given by

$$\ell_{\text{sur}}(Z, \hat{Z}) \triangleq \sum_{j \notin \text{sur}(i)} \mathbb{1}([\mathbf{H} \cdot \mathbf{G}]_{i,j} \geq \eta), \quad \text{set } \eta = 0.1. \quad (88)$$

Table 5 shows that when using perfect scores, LSCALE-I performs nearly perfectly, verifying the results of Theorem 2. A difference in this setting compared to the linear causal models is that we estimate the score functions of the observed variables using SSM-VR since p_X is not amenable to parameter estimation. When using noisy scores, we still have strong latent variable recovery indicated by MCC over 0.85. For incorrect mixing entries, note that the number of entries in an effective mixing matrix $\mathbf{H} \cdot \mathbf{G}$ is $n^2 = 25$, hence, $\ell_{\text{sur}} < 6$ also indicates a strong performance. On the other hand, the performance at the graph recovery is relatively weaker, demonstrating the effect of noisy scores, which we elaborate on more later in the sequel.

7.2 GSCALE-I Algorithm for General Transformations

Next, we focus on nonlinear transformations to showcase the settings for which the existing literature lacks achievability results and provides only identifiability results. In particular, we focus on quadratic causal models under a nonlinear transformation.

To generate \mathcal{G} we use the Erdős-Rényi model with density 0.5 and $n = 5$ nodes. For observational causal mechanisms, we use (85) and the parameterization therein. For the two hard interventions on node i , Z_i is set to $N_{q,i} \sim \mathcal{N}(0, \sigma_{q,i}^2)$ and $N_{\bar{q},i} \sim \mathcal{N}(0, \sigma_{\bar{q},i}^2)$, where we set $\sigma_{q,i}^2 = \sigma_i^2 + 1$ and $\sigma_{\bar{q},i}^2 = \sigma_i^2 + 2$. We consider target dimension values $d \in \{5, 25, 100\}$, and for each d value, we generate 100 latent graphs and $n_s = 30000$ samples per graph.

Choice of nonlinearity and evaluation metrics. As the transformation, we first consider a generalized linear model,

$$X = g(Z) = \tanh(\mathbf{G} \cdot Z), \quad (89)$$

in which \tanh is applied element-wise, and parameter $\mathbf{G} \in \mathbb{R}^{d \times n}$ is a randomly sampled full-rank matrix. By being a relatively simple nonlinear transform, this setting allows us to evaluate the

Table 6: GSCALE-I for a quadratic causal model with **two coupled hard** interventions per node ($n = 5$) when using $n_s = 300$ samples. Noisy scores are obtained using SSM-VR with $n_{\text{score}} = 30000$ samples.

n	d	perfect scores			noisy scores		
		MCC	$\ell(Z, \hat{Z})$	$\text{SHD}(\mathcal{G}, \hat{\mathcal{G}})$	MCC	$\ell(Z, \hat{Z})$	$\text{SHD}(\mathcal{G}, \hat{\mathcal{G}})$
5	5	1.00 ± 0.00	0.02 ± 0.00	0.06 ± 0.03	0.71 ± 0.01	1.04 ± 0.07	5.45 ± 0.41
5	25	1.00 ± 0.00	0.04 ± 0.01	0.04 ± 0.04	0.75 ± 0.74	0.74 ± 0.04	5.10 ± 0.34
5	100	1.00 ± 0.00	0.04 ± 0.01	0.02 ± 0.02	0.73 ± 0.01	0.86 ± 0.05	5.00 ± 0.32

performance of GSCALE-I better (for more general transformations, see experiments on images in Section 7.3). Specifically, leveraging (89), we parameterize valid encoders h with parameter $\mathbf{H} \in \mathbb{R}^{n \times d}$, which gives

$$\hat{Z}(X; h) = h(X) = \mathbf{H} \cdot \text{arctanh}(X) , \quad (90)$$

$$\hat{X} = h^{-1}(\hat{Z}(X; h)) = \tanh\left(\mathbf{H}^\dagger \cdot \hat{Z}(X; h)\right) , \quad (91)$$

$$\hat{Z} = \phi_h(Z) = \mathbf{H} \cdot \mathbf{G} \cdot Z . \quad (92)$$

Hence, the only element-wise diffeomorphism between Z and \hat{Z} is an element-wise scaling. Then, we can evaluate the estimated latent variables against the scaling consistency objective. This simplification has two benefits. First, we can still use the normalized ℓ_2 error metric specified in (86). Second, recall that for general transformations, we can only guarantee $\hat{Z}_i = \phi_i(Z_i)$ for a diffeomorphism ϕ_i . However, $\text{MCC}(Z_i, \phi(Z_i))$ can largely deviate from 1 for nonlinear ϕ_i . For instance, for $Z_i \sim \mathcal{N}(0, 1)$ and $\phi(Z_i) = Z_i^3 + 0.1Z_i$, we have $\text{MCC}(Z_i, \phi(Z_i)) \approx 0.786$. On the other hand, when we use the parameterization in (90), MCC remains a perfectly informative metric. To learn parameters \mathbf{H} of h , we adapt the objective in (70) and minimize

$$\text{loss}_{\text{score}} = \|\mathbf{D}_t(h) - \mathbf{I}_{n \times n}\|_{1,1} \quad (93)$$

that is the sum of absolute entries, computed with empirical expectations. We also add proper regularization terms to ensure that the estimated parameter \mathbf{H} will be full-rank.

Observations. Table 6 shows that by using perfect scores, we can almost perfectly recover the latent variables and the latent DAG for $n = 5$ nodes. We also observe that increasing dimension d of the observational data does not degrade the performance (as was the case for LSCALE-I), confirming our analysis that GSCALE-I is agnostic to the dimension of observations.

The effect of the quality of score estimation. When using noisy scores, the performance of GSCALE-I degrades significantly, for instance, MCC goes down to approximately 0.73. This degradation is similar to what happens when using LSCALE-I on quadratic causal models in Table 5. It is noteworthy that the transition from perfect to noisy scores is remarkably smoother when using LSCALE-I on linear causal models (Tables 3 and 4). This discrepancy is attributed to the distinct score estimation procedures adopted in the two experiment settings. Specifically, linear Gaussian latent models allow us to directly estimate the parameters of the closed-form score function s_X . However, when using a quadratic latent model, we rely on a nonparametric score estimation via SSM-VR (Song et al., 2020). This comparison between two experiment settings and results underscores

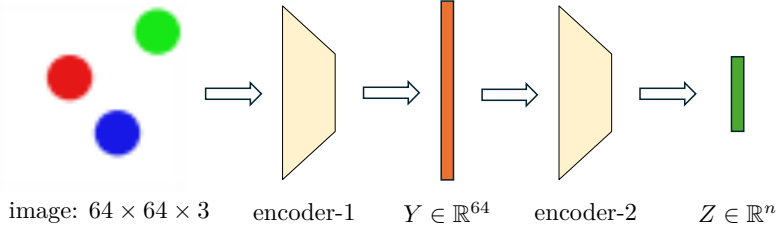


Figure 3: Learning the latent variables from images. Autoencoder-1 is trained to minimize only the reconstruction loss. Autoencoder-2 is trained to minimize the score-based loss in (93) while using the reconstruction loss as regularization.

that the performance gap between the theoretical guarantees and practical results can be significantly mitigated through the advances in general score estimation techniques. In Section 7.4, we provide a further empirical evaluation of how the quality of the score estimation affects the final performance.

7.3 Experiments on Image Data

In this section, we perform experiments on CRL where the general transformation is image rendering, a highly nonlinear transformation, by applying the GSCALE-I algorithm on synthetic image data.

Image data generation. For image-based experiments, we follow the setup of the closely related studies in (Ahuja et al., 2023; Buchholz et al., 2023). Specifically, we consider images of the form in Figure 4, which are generated as follows. The pairs of latent variables (Z_{2i-1}, Z_{2i}) describe the coordinates of the i -th ball’s center in a $64 \times 64 \times 3$ RGB image. We use three balls in our experiments, which corresponds to $n = 6$ latent variables. We sample the latent graph \mathcal{G} from Erdős–Rényi model for 6 nodes and set the expected number of edges to 12. Given this graph \mathcal{G} , we adopt a *truncated* linear Gaussian latent causal model. The details of the linear model are the same as the Section 7.1, with the addition of a second set of interventions represented by the causal mechanisms \tilde{q}_i , by setting $Z_i = \tilde{N}_i$, where $\tilde{N}_i \sim \mathcal{N}(0, \frac{\sigma_i^2}{4})$. Latent variables z are sampled from the distribution defined by this linear model, but samples with any coordinate absolute value greater than 1 are discarded to truncate the distribution in the box $[-1, 1]^6$. For each latent sample z , we render an image of the balls centered at the specified coordinates (shifted and scaled to fit entirely within rendered image boundaries) with a radius of 8 pixels and use these as our observed data x . Balls are color-coded, filled with three different colors, and the background is white. We generate 5 graphs and 10000 samples from each graph under each environment.

Candidate encoder and training. For learning the latent variables, we construct a two-step autoencoder, depicted in Figure 3. Specifically, in step one, we train an autoencoder on the observational image data set with a bottleneck dimension of 64 using only a reconstruction objective. In step two, we train another autoencoder on the 64-dimensional output of the first encoder with the bottleneck dimension of $n = 6$ (the latent dimension) using both reconstruction loss and the score-based loss described earlier in Section 7.2. Architecture details and training schedule are given in Table 7.

Score difference estimation. The main loss function for the second autoencoder of our setup is the score-based loss in (93), $\|\mathbf{D}_t(h) - \mathbf{I}_{n \times n}\|_{1,1}$. For computing $\mathbf{D}_t(h)$ for an encoder h , we need to compute the score differences of image datasets. To this end, we adopt a binary classifier-based log

Table 7: 2-step autoencoder architecture for learning latent representations of images.

Step	Details
Step 1 Encoder	Input: Image $X \in \mathbb{R}^{64 \times 64 \times 3}$ Flatten FC(256), ReLU, LayerNorm FC(64) \triangleright Intermediate representation Y
Step 1 Decoder	FC(256), ReLU, LayerNorm FC($64 \times 64 \times 3$), Sigmoid \triangleright Reconstructed image \hat{X}_c
Autoencoder-1	Training: 100 epochs, Adam optimizer, batch size: 16 Learning rate: 10^{-3} , weight decay: 0.01 Minimize $\mathbb{E}[\ X - \hat{X}_c\ ^2]$ \triangleright recons. loss
Step 2 Encoder	Input: $Y \in \mathbb{R}^{64}$ FC(256), ReLU, LayerNorm FC(6) \triangleright Latent causal variables \hat{Z}
Step 2 Decoder	FC(256), ReLU, LayerNorm FC(64) \triangleright Reconstructed \hat{Y}
Autoencoder-2	Training: 100 epochs, Adam optimizer, batch size: 16, weight decay: 0.01 Learning rate: 0.95 decay/epoch for 75 epochs, reset to 10^{-3} for 25 epochs Minimize $\ \mathbf{D}_t(h) - \mathbf{I}_{n \times n}\ _{1,1} + \lambda \mathbb{E}[\ Y - \hat{Y}\ ^2]$ \triangleright score loss + recons. loss

Table 8: Architecture for LDR (log-density-ratio) model for score-difference estimation.

Layers:	Input: Image $X \in \mathbb{R}^{64 \times 64 \times 3}$, class (intervention) label $y \in \{0, 1\}$ Conv(3, 32, kernel size=3, stride=1, padding=1), ReLU, BatchNorm, Dropout(0.1) MaxPool(kernel size=2, stride=2) Conv(32, 64, kernel size=3, stride=1, padding=1), ReLU, BatchNorm, Dropout(0.1) MaxPool(kernel size=2, stride=2) Flatten, FC(128), ReLU FC(1)
Training:	10 epochs, Adam optimizer, weight decay: 0.01, batch size: 16 Learning rate: 10^{-5} Minimize binary cross entropy between sigmoid of negation of output and labels

density ratio (LDR) estimator and use the gradients of these learned LDRs as our score difference functions as described earlier. Specifically, we parameterize the LDR at any image through a CNN-based model, details of which are given in Table 8. The output of this model is used to compute class probabilities, which is used to minimize cross entropy to train the model. We train one LDR model for each pair of hard interventions on the same node, and one for the observational-interventional environment pairs for one set of hard interventions.

Results. GSCALE-I ensures perfect graph recovery, and latent variables recovery up to permutation and element-wise scaling. Similarly to related work (Ahuja et al., 2023; Buchholz et al., 2023), we report MCC between \hat{Z} and Z as a metric of latent variables recovery. Over 5 different image

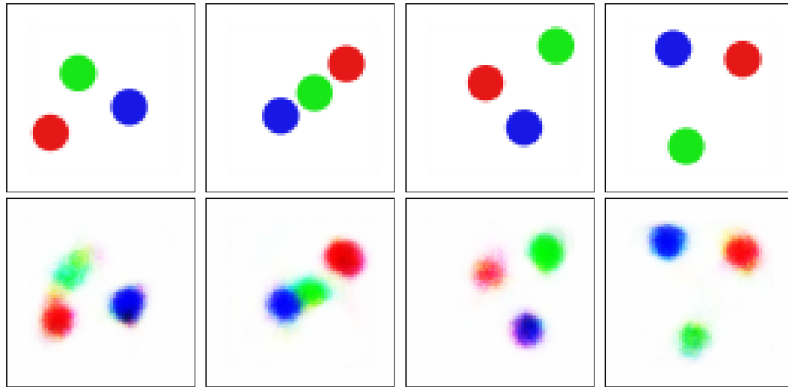


Figure 4: Sample images (top row) versus their reconstructions (bottom row).

datasets, we observe MCC values of

run-1: 0.977	run-2: 0.490	run-3: 0.645	run-4: 0.874	run-5: 0.811	mean: 0.760	std: 0.173
--------------	--------------	--------------	--------------	--------------	-------------	------------

During training, we observed that MCC highly correlates with the reconstruction performance, i.e., when reconstruction errors in both autoencoders converge to small values, latent variable recovery is also successful (e.g., MCC is 0.98 in run-1). We note that the reconstruction does not have to be perfect. For instance, the samples in Figure 4 are from the setting with an MCC of 0.98. Conversely, for the runs with nonconvergent reconstruction loss in either of the autoencoder training steps, latent variable recovery also struggled (e.g., MCC of 0.49 in run-2). Hence, as long as we can ensure reasonable reconstruction performance when we are minimizing the score-based loss, our algorithm manages to disentangle the true causal variables embedded in the latent domain. We discuss these results compared to the related work as follows.

- Ahuja et al. (2023) consider 5 runs on the *same image dataset* of 2 balls. For this setting, they report MCC for linear SCMs when using varying numbers of *do* interventions per node. For instance, for 3 interventions per node, they achieve an MCC of 0.73 and require at least 5 interventions per node to achieve a higher MCC (e.g., 0.85). Therefore, our result with 0.76 average MCC is highly competitive, considering that we use three balls, less restrictive stochastic interventions, and two interventions per node.
- Buchholz et al. (2023) similarly report 5 runs on the *same image dataset* for varying numbers of balls. They report significantly better results than (Ahuja et al., 2023) via using contrastive learning, e.g., MCC of 0.87 for 2 balls and 0.94 for five balls. They also report that some other commonly used methods for CRL, e.g., vanilla variational autoencoder, are not competitive in this setting.

We emphasize that our results on *5 different image datasets* demonstrate the dependence of the performance on the specific dataset, indicated by a standard deviation of 0.17 in MCC. Therefore, our results are not directly comparable to those in the related work which only report results for one dataset. Our goal in this setting is to showcase the potential of our framework on complex non-linear transforms, e.g., image rendering, and we achieve this goal by demonstrating a competitive performance at latent variable recovery.

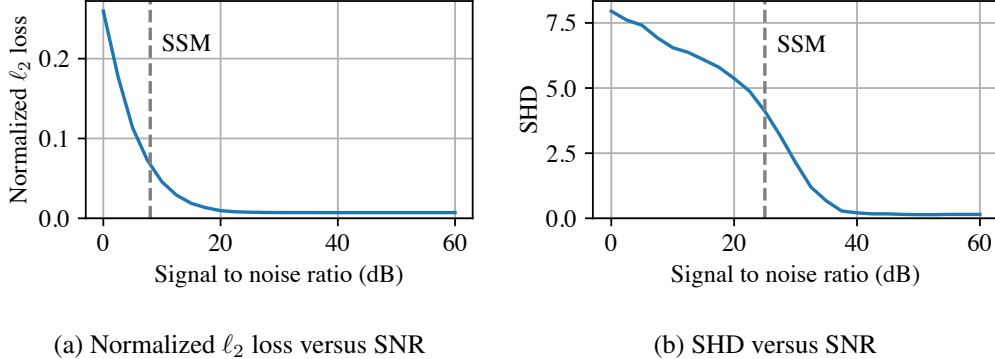


Figure 5: The performance of LSCALE-I under noisy scores with varying SNR for $n = 5$ and $d = 25$. The dashed vertical lines correspond to SNR values that correspond to the performance attained by SSM-VR.

7.4 Sensitivity to Score Estimation Noise

As discussed earlier, score estimators can be modularly incorporated into our algorithm. For the cases where p_X is not amenable to parameter estimation, we can use the noisy score estimates generated by SSM-VR as achievable baselines. In Section 7.3 and Appendix E.2, we follow this procedure for the LSCALE-I algorithm with a quadratic latent causal model specified in (85) and report the results in Table 5 and Table 12, for soft and hard interventions, respectively. In this subsection, we assess how much performance improvement we can have as the score estimates become more accurate. To this end, we test the LSCALE-I algorithm under varying score estimation noise levels. Specifically, we run LSCALE-I algorithm using the scores generated by the following model:

$$\hat{s}_X(x; \sigma^2) = s_X(x) \cdot (1 + \Xi), \quad \text{where } \Xi \sim \mathcal{N}(0, \sigma^2 \cdot \mathbf{I}_{d \times d}). \quad (94)$$

We consider hard interventions on graph size of $n = 5$, set $d = 25$, and vary the value of σ^2 within $[10^{-4}, 10^{-2}]$. We repeat the experiments 100 times with $n_s = 10000$ samples from each environment. We plot the evaluation metrics mean Z error and mean SHD in Figure 5 with respect to the signal-to-noise ratio (SNR). It is clear that when the score estimation error is small, indicated by a high SNR value, LSCALE-I algorithm demonstrates a strong performance in recovering both latent causal variables and the latent graph. We also note that the baseline results with noisy scores computed via SSM-VR in Table 12 yield similar success at graph recovery at the SNR of approximately 25 dB and latent recovery at the SRM of approximately 8 dB. The trend of the curves in Figure 5 indicates that our algorithm would greatly benefit from a better score estimator.

8. Discussion and Concluding Remarks

In this paper, we have proposed a score function-based CRL framework that uses stochastic interventions to learn latent causal representations and the latent causal graph underlying them. In this framework, by uncovering novel connections between score functions and CRL, we have established identifiability results for linear and general transformations without restricting the latent causal models, and designed LSCALE-I and GSCALE-I algorithms that achieve these identifiability guarantees. There are several exciting directions for future work.

As discussed in Section 3.4 after defining the identifiability objectives, and emphasized when presenting the corresponding results through the paper, our results are tight *given a complete set of atomic interventions*. A natural direction for future work is relaxing the atomic intervention requirement. In this aspect, the paper (Varıcı et al., 2024) extends the score-based framework for linear transformations into the setting of unknown multi-node interventions by using combinations of multi-node score differences. Given a sufficiently diverse multi-node intervention set, similar identifiability results to those in Section 5 are shown. That being said, establishing the *necessary* conditions for multi-node interventions and the case of general transformations remains an open problem. In another direction, partial identifiability from an incomplete set of interventions is an underexplored setting, especially for general transformations. Next, we note that our LSCALE-I algorithm for *linear transformations* is agnostic to the intervention type and latent causal model, meaning that it can be used for both soft and hard interventions and different causal models. Designing similar universal CRL algorithms that can handle general transformations under different sizes and types of interventional environments is the ultimate goal for studying the identifiability of CRL from interventions. Finally, a missing component of existing CRL literature is the finite-sample analysis. Probabilistic identifiability results for a given number of interventional data samples can be useful, especially in applications where performing interventions is costly. Hence, it is an exciting future direction to infer partial causal information from a limited number of samples and knowledge about unseen interventions from available interventions.

References

K. Ahuja, J. S. Hartford, and Y. Bengio. Properties from mechanisms: An equivariance perspective on identifiable representation learning. In *Proc. International Conference on Learning Representations*, virtual, April 2022.

K. Ahuja, D. Mahajan, Y. Wang, and Y. Bengio. Interventional causal representation learning. In *Proc. International Conference on Machine Learning*, Honolulu, Hawaii, July 2023.

K. Ahuja, A. Mansouri, and Y. Wang. Multi-domain causal representation learning via weak distributional invariances. In *Proc. International Conference on Artificial Intelligence and Statistics*, Valencia, Spain, May 2024.

S. Bing, U. Ninad, J. Wahl, and J. Runge. Identifying linearly-mixed causal representations from multi-node interventions. In *Proc. Causal Learning and Reasoning*, Los Angeles, CA, April 2024.

W. M. Boothby. *An introduction to differentiable manifolds and Riemannian geometry, Revised*, volume 120. Gulf Professional Publishing, 2003.

J. Brehmer, P. De Haan, P. Lippe, and T. S. Cohen. Weakly supervised causal representation learning. In *Proc. Advances in Neural Information Processing Systems*, New Orleans, LA, December 2022.

S. Buchholz, G. Rajendran, E. Rosenfeld, B. Aragam, B. Schölkopf, and P. Ravikumar. Learning linear causal representations from interventions under general nonlinear mixing. In *Proc. Advances in Neural Information Processing Systems*, New Orleans, LA, December 2023.

G. Cybenko. Approximation by superpositions of a sigmoidal function. *Mathematics of control, signals and systems*, 2(4):303–314, 1989.

M. U. Gutmann and A. Hyvärinen. Noise-contrastive estimation of unnormalized statistical models, with applications to natural image statistics. *Journal of machine learning research*, 13(2), 2012.

H. Hälvä and A. Hyvärinen. Hidden Markov nonlinear ICA: Unsupervised learning from nonstationary time series. In *Proc. Conference on Uncertainty in Artificial Intelligence*, virtual, August 2020.

A. Hyvärinen and H. Morioka. Nonlinear ICA of temporally dependent stationary sources. In *Proc. International Conference on Artificial Intelligence and Statistics*, Ft. Lauderdale, FL, April 2017.

A. Hyvärinen and P. Pajunen. Nonlinear independent component analysis: Existence and uniqueness results. *Neural Networks*, 12(3):429–439, April 1999.

A. Hyvärinen, H. Sasaki, and R. Turner. Nonlinear ICA using auxiliary variables and generalized contrastive learning. In *Proc. International Conference on Artificial Intelligence and Statistics*, Naha, Japan, April 2019.

Y. Jiang and B. Aragam. Learning nonparametric latent causal graphs with unknown interventions. In *Proc. Advances in Neural Information Processing Systems*, New Orleans, LA, December 2023.

J. Jin and V. Syrgkanis. Learning causal representations from general environments: Identifiability and intrinsic ambiguity. *arXiv:2311.12267*, 2023.

I. Khemakhem, D. Kingma, R. Monti, and A. Hyvärinen. Variational autoencoders and nonlinear ICA: A unifying framework. In *Proc. International Conference on Artificial Intelligence and Statistics*, virtual, August 2020a.

I. Khemakhem, R. Monti, D. Kingma, and A. Hyvärinen. Ice-beem: Identifiable conditional energy-based deep models based on nonlinear ICA. In *Proc. Advances in Neural Information Processing Systems*, virtual, December 2020b.

B. Kivva, G. Rajendran, P. Ravikumar, and B. Aragam. Identifiability of deep generative models under mixture priors without auxiliary information. In *Proc. Advances in Neural Information Processing Systems*, New Orleans, LA, December 2022.

S. Lachapelle, P. R. López, Y. Sharma, K. Everett, R. L. Priol, A. Lacoste, and S. Lacoste-Julien. Nonparametric partial disentanglement via mechanism sparsity: Sparse actions, interventions and sparse temporal dependencies. *arXiv:2401.04890*, 2024.

T. E. Lee, J. A. Zhao, A. S. Sawhney, S. Girdhar, and O. Kroemer. Causal reasoning in simulation for structure and transfer learning of robot manipulation policies. In *Proc. IEEE International Conference on Robotics and Automation*, Xi'an, China, May 2021.

Z. Li, Y. Shen, K. Zheng, R. Cai, X. Song, M. Gong, Z. Hao, Z. Zhu, G. Chen, and K. Zhang. On the identification of temporally causal representation with instantaneous dependence. *arXiv:2405.15325*, 2024.

W. Liang, A. Kekić, J. von Kügelgen, S. Buchholz, M. Besserve, L. Gresele, and B. Schölkopf. Causal component analysis. In *Proc. Advances in Neural Information Processing Systems*, New Orleans, LA, December 2023.

P. Lippe, S. Magliacane, S. Löwe, Y. M. Asano, T. Cohen, and E. Gavves. Intervention design for causal representation learning. In *UAI 2022 Workshop on Causal Representation Learning*, Eindhoven, Netherlands, 2022.

P. Lippe, S. Magliacane, S. Löwe, Y. M. Asano, T. Cohen, and E. Gavves. Causal representation learning for instantaneous and temporal effects in interactive systems. In *Proc. International Conference on Learning Representations*, Kigali, Rwanda, May 2023a.

P. Lippe, S. Magliacane, S. Löwe, Y. M. Asano, T. Cohen, and E. Gavves. Biscuit: Causal representation learning from binary interactions. In *Proc. Uncertainty in Artificial Intelligence*, Pittsburgh, PA, August 2023b.

F. Locatello, S. Bauer, M. Lucic, G. Raetsch, S. Gelly, B. Schölkopf, and O. Bachem. Challenging common assumptions in the unsupervised learning of disentangled representations. In *Proc. International Conference on Machine Learning*, Long Beach, CA, June 2019.

F. Locatello, B. Poole, G. Rätsch, B. Schölkopf, O. Bachem, and M. Tschannen. Weakly-supervised disentanglement without compromises. In *Proc. International Conference on Machine Learning*, virtual, April 2020.

F. Montagna, A. A. Mastakouri, E. Eulig, N. Noceti, L. Rosasco, D. Janzing, B. Aragam, and F. Locatello. Assumption violations in causal discovery and the robustness of score matching. In *Proc. Advances in Neural Information Processing Systems*, New Orleans, LA, December 2023a.

F. Montagna, N. Noceti, L. Rosasco, K. Zhang, and F. Locatello. Scalable causal discovery with score matching. In *Proc. Conference on Causal Learning and Reasoning*, Tübingen, Germany, April 2023b.

H. Morioka and A. Hyvärinen. Causal representation learning made identifiable by grouping of observational variables. *arXiv:2310.15709*, 2023.

J. Pearl. *Causality*. Cambridge University Press, Cambridge, UK, 2009.

P. Rolland, V. Cevher, M. Kleindessner, C. Russell, D. Janzing, B. Schölkopf, and F. Locatello. Score matching enables causal discovery of nonlinear additive noise models. In *Proc. International Conference on Machine Learning*, Baltimore, MD, July 2022.

S. Saengkyongam, E. Rosenfeld, P. Ravikumar, N. Pfister, and J. Peters. Identifying representations for intervention extrapolation. In *Proc. International Conference on Learning Representations*, Vienna, Austria, May 2024.

B. Schölkopf, F. Locatello, S. Bauer, N. R. Ke, N. Kalchbrenner, A. Goyal, and Y. Bengio. Toward causal representation learning. *Proceedings of the IEEE*, 109(5):612–634, May 2021.

X. Shen, F. Liu, H. Dong, Q. Lian, Z. Chen, and T. Zhang. Weakly supervised disentangled generative causal representation learning. *Journal of Machine Learning Research*, 23(1):10994–11048, 2022.

R. Shu, Y. Chen, A. Kumar, S. Ermon, and B. Poole. Weakly supervised disentanglement with guarantees. In *Proc. International Conference on Learning Representations*, virtual, May 2020.

L. Simon. Introduction to geometric measure theory. *Tsinghua Lectures*, 2014.

Y. Song, S. Garg, J. Shi, and S. Ermon. Sliced score matching: A scalable approach to density and score estimation. In *Proc. Uncertainty in Artificial Intelligence*, virtual, August 2020.

C. Squires, A. Seigal, S. S. Bhate, and C. Uhler. Linear causal disentanglement via interventions. In *Proc. International Conference on Machine Learning*, Honolulu, Hawaii, July 2023.

N. Sturma, C. Squires, M. Drton, and C. Uhler. Unpaired multi-domain causal representation learning. In *Proc. Advances in Neural Information Processing Systems*, New Orleans, LA, December 2023.

A. Tejada-Lapuerta, P. Bertin, S. Bauer, H. Aliee, Y. Bengio, and F. J. Theis. Causal machine learning for single-cell genomics. *arXiv:2310.14935*, 2023.

B. Varıcı, E. Acartürk, K. Shanmugam, and A. Tajer. Linear causal representation learning from unknown multi-node interventions. *arXiv:2406.05937*, 2024.

B. Varıcı, E. Acartürk, K. Shanmugam, A. Kumar, and A. Tajer. Score-based causal representation learning with interventions. *arXiv:2301.08230*, 2023.

J. von Kügelgen, Y. Sharma, L. Gresele, W. Brendel, B. Schölkopf, M. Besserve, and F. Locatello. Self-supervised learning with data augmentations provably isolates content from style. In *Proc. Advances in Neural Information Processing Systems*, virtual, December 2021.

J. von Kügelgen, M. Besserve, W. Liang, L. Gresele, A. Kekić, E. Bareinboim, D. M. Blei, and B. Schölkopf. Nonparametric identifiability of causal representations from unknown interventions. In *Proc. Advances in Neural Information Processing Systems*, New Orleans, LA, December 2023.

E. W. Weisstein. Sigmoid function. <https://mathworld.wolfram.com/>, 2002.

M. Welling and Y. W. Teh. Bayesian learning via stochastic gradient langevin dynamics. In *Proceedings of the 28th international conference on machine learning (ICML-11)*, pages 681–688. Citeseer, 2011.

D. Yao, D. Rancati, R. Cadei, M. Fumero, and F. Locatello. Unifying causal representation learning with the invariance principle. *arXiv:2409.02772*, 2024a.

D. Yao, D. Xu, S. Lachapelle, S. Magliacane, P. Taslakian, G. Martius, J. von Kügelgen, and F. Locatello. Multi-view causal representation learning with partial observability. In *Proc. International Conference on Learning Representations*, Vienna, Austria, May 2024b.

W. Yao, Y. Sun, A. Ho, C. Sun, and K. Zhang. Learning temporally causal latent processes from general temporal data. In *Proc. International Conference on Learning Representations*, virtual, April 2022.

J. Zhang, C. Squires, K. Greenewald, A. Srivastava, K. Shanmugam, and C. Uhler. Identifiability guarantees for causal disentanglement from soft interventions. In *Proc. Advances in Neural Information Processing Systems*, New Orleans, LA, December 2023.

Z. Zhu, F. Locatello, and V. Cevher. Sample complexity bounds for score-matching: Causal discovery and generative modeling. In *Proc. Advances in Neural Information Processing Systems*, New Orleans, LA, December 2023.

Appendix

Table of Contents

A Proofs of Score Function Properties and Transformations	50
A.1 Proof of Lemma 1	50
A.2 Proof of Lemma 2	53
A.3 Proof of Lemma 14	55
B Proofs of the Results for Linear Transformations	57
B.1 Proof of Lemma 3	57
B.2 Proof of Lemma 4	58
B.3 Proofs of Lemma 5 and Lemma 6	59
B.4 Proof of Lemma 8	63
B.5 Proof of Lemma 7	66
B.6 Proof of Lemma 15	69
C Proofs of the Results for General Transformations	70
C.1 Proof of Lemma 11	70
C.2 Proof of Theorem 4	71
C.3 Proof of Theorem 5	73
C.4 Proof of Lemma 12	75
C.5 Proof of Lemma 13	77
C.6 Proof of Theorem 6	78
D Analysis of the Assumptions	78
D.1 Analysis of Assumption 1	78
D.2 Analysis of Assumption 2	80
D.3 Assumptions of (Zhang et al., 2023)	88
E Empirical Evaluations: Details and Additional Results	89
E.1 Implementation Details of LSCALE-I Algorithm	89
E.2 Additional Results for LSCALE-I	91
E.3 Implementation Details of GSCALE-I Algorithm	92
E.4 Additional Results for GSCALE-I	94

Table 9: Notation.

ground-truth variables	$[n]$	$\{1, \dots, n\}$
	$\mathbf{1}$	indicator function
	\mathcal{G}	latent causal graph over Z
	\mathcal{G}_{tc}	transitive closure of \mathcal{G}
	\mathcal{G}_{tr}	transitive reduction of \mathcal{G}
	$\text{pa}(i)$	parents of node i in \mathcal{G}
	$\text{ch}(i)$	children of node i in \mathcal{G}
	$\text{an}(i)$	ancestors of node i in \mathcal{G}
	$\text{de}(i)$	descendants of node i in \mathcal{G}
	X	$[X_1, \dots, X_d]^{\top}$ observed random variables
intervention notations	Z	$[Z_1, \dots, Z_n]^{\top}$ latent random variables
	$Z_{\text{pa}(i)}$	vector formed by Z_i for all $i \in \text{pa}(i)$
	g	true decoder
	h	a valid encoder
	\mathcal{H}	the set of valid encoders h
	\mathbf{G}	true linear decoder
	\mathbf{H}	a valid linear encoder
	\mathcal{E}^0	observational environment
	\mathcal{E}	$(\mathcal{E}^1, \dots, \mathcal{E}^n)$ first interventional environments
	$\tilde{\mathcal{E}}$	$(\tilde{\mathcal{E}}^1, \dots, \tilde{\mathcal{E}}^n)$ second interventional environments
statistical models	I^m	the intervened nodes in \mathcal{E}^m
	\tilde{I}^m	the intervened nodes in $\tilde{\mathcal{E}}^m$
	\mathcal{I}	the set of intervened nodes (I^1, \dots, I^n)
	$\tilde{\mathcal{I}}$	the set of intervened nodes $(\tilde{I}^1, \dots, \tilde{I}^n)$
	$\hat{Z}(X)$	generic estimator of Z given X
	$\hat{Z}(X; h)$	an auxiliary estimator of Z given X and encoder h
	$\hat{\mathcal{G}}$	estimate of \mathcal{G}
	p, p^m, \tilde{p}^m	pdfs of Z in $\mathcal{E}^0, \mathcal{E}^m$, and $\tilde{\mathcal{E}}^m$
	$p_X, p_X^m, \tilde{p}_X^m$	pdfs of X in $\mathcal{E}^0, \mathcal{E}^m$, and $\tilde{\mathcal{E}}^m$
	s, s^m, \tilde{s}^m	score functions of Z in $\mathcal{E}^0, \mathcal{E}^m$, and $\tilde{\mathcal{E}}^m$
matrix notations	$s_X, s_X^m, \tilde{s}_X^m$	score functions of X in $\mathcal{E}^0, \mathcal{E}^m$, and $\tilde{\mathcal{E}}^m$
	$s_{\hat{Z}}, s_{\hat{Z}}^m, \tilde{s}_{\hat{Z}}^m$	score functions of \hat{Z} in $\mathcal{E}^0, \mathcal{E}^m$, and $\tilde{\mathcal{E}}^m$ for encoder h
	$\hat{\text{pa}}(i)$	parents of node i in $\hat{\mathcal{G}}$
	\mathbf{A}^{\dagger}	Pseudo-inverse of matrix \mathbf{A}
	\mathbf{A}_i	row i of matrix \mathbf{A}
	$\mathbf{A}_{i,j}$	entry of matrix \mathbf{A} at row i and column j
	\mathbf{P}_{π}	Permutation matrix associated with permutation π of $[n]$
	$\mathcal{R}(f)$	$\dim(\text{im}(f))$ for a function f
	$\mathcal{R}(\mathcal{F})$	$\dim(\text{im}(\mathcal{F}))$ for a set of functions \mathcal{F}
	$\mathbf{D}, \tilde{\mathbf{D}}, \mathbf{D}_t$	True score change matrices
	$\mathbf{D}(h), \tilde{\mathbf{D}}(h), \mathbf{D}_t(h)$	Score change matrices under encoder h

Appendix A. Proofs of Score Function Properties and Transformations

We start by providing the following facts that will be used repeatedly in the proofs.

Proposition 2 *Consider two continuous functions $f, g : \mathbb{R}^n \rightarrow \mathbb{R}$ with full support. Then, for any $\alpha > 0$,*

$$\exists z \in \mathbb{R}^n \quad f(z) \neq g(z) \iff \mathbb{E}[|f(Z) - g(Z)|^\alpha] \neq 0. \quad (95)$$

Specifically, for $\alpha = 1$, we have

$$\exists z \in \mathbb{R}^n \quad f(z) \neq g(z) \iff \mathbb{E}[|f(Z) - g(Z)|] \neq 0. \quad (96)$$

Proof: If there exists $z \in \mathbb{R}^n$ such that $f(z) \neq g(z)$, then $f(z) - g(z)$ is non-zero over a non-zero-measure set due to continuity. Then, $\mathbb{E}[|f(Z) - g(Z)|^\alpha] \neq 0$ since p (pdf of Z) has full support. On the other direction, if $f(z) = g(z)$ for all $z \in \mathbb{R}^n$, then $\mathbb{E}[|f(Z) - g(Z)|^\alpha] = 0$. This means that $\mathbb{E}[|f(Z) - g(Z)|^\alpha] \neq 0$ implies that there exists $z \in \mathbb{R}^n$ such that $f(z) \neq g(z)$.

A.1 Proof of Lemma 1

Our score-based methodology builds on the changes in score functions under interventions. For proving Lemma 1, we start by showing that $\mathbb{E}[|[s(Z) - s^m(Z)]_i|] \neq 0 \implies i \in \overline{\text{pa}}(I^m)$, which holds true regardless of the causal model and the intervention type.

Proof of $\mathbb{E}[|[s(Z) - s^m(Z)]_i|] \neq 0 \implies i \in \overline{\text{pa}}(I^m)$: Let ℓ denote the node intervened in \mathcal{E}^m , i.e. $I^m = \ell$. Recalling (18) and (19), the latent scores $s(z)$ and $s^m(z)$ are decomposed as

$$s(z) = \nabla_z \log p_\ell(z_\ell | z_{\text{pa}(\ell)}) + \sum_{i \neq \ell} \nabla_z \log p_i(z_i | z_{\text{pa}(i)}), \quad (97)$$

$$\text{and } s^m(z) = \nabla_z \log q_\ell(z_\ell | z_{\text{pa}(\ell)}) + \sum_{i \neq \ell} \nabla_z \log p_i(z_i | z_{\text{pa}(i)}). \quad (98)$$

Hence, $s(z)$ and $s^m(z)$ differ in only the causal mechanism of node ℓ . Next, we check the derivatives of $p_\ell(z_\ell | z_{\text{pa}(\ell)})$ and $q_\ell(z_\ell | z_{\text{pa}(\ell)})$ in their i -th coordinates. Note that these two depend on Z only through $\{Z_j : j \in \overline{\text{pa}}(\ell)\}$. Therefore, if $i \notin \overline{\text{pa}}(\ell)$,

$$\frac{\partial}{\partial z_i} \log p_\ell(z_\ell | z_{\text{pa}(\ell)}) = \frac{\partial}{\partial z_i} \log q_\ell(z_\ell | z_{\text{pa}(\ell)}) = 0, \quad (99)$$

which indicates that if $i \notin \overline{\text{pa}}(\ell)$, then $[s(z)]_i = [s^m(z)]_i$ for all z . This, equivalently, means that if $\mathbb{E}[|[s(Z) - s^m(Z)]_i|] \neq 0$, then $i \in \overline{\text{pa}}(\ell)$. \square

For the reverse direction, we will use the following intermediate result which formalizes the weakest possible requirement for a meaningful intervention and shows that it is a property of (i) hard interventions under any causal model, and (ii) additive noise model under either soft or hard interventions.

Lemma 14 (Interventional Regularity) *Causal mechanisms p_i and q_i of node i are said to satisfy interventional regularity if*

$$\exists z \in \mathbb{R}^n \text{ such that } \frac{\partial}{\partial z_k} \frac{q_i(z_i | z_{\text{pa}(i)})}{p_i(z_i | z_{\text{pa}(i)})} \neq 0, \quad \forall k \in \text{pa}(i). \quad (100)$$

Then, p_i and q_i satisfy interventional regularity if at least one of the following conditions is true:

1. The intervention is hard, i.e., $q_i(z_i | z_{\text{pa}(i)}) = q_i(z_i)$.
2. The causal model is an additive noise model in which the pdfs of the noise variables are analytic.

Proof: See Appendix A.3.

Case (i) and Case (ii). $\mathbb{E}\left[\left| [s(Z) - s^m(Z)]_i \right| \right] \neq 0 \implies i \in \overline{\text{pa}}(I^m)$ is already shown above. For the reverse direction, we give the proof for soft interventions on additive noise models, Case (ii). We will use interventional regularity since Lemma 14 shows that it is satisfied for additive noise models. The proof for hard interventions, Case (i), follows from similar arguments since interventional regularity is also satisfied for hard interventions by Lemma 14.

Proof of $i \in \overline{\text{pa}}(I^m)$ $\implies \mathbb{E}\left[\left| [s(Z) - s^m(Z)]_i \right| \right] \neq 0$: Note that the two score functions s and s^m are equal in their coordinate $i \in \overline{\text{pa}}(\ell)$ only if

$$0 = \frac{\partial \log q_\ell(z_\ell | z_{\text{pa}(\ell)})}{\partial z_i} - \frac{\partial \log p_\ell(z_\ell | z_{\text{pa}(\ell)})}{\partial z_i} = \frac{\partial}{\partial z_i} \log \frac{q_\ell(z_\ell | z_{\text{pa}(i)})}{p_\ell(z_\ell | z_{\text{pa}(\ell)})}. \quad (101)$$

However, (101) contradicts with interventional regularity. Therefore, if $i \in \overline{\text{pa}}(\ell)$, $[s(z)_i]$ and $[s^m(z)]_i$ are not identical and by Proposition 2, $\mathbb{E}\left[\left| [s(Z) - s^m(Z)]_i \right| \right] \neq 0$.

Case (iii) Coupled environments. Suppose that $I^m = \tilde{I}^m = \ell$. Following (16), we have

$$s^m(z) = \nabla_z \log q_\ell(z_\ell) + \sum_{i \neq \ell} \nabla_z \log p_i(z_i | z_{\text{pa}(i)}), \quad (102)$$

$$\text{and } \tilde{s}^m(z) = \nabla_z \log \tilde{q}_\ell(z_\ell) + \sum_{i \neq \ell} \nabla_z \log p_i(z_i | z_{\text{pa}(i)}). \quad (103)$$

Then, subtracting (103) from (102) and looking at i -th coordinate, we have

$$[s^m(z) - \tilde{s}^m(z)]_i = \frac{\partial \log q_\ell(z_\ell)}{\partial z_i} - \frac{\partial \log \tilde{q}_\ell(z_\ell)}{\partial z_i}. \quad (104)$$

If $i \neq \ell$, the right-hand side is zero and we have $[s^m(z) - \tilde{s}^m(z)]_i = 0$ for all z . On the other hand, if $i = \ell$, since $q_\ell(z_\ell)$ and $\tilde{q}_\ell(z_\ell)$ are distinct, there exists $z \in \mathbb{R}^n$ such that $q_\ell(z_\ell) \neq \tilde{q}_\ell(z_\ell)$. Subsequently, by Proposition 2, we have $\mathbb{E}\left[\left| [s^m(Z) - \tilde{s}^m(Z)]_i \right| \right] \neq 0$.

Case (iv) Uncoupled environments. Suppose that $I^m = \ell$ and $\tilde{I}^m = j$, and $\ell \neq j$. Following (16), we have

$$s^m(z) = \nabla_z \log q_\ell(z_\ell) + \nabla_z \log p_j(z_j | z_{\text{pa}(j)}) + \sum_{k \in [n] \setminus \{\ell, j\}} \nabla_z \log p_k(z_k | z_{\text{pa}(k)}), \quad (105)$$

$$\text{and } \tilde{s}^m(z) = \nabla_z \log q_j(z_j) + \nabla_z \log p_\ell(z_\ell | z_{\text{pa}(\ell)}) + \sum_{k \in [n] \setminus \{\ell, j\}} \nabla_z \log p_k(z_k | z_{\text{pa}(k)}). \quad (106)$$

Then, subtracting (106) from (105) we have

$$s^m(z) - \tilde{s}^m(z) = \nabla_z \log q_\ell(z_\ell) + \nabla_z \log p_j(z_j | z_{\text{pa}(j)}) - \nabla_z \log q_j(z_j) - \nabla_z \log p_\ell(z_\ell | z_{\text{pa}(\ell)}). \quad (107)$$

Scrutinizing the i -th coordinate, we have

$$[s^m(z) - \tilde{s}^m(z)]_i = \frac{\partial \log q_\ell(z_\ell)}{\partial z_i} + \frac{\partial \log p_j(z_j \mid z_{\text{pa}(j)})}{\partial z_i} - \frac{\partial \log q_j(z_j)}{\partial z_i} - \frac{\partial \log p_\ell(z_\ell \mid z_{\text{pa}(\ell)})}{\partial z_i}. \quad (108)$$

Proof of $\mathbb{E}[[s^m(Z) - \tilde{s}^m(Z)]_i] \neq 0 \implies i \in \overline{\text{pa}}(\ell, j)$: Suppose that $i \notin \overline{\text{pa}}(\ell, j)$. Then, none of the terms in the RHS of (108) is a function of z_i . Therefore, all the terms in the RHS of (108) are zero, and we have $[s^m(z) - \tilde{s}^m(z)]_i = 0$ for all z . By Proposition 2, $\mathbb{E}[[s^m(Z) - \tilde{s}^m(Z)]_i] = 0$. This, equivalently, means that if $\mathbb{E}[[s^m(Z) - \tilde{s}^m(Z)]_i] \neq 0$, then $i \in \overline{\text{pa}}(\ell, j)$.

Proof of $\mathbb{E}[[s^m(Z) - \tilde{s}^m(Z)]_i] \neq 0 \iff i \in \overline{\text{pa}}(\ell, j)$: We prove it by contradiction. Assume that $[s^m(z) - \tilde{s}^m(z)]_i = 0$ for all z . Without loss of generality, let $\ell \notin \overline{\text{pa}}(j)$.

1. **If $i = \ell$.** In this case, (108) is simplified to

$$0 = [s^m(z) - \tilde{s}^m(z)]_\ell = \frac{\partial \log q_\ell(z_\ell)}{\partial z_\ell} - \frac{\partial \log p_\ell(z_\ell \mid z_{\text{pa}(\ell)})}{\partial z_\ell}. \quad (109)$$

If ℓ is a root node, i.e., $\text{pa}(\ell) = \emptyset$, (109) implies that $(\log q_\ell)'(z_\ell) = (\log p_\ell)'(z_\ell)$ for all z_ℓ . Integrating, we get $p_\ell(z_\ell) = \alpha q_\ell(z_\ell)$ for some constant α . Since both p_ℓ and q_ℓ are pdfs, they both integrate to one, implying $\alpha = 1$ and $p_\ell(z_\ell) = q_\ell(z_\ell)$, which contradicts the premise that observational and interventional mechanisms are distinct. If ℓ is not a root node, consider some $k \in \text{pa}(\ell)$. Then, taking the derivative of (109) with respect to z_k , we have

$$0 = \frac{\partial^2 \log p_\ell(z_\ell \mid z_{\text{pa}(\ell)})}{\partial z_\ell \partial z_k}. \quad (110)$$

Recall the equation $Z_\ell = f_\ell(Z_{\text{pa}(\ell)}) + N_\ell$ for additive noise models specified in (7). Denote the pdf of the noise term N_ℓ by p_N . Then, the conditional pdf $p_\ell(z_\ell \mid z_{\text{pa}(\ell)})$ is given by $p_\ell(z_\ell \mid z_{\text{pa}(\ell)}) = p_N(z_\ell - f_\ell(z_{\text{pa}(\ell)}))$. Denoting the score function of p_N by r_p ,

$$r_p(u) \triangleq \frac{d}{du} \log p_N(u), \quad (111)$$

we have

$$\frac{\partial \log p_\ell(z_\ell \mid z_{\text{pa}(\ell)})}{\partial z_\ell} = \frac{\partial \log p_N(z_\ell - f_\ell(z_{\text{pa}(\ell)}))}{\partial z_\ell} = r_p(z_\ell - f_\ell(z_{\text{pa}(\ell)})). \quad (112)$$

Substituting this into (110), we obtain

$$0 = \frac{\partial r_p(z_\ell - f_\ell(z_{\text{pa}(\ell)}))}{\partial z_k} = -\frac{\partial f_\ell(z_{\text{pa}(\ell)})}{\partial z_k} \cdot r'_p(z_\ell - f_\ell(z_{\text{pa}(\ell)})), \quad \forall z \in \mathbb{R}^n. \quad (113)$$

Since k is a parent of ℓ , there exists a fixed $Z_{\text{pa}(\ell)} = z_{\text{pa}(\ell)}^*$ realization for which $\partial f_\ell(z_{\text{pa}(\ell)}^*)/\partial z_k$ is non-zero. Otherwise, $f_\ell(z_{\text{pa}(\ell)})$ would not be sensitive to z_k which is contradictory to k being a parent of ℓ . Note that Z_ℓ can vary freely after fixing $Z_{\text{pa}(\ell)}$. Therefore, for (113) to hold, the derivative of r_p must always be zero. However, the score function of a valid pdf with full support cannot be constant. Therefore, $[s^m(z)_i - \tilde{s}^m(z)]_i$ is not always zero, and we have $\mathbb{E}[[s^m(Z) - \tilde{s}^m(Z)]_i] \neq 0$.

2. **If $i \neq \ell$.** In this case, (108) is simplified to

$$0 = [s^m(z) - \tilde{s}^m(z)]_i = \frac{\partial \log p_j(z_j | z_{\text{pa}(j)})}{\partial z_i} - \frac{\partial \log q_j(z_j)}{\partial z_i} - \frac{\partial \log p_\ell(z_\ell | z_{\text{pa}(\ell)})}{\partial z_i}. \quad (114)$$

We investigate case by case and reach a contradiction for each case. First, suppose that $i \notin \text{pa}(\ell)$. Then, we have $i \in \overline{\text{pa}}(j)$, and (114) becomes

$$0 = [s^m(z) - \tilde{s}^m(z)]_i = \frac{\partial \log p_j(z_j | z_{\text{pa}(j)})}{\partial z_i} - \frac{\partial \log q_j(z_j)}{\partial z_i}. \quad (115)$$

If $i = j$, the impossibility of (115) directly follows from the impossibility of (109). The remaining case is $i \in \text{pa}(j)$. In this case, taking the derivative of the right-hand side of (115) with respect to z_j , we obtain

$$0 = \frac{\partial^2 \log p_j(z_j | z_{\text{pa}(j)})}{\partial z_i \partial z_j}, \quad (116)$$

which is a realization of (110) for $i \in \text{pa}(j)$ and j in place of $k \in \text{pa}(\ell)$ and ℓ , which we proved to be impossible in $i = \ell$ case. Therefore, $i \notin \text{pa}(\ell)$ is not viable. Finally, suppose that $i \in \text{pa}(\ell)$. Then, taking the derivative of the right-hand side of (114) with respect to z_ℓ , we obtain

$$0 = \frac{\partial^2 \log p_\ell(z_\ell | z_{\text{pa}(\ell)})}{\partial z_i \partial z_\ell}, \quad (117)$$

which is again a realization of (110) for $k = i$, which we proved to be impossible.

Hence, we showed that $[s^m(z) - \tilde{s}^m(z)]_i$ cannot be zero for all z values. Then, by Proposition 2 we have $\mathbb{E}[|[s^m(Z) - \tilde{s}^m(Z)]_i|] \neq 0$, and the proof is concluded.

A.2 Proof of Lemma 2

Let us recall the setting. Consider random vectors $Y_1, Y_2 \in \mathbb{R}^r$ and $W_1, W_2 \in \mathbb{R}^s$ that are related through $Y_1 = f(W_1)$ and $Y_2 = f(W_2)$ such that $r \geq s$, probability measures of W_1, W_2 are absolutely continuous with respect to the s -dimensional Lebesgue measure and $f : \mathbb{R}^s \rightarrow \mathbb{R}^r$ is an injective and continuously differentiable function.

In this setting, the realizations of W_1 and Y_1 , and that of W_2 and Y_2 , are related through $y = f(w)$. Since f is injective and continuously differentiable, volume element dw in \mathbb{R}^s gets mapped to $|\det([J_f(w)]^\top \cdot J_f(w))|^{1/2} dw$ on $\text{im}(f)$. Since W_1 has density p_{W_1} absolutely continuous with respect to the s -dimensional Lebesgue measure, using the area formula (Boothby, 2003), we can define a density for Y_1 , denoted by p_{Y_1} , supported only on manifold $\mathcal{M} \triangleq \text{im}(f)$ which is absolutely continuous with respect to the s -dimensional Hausdorff measure:

$$p_{Y_1}(y) = p_{W_1}(w) \cdot \left| \det \left([J_f(w)]^\top \cdot J_f(w) \right) \right|^{-1/2}, \quad \text{where } y = f(w). \quad (118)$$

Densities p_{Y_2} and p_{W_2} of Y_2 and W_2 are related similarly. Subsequently, score functions of $\{W_1, W_2\}$ and $\{Y_1, Y_2\}$ are specified similarly to (9) and (14), respectively. Denote the Jacobian matrix of f at point $w \in \mathbb{R}^s$ by $J_f(w)$, which is an $r \times s$ matrix with entries given by

$$[J_f(w)]_{i,j} = \frac{\partial [f(w)]_i}{\partial w_j} = \frac{\partial y_i}{\partial w_j}, \quad \forall i \in [r], j \in [s]. \quad (119)$$

Next, consider a function $\phi: \mathcal{M} \rightarrow \mathbb{R}$. Since the domain of ϕ is a manifold, its differential, denoted by $D\phi$, is defined according to (12). By noting $y = f(w)$, we can also differentiate ϕ with respect to $w \in \mathbb{R}^s$ as (Simon, 2014, p. 57)

$$\nabla_w \phi(y) = \nabla_w (\phi \circ f)(w) = [J_f(w)]^\top \cdot D\phi(y). \quad (120)$$

Next, given the identities in (118) and (120), we find the relationship between score functions of W_1 and Y_1 as follows.

$$s_{W_1}(w) = \nabla_w \log p_{W_1}(w) \quad (121)$$

$$\stackrel{(118)}{=} \nabla_w \log p_{Y_1}(y) + \nabla_w \log \left| \det([J_f(w)]^\top \cdot J_g(w)) \right|^{1/2} \quad (122)$$

$$\stackrel{(120)}{=} [J_f(w)]^\top \cdot D \log p_{Y_1}(y) + \nabla_w \log \left| \det([J_f(w)]^\top \cdot J_f(w)) \right|^{1/2} \quad (123)$$

$$= [J_f(w)]^\top \cdot s_{Y_1}(y) + \nabla_w \log \left| \det([J_f(w)]^\top \cdot J_f(w)) \right|^{1/2}. \quad (124)$$

Following the similar steps that led to (124) for W_2 and Y_2 , we obtain

$$s_{W_2}(w) = [J_f(w)]^\top \cdot s_{Y_2}(y) + \nabla_w \log \left| \det([J_f(w)]^\top \cdot J_f(w)) \right|^{1/2}. \quad (125)$$

Subtracting (125) from (124), we obtain the desired result

$$s_{W_1}(w) - s_{W_2}(w) = [J_f(w)]^\top \cdot [s_{Y_1}(y) - s_{Y_2}(y)]. \quad (126)$$

Corollary 2 *In Lemma 2, if f is a linear transform, that is $Y = \mathbf{F} \cdot W$ for a full-rank matrix $\mathbf{F} \in \mathbb{R}^{r \times s}$, then the score functions of Y and W are related through $s_W(w) = \mathbf{F}^\top \cdot s_Y(y)$, where $y = \mathbf{F} \cdot w$.*

Proof: For the given linear transform, we have $J_f(w) = \mathbf{F}$, which is independent of w . Then, in the proof of Lemma 2, (124) reduces to $s_W(w) = \mathbf{F}^\top \cdot s_Y(y)$. Finally, we note that the score difference of Y can be similarly written in terms of the score difference of W .

Corollary 1 *Under the same setting and the assumptions as Lemma 2, we have*

$$s_{Y_1}(y) - s_{Y_2}(y) = [[J_f(w)]^\dagger]^\top \cdot [s_{W_1}(w) - s_{W_2}(w)], \quad \text{where } y = f(w). \quad (127)$$

Proof: Multiplying (126) from left with $[[J_f(w)]^\dagger]^\top$, we obtain

$$[[J_f(w)]^\dagger]^\top \cdot [s_{W_1}(w) - s_{W_2}(w)] = [[J_f(w)]^\dagger]^\top \cdot [J_f(w)]^\top \cdot [s_{Y_1}(y) - s_{Y_2}(y)]. \quad (128)$$

Note that

$$[[J_f(w)]^\dagger]^\top \cdot [J_f(w)]^\top = J_f(w) \cdot [J_f(w)]^\dagger. \quad (129)$$

Note that, by properties of the Moore-Penrose inverse, for any matrix \mathbf{A} , we have $\mathbf{A} \cdot \mathbf{A}^\dagger \cdot \mathbf{A} = \mathbf{A}$. This means that $\mathbf{A} \cdot \mathbf{A}^\dagger$ acts as a left identity for vectors in the column space of \mathbf{A} . By definition, s_{Y_1} and s_{Y_2} have values in $T_w \text{im}(f)$, the tangent space of the image manifold f at point w . This space is equal to the column space of matrix $J_f(w)$. Therefore, $J_f(w) \cdot [J_f(w)]^\dagger$ acts as a left identity for $s_{Y_1}(y)$ and $s_{Y_2}(y)$, and we have

$$J_f(w) \cdot [J_f(w)]^\dagger \cdot [s_{Y_1}(y) - s_{Y_2}(y)] = s_{Y_1}(y) - s_{Y_2}(y). \quad (130)$$

Substituting (129) and (130) into (128) completes the proof.

A.3 Proof of Lemma 14

We will prove that causal mechanisms p_i and q_i satisfy interventional regularity for (i) hard interventions and (ii) additive noise models. To this end, we first define

$$\psi(z_i, z_{\text{pa}(i)}) \triangleq \frac{q_i(z_i \mid z_{\text{pa}(i)})}{p_i(z_i \mid z_{\text{pa}(i)})}. \quad (131)$$

We start by showing that $\psi(z_i, z_{\text{pa}(i)})$ varies with z_i . We prove it by contradiction. Assume the contrary, i.e., let $\psi(z_i, z_{\text{pa}(i)}) = \psi(z_{\text{pa}(i)})$. By rearranging (131) we have

$$q_i(z_i \mid z_{\text{pa}(i)}) = \psi(z_{\text{pa}(i)}) p_i(z_i \mid z_{\text{pa}(i)}). \quad (132)$$

Fix a realization of $z_{\text{pa}(i)} = z_{\text{pa}(i)}^*$ and integrate both sides of (132) with respect to z_i . Since both p_i and q_i are pdfs, we have

$$1 = \int_{\mathbb{R}} q_i(z_i \mid z_{\text{pa}(i)}^*) dz_i = \int_{\mathbb{R}} \psi(z_{\text{pa}(i)}^*) p_i(z_i \mid z_{\text{pa}(i)}^*) dz_i dz_i \quad (133)$$

$$= \psi(z_{\text{pa}(i)}^*) \int_{\mathbb{R}} p_i(z_i \mid z_{\text{pa}(i)}^*) dz_i \quad (134)$$

$$= \psi(z_{\text{pa}(i)}^*). \quad (135)$$

This identity implies that $p_i(z_i \mid z_{\text{pa}(i)}^*) = q_i(z_i \mid z_{\text{pa}(i)}^*)$ for any arbitrary realization $z_{\text{pa}(i)}^*$. This contradicts the premise that observational and interventional distributions are distinct. As a result, to check if a model satisfies interventional regularity for node i , it suffices to investigate whether the function ψ is not invariant with respect to z_k for $k \in \text{pa}(i)$. To this end, from (131) we know that $\psi(z_i, z_{\text{pa}(i)})$ varies with z_k if and only if

$$\frac{\partial}{\partial z_i} \log \psi(z_i, z_{\text{pa}(i)}) = \frac{\partial q_i(z_i \mid z_{\text{pa}(i)})}{\partial z_i} \cdot \frac{1}{q_i(z_i \mid z_{\text{pa}(i)})} - \frac{\partial p_i(z_i \mid z_{\text{pa}(i)})}{\partial z_i} \cdot \frac{1}{p_i(z_i \mid z_{\text{pa}(i)})} \neq 0. \quad (136)$$

Next, we investigate the sufficient conditions listed in the Lemma 14.

A.3.1 HARD INTERVENTIONS

Under hard interventions, note that for any $k \in \text{pa}(i)$,

$$\frac{\partial}{\partial z_k} p_i(z_i \mid z_{\text{pa}(i)}) \neq 0, \quad \text{and} \quad \frac{\partial}{\partial z_k} q_i(z_i) = 0. \quad (137)$$

Then, it follows directly from (136) that

$$\frac{\partial}{\partial z_k} \log \psi(z_i, z_{\text{pa}(i)}) = \underbrace{\frac{\partial q_i(z_i)}{\partial z_k}}_{=0} \cdot \frac{1}{q_i(z_i)} - \underbrace{\frac{\partial p_i(z_i \mid z_{\text{pa}(i)})}{\partial z_k}}_{\neq 0} \cdot \frac{1}{p_i(z_i \mid z_{\text{pa}(i)})} \neq 0. \quad (138)$$

Thus, hard interventions on any latent causal model satisfy interventional regularity.

A.3.2 ADDITIVE NOISE MODELS

The additive noise model for node i is given by

$$Z_i = f_i(Z_{\text{pa}(i)}) + N_i, \quad (139)$$

as specified in (7). When node i is soft intervened, Z_i is generated according to

$$Z_i = \bar{f}_i(Z_{\text{pa}(i)}) + \bar{N}_i, \quad (140)$$

in which \bar{f}_i and \bar{N}_i specify the interventional mechanism for node i . Then, denoting the pdfs of N_i and \bar{N}_i by p_N and q_N , respectively, (139) and (140) imply that

$$p_i(z_i | z_{\text{pa}(i)}) = p_N(z_i - f_i(z_{\text{pa}(i)})), \quad \text{and} \quad q_i(z_i | z_{\text{pa}(i)}) = q_N(z_i - \bar{f}_i(z_{\text{pa}(i)})). \quad (141)$$

Denote the score functions associated with p_N and q_N by

$$r_p(u) \triangleq \frac{d}{du} \log p_N(u) = \frac{p'_N(u)}{p_N(u)}, \quad \text{and} \quad r_q(u) \triangleq \frac{d}{du} \log q_N(u) = \frac{q'_N(u)}{q_N(u)}. \quad (142)$$

We will prove that (136) holds by contradiction. Assume the contrary and let

$$\frac{\partial q_i(z_i | z_{\text{pa}(i)})}{\partial z_k} \cdot \frac{1}{q_i(z_i | z_{\text{pa}(i)})} = \frac{\partial p_i(z_i | z_{\text{pa}(i)})}{\partial z_k} \cdot \frac{1}{p_i(z_i | z_{\text{pa}(i)})}. \quad (143)$$

From (141) and (142), for the numerators in (143) we have,

$$\frac{\partial p_i(z_i | z_{\text{pa}(i)})}{\partial z_k} = -\frac{\partial f_i(z_{\text{pa}(i)})}{\partial z_k} \cdot p'_N(z_i - f_i(z_{\text{pa}(i)})), \quad (144)$$

$$\text{and} \quad \frac{\partial q_i(z_i | z_{\text{pa}(i)})}{\partial z_k} = -\frac{\partial \bar{f}_i(z_{\text{pa}(i)})}{\partial z_k} \cdot q'_N(z_i - \bar{f}_i(z_{\text{pa}(i)})). \quad (145)$$

Hence, the identity in (143) can be written as

$$\frac{\partial f_i(z_{\text{pa}(i)})}{\partial z_k} \cdot r_p(z_i - f_i(z_{\text{pa}(i)})) = \frac{\partial \bar{f}_i(z_{\text{pa}(i)})}{\partial z_k} \cdot r_q(z_i - \bar{f}_i(z_{\text{pa}(i)})). \quad (146)$$

Define n_i and \bar{n}_i as the realizations of N_i and \bar{N}_i when $Z_i = z_i$ and $Z_{\text{pa}(i)} = z_{\text{pa}(i)}$. By defining $\delta(z_{\text{pa}(i)}) \triangleq f_i(z_{\text{pa}(i)}) - \bar{f}_i(z_{\text{pa}(i)})$, we have $\bar{n}_i = n_i + \delta(z_{\text{pa}(i)})$. Then, (146) can be rewritten as

$$\frac{\partial f_i(z_{\text{pa}(i)})}{\partial z_k} \cdot r_p(n_i) = \frac{\partial \bar{f}_i(z_{\text{pa}(i)})}{\partial z_k} \cdot r_q(n_i + \delta(z_{\text{pa}(i)})). \quad (147)$$

Note that $\frac{\partial f_i(z_{\text{pa}(i)})}{\partial z_k}$ is a non-zero continuous function. Hence, there exists an interval $\Phi \subseteq \mathbb{R}^{|\text{pa}(i)|}$ over which $\frac{\partial f_i(z_{\text{pa}(i)})}{\partial z_k} \neq 0$. Likewise, $r_p(n_i)$ cannot be constantly zero over all possible intervals $\Omega \subseteq \mathbb{R}$. This is because otherwise, it would have to necessarily be a constant zero function (since it is analytic), which is an invalid score function. Hence, there exists an open interval $\Omega \subseteq \mathbb{R}$ over which $r_p(n_i)$ is non-zero for all $n_i \in \Omega$. Then, we can rearrange (147) as

$$\frac{r_p(n_i)}{r_q(n_i + \delta(z_{\text{pa}(i)}))} = \frac{\frac{\partial \bar{f}_i(z_{\text{pa}(i)})}{\partial z_k}}{\frac{\partial f_i(z_{\text{pa}(i)})}{\partial z_k}}, \quad \forall (n_i, z_{\text{pa}(i)}) \in \Omega \times \Phi. \quad (148)$$

Note that the RHS of (148) is not a function of n_i . Then, taking the derivative of both sides with respect to n_i , we get

$$\frac{r'_p(n_i)}{r_p(n_i)} = \frac{r'_q(n_i + \delta(z_{\text{pa}(i)}))}{r_q(n_i + \delta(z_{\text{pa}(i)}))}. \quad (149)$$

In the next step, we show that δ is not a constant function. We prove this by contradiction. Suppose that $\delta(z_{\text{pa}(i)}) = \delta^*$ is a constant function. Then, the gradients of f_i and \bar{f}_i are equal. From (148), this implies that

$$r_p(n_i) = r_q(n_i + \delta^*), \quad \forall n_i \in \Omega. \quad (150)$$

Since $r_p(n_i)$ and $r_q(n_i + \delta^*)$ are analytic functions that agree on an open interval of \mathbb{R} , they are equal for all $n_i \in \mathbb{R}$. This implies that $p_N(n_i) = \eta q_N(n_i + \delta^*)$ for some constant $\eta \in \mathbb{R}$. Since p_N and q_N are pdfs, $\eta = 1$ is the only choice that maintains p_N and q_N are pdfs. Therefore, $p_N(n_i) = q_N(n_i + \delta^*)$. However, using (141), this implies that $p_i(z_i \mid z_{\text{pa}(i)}) = q_i(z_i \mid z_{\text{pa}(i)})$, which contradicts the premise that an intervention changes the causal mechanism of target node i . Therefore δ is a continuous, non-constant function, and its image over $z_{\text{pa}(i)} \in \Phi$ includes an open interval $\Theta \subseteq \mathbb{R}$. With this result in mind, we return to (149). Consider a fixed realization $n_i = n_i^*$ and denote the value of the left-hand side (LHS) for n_i^* by α . By defining $u \triangleq \delta(z_{\text{pa}(i)})$, we get

$$\alpha = \frac{r'_q(n_i^* + u)}{r_q(n_i^* + u)}, \quad \forall u \in \Theta. \quad (151)$$

This is only possible if r_q is an exponential function, i.e., $r_q(u) = k_1 \exp(\alpha u)$ over interval $u \in \Theta$. Since r_q is an analytic function, it is, therefore, exponential over entire \mathbb{R} . Then, the associated pdf must have the form $q_N(u) = k_2 \exp((k_1/\alpha) \exp(\alpha u))$. However, the integral of this function over the entire domain \mathbb{R} diverges. Hence, it is not a valid pdf, rendering a contradiction. Hence, the additive noise model satisfies interventional regularity.

Appendix B. Proofs of the Results for Linear Transformations

B.1 Proof of Lemma 3

Consider environment \mathcal{E}^m and denote the intervened node by $\ell = I^m$. Lemma 1(i) and (ii) imply that, for any $m \in [n]$, the image of the function $(s - s^m)$ contains a vector $z \in \mathbb{R}^n$ for which $z_\ell \neq 0$ and $z_j = 0$ for $j \notin \overline{\text{pa}}(\ell)$. Since (Z_1, \dots, Z_n) are topologically ordered, this implies $z_j = 0$ for $j \geq (\ell + 1)$. Then, for different values of m , these specified vectors are linearly independent. Hence, $\text{im}(\{s - s^m : m \in \mathcal{A}\})$ contains at least $|\mathcal{A}|$ linearly independent vectors and we have

$$\mathcal{R}(\{s - s^m : m \in \mathcal{A}\}) \geq |\mathcal{A}|. \quad (152)$$

On the other hand, using Lemma 1, the term $s(Z) - s^m(Z)$ can have non-zero entries only at the coordinates $\overline{\text{pa}}(\ell)$. Therefore, in any vector in $\text{im}(\{s - s^m : m \in \mathcal{A}\})$, the j -th coordinate is zero if $j \notin \overline{\text{pa}}(I^{\mathcal{A}})$. Subsequently, we have

$$\mathcal{R}(\{s - s^m : m \in \mathcal{A}\}) \leq |\overline{\text{pa}}(I^{\mathcal{A}})|. \quad (153)$$

Finally, if $I^{\mathcal{A}}$ is ancestrally closed, we have $\overline{\text{pa}}(I^{\mathcal{A}}) = I^{\mathcal{A}}$. This implies that the inequalities in (152) and (153) hold with equality and we have

$$\mathcal{R}(\{s - s^m : m \in \mathcal{A}\}) = |\mathcal{A}| = |\overline{\text{pa}}(I^{\mathcal{A}})|. \quad (154)$$

B.2 Proof of Lemma 4

We consider a set \mathcal{A} for which $I^{\mathcal{A}}$ is ancestrally closed, i.e., $\text{an}(I^{\mathcal{A}}) \subseteq I^{\mathcal{A}}$, and consider the score function differences $\{s - s^m : m \in \mathcal{A} \setminus \{k\}\}$ for some $k \in \mathcal{A}$. First, we use Lemma 3 to show that the rank of the image of these functions is either $|\mathcal{A}|$ or $|\mathcal{A}| - 1$. Note that $\overline{\text{pa}}(I^{\mathcal{A}}) = \overline{\text{pa}}(I^{\mathcal{A} \setminus \{k\}}) \cup \overline{\text{pa}}(I^k)$. Subsequently, since $I^{\mathcal{A}}$ is ancestrally closed, we have

$$|\overline{\text{pa}}(I^{\mathcal{A} \setminus \{k\}})| \leq |\overline{\text{pa}}(I^{\mathcal{A}})| = |I^{\mathcal{A}}| = |\mathcal{A}|. \quad (155)$$

Then, using Lemma 3, we have

$$|\mathcal{A}| \geq \mathcal{R}\left(\{s - s^m : m \in \mathcal{A} \setminus \{k\}\}\right) \geq |\mathcal{A}| - 1. \quad (156)$$

Next, consider two cases as follows.

Case (i): I^k does not have a child in $I^{\mathcal{A}}$. In this case, $I^{\mathcal{A} \setminus \{k\}}$ is ancestrally closed, which implies

$$|\overline{\text{pa}}(I^{\mathcal{A} \setminus \{k\}})| = |I^{\mathcal{A} \setminus \{k\}}| = |\mathcal{A}| - 1. \quad (157)$$

Then, using Lemma 3 and (156), we have

$$\mathcal{R}\left(\{s - s^m : m \in \mathcal{A} \setminus \{k\}\}\right) = |\mathcal{A}| - 1. \quad (158)$$

Case (ii): I^k has a child in $I^{\mathcal{A}}$. Suppose that I^j is the eldest child of I^k in $I^{\mathcal{A}}$. This means that ancestors of I^j and children of I^k do not intersect, $\text{an}(I^j) \cap \text{ch}(I^k) = \emptyset$. Let γ be a permutation of the nodes in \mathcal{A} such that $\{I^{\gamma_1}, \dots, I^{\gamma_{|\mathcal{A}|}}\}$ are topologically ordered. This implies that

$$I^{\gamma_j} < I^{\gamma_\ell}, \quad \forall \ell \in \text{ch}(k) \setminus \{j\}. \quad (159)$$

Denote the index of k and j in γ by u and v , i.e., $\gamma_u = k$ and $\gamma_v = j$. Consider the set

$$\mathcal{M} = \{\gamma_1, \dots, \gamma_{u-1}, \gamma_{u+1}, \dots, \gamma_{v-1}\}. \quad (160)$$

Since I^j is the eldest child of I^k in \mathcal{A} , we know that $I^{\mathcal{M}}$ is ancestrally closed. Then, using Lemma 3, we have

$$\mathcal{R}(\{s - s^m : m \in \mathcal{M}\}) = |\mathcal{M}|. \quad (161)$$

Note that the vectors in $\text{im}(\{s - s^m : m \in \mathcal{M}\})$ have zeros in coordinates I^k and I^j since $I^{\mathcal{M}}$ does not contain any children of I^k or I^j . Since $I^k \in \text{pa}(I^j)$, Assumption 1 implies that $\text{im}(s - s^j)$ contains two linearly independent vectors $a, b \in \mathbb{R}^n$ such that

$$\exists a, b \in \text{im}(s - s^j) : \quad a_{I^k} \neq 0 \quad \text{and} \quad b_{I^j} \neq 0. \quad (162)$$

Since $\text{pa}(I^j) \setminus \{I^k\} \subseteq \mathcal{M}$, the set $\text{im}(\{s - s^m : m \in \mathcal{M} \cup \{j\}\})$ contains $|\mathcal{M}| + 2$ linearly independent vectors. Finally, we use the same argument as in the proof of Lemma 3 as follows. For each $m \in \mathcal{A} \setminus (\mathcal{M} \cup \{k, j\})$, we have

$$\exists z \in \text{im}(s - s^m) : \quad z_{I^m} \neq 0 \quad \text{and} \quad z_j = 0, \quad \forall j \geq (I^m + 1). \quad (163)$$

Then, these specified vectors are linearly independent and are not contained in $\text{im}(\{s - s^m : m \in \mathcal{M} \cup \{j\}\})$. Therefore, $\text{im}(\{s - s^m : m \in \mathcal{A} \setminus \{k\}\})$ contains at least $|\mathcal{A}|$ linearly independent vectors – two vectors from $\text{im}(s - s^j)$ and one vector from $\text{im}(s - s^m)$ for each $m \in \mathcal{A} \setminus \{k, j\}$, and the proof is complete.

B.3 Proofs of Lemma 5 and Lemma 6

First, we provide a linear algebraic property, which will be used in the proofs.

Lemma 15 *Consider the latent causal graph \mathcal{G} , and a matrix $\mathbf{L} \in \mathbb{R}^{n \times n}$.*

1. *Let \mathbf{L}_{an} be a binary matrix that denotes the ancestral relationships in \mathcal{G} , i.e.,*

$$[\mathbf{L}_{\text{an}}]_{i,j} \triangleq \begin{cases} 1, & \text{if } i \in \overline{\text{an}}(j), \\ 0, & \text{otherwise} \end{cases} . \quad (164)$$

Then, if $\mathbf{I}_{n \times n} \preceq \mathbf{1}(\mathbf{L}) \preceq \mathbf{L}_{\text{an}}$, we also have $\mathbf{I}_{n \times n} \preceq \mathbf{1}(\mathbf{L}^{-1}) \preceq \mathbf{L}_{\text{an}}$.

2. *Let \mathbf{L}_{sur} be a binary matrix that denotes the surrounding relationships in \mathcal{G} , i.e.,*

$$[\mathbf{L}_{\text{sur}}]_{i,j} \triangleq \begin{cases} 1, & \text{if } i = j, \\ 1, & \text{if } \overline{\text{ch}}(j) \subseteq \text{ch}(i), \\ 0, & \text{otherwise} \end{cases} . \quad (165)$$

Then, if $\mathbf{I}_{n \times n} \preceq \mathbf{1}(\mathbf{L}) \preceq \mathbf{L}_{\text{sur}}$, we also have $\mathbf{I}_{n \times n} \preceq \mathbf{1}(\mathbf{L}^{-1}) \preceq \mathbf{L}_{\text{sur}}$.

Proof: See Appendix B.6.

Reducing to equivalent optimization problems. We investigate the optimization problems in Algorithms 2 and 3. Note that if $a \in \text{im}(\mathbf{G})$, there exists some $b \in \mathbb{R}^n$ such that $a = \mathbf{G} \cdot b$. Also, recall (45) that

$$s(Z) - s^m(Z) = \mathbf{G}^\top \cdot [s_X(X) - s_X^m(X)] , \quad \forall m \in [n] , \text{ where } X = \mathbf{G} \cdot Z , \quad (166)$$

which implies that, by pre-multiplying both sides by b , we have

$$b^\top \cdot [s(Z) - s^m(Z)] = (\mathbf{G} \cdot b)^\top \cdot [s_X(X) - s_X^m(X)] = a^\top \cdot [s_X(X) - s_X^m(X)] . \quad (167)$$

Then, by defining $\mathbf{B}_{\pi_j} = \mathbf{A}_{\pi_j} \cdot (\mathbf{G}^\dagger)^\top$ for all $j \in \{t+1, \dots, n\}$ at step t of Algorithm 2, the feasible set \mathcal{F}_t corresponds to $\tilde{\mathcal{F}}_t \triangleq \mathbb{R}^n \setminus \text{span}(\mathbf{B}_{\pi_{t+1}}^\top, \dots, \mathbf{B}_{\pi_n}^\top)$. Hence, for any set $\mathcal{M} \subseteq [n]$,

$$\min_{a \in \mathcal{F}_t} \sum_{m \in \mathcal{M}} \mathbb{E} \left[\left| a^\top \cdot [s_X(X) - s_X^m(X)] \right| \right] \quad (168)$$

is equivalent to the optimization problem

$$\min_{b \in \tilde{\mathcal{F}}_t} \sum_{m \in \mathcal{M}} \mathbb{E} \left[\left| b^\top \cdot [s(Z) - s^m(Z)] \right| \right] . \quad (169)$$

Furthermore, in the algorithm steps, we are only interested in whether the optimal value of the optimization problems in (168) and (169) are zero. Next, using Proposition 2, for any $b \in \mathbb{R}^n$ and $m \in [n]$, we have

$$\exists z^* \in \mathbb{R}^n : b^\top \cdot [s(z^*) - s^m(z^*)] \neq 0 \iff \mathbb{E} \left[\left| b^\top \cdot [s(z^*) - s^m(z^*)] \right| \right] > 0 . \quad (170)$$

Therefore, for any $\mathcal{M} \subseteq [n]$, the terms in (168) and (169) are zero if and only if

$$\exists b \in \tilde{\mathcal{F}}_t : b^\top \cdot [s(z) - s^m(z)] = 0 , \quad \forall z \in \mathbb{R}^n, \forall m \in \mathcal{M} . \quad (171)$$

B.3.1 PROOF OF LEMMA 5

We use the equivalency relationships in (169) and (171) to prove the statements in Lemma 5. Recall that \mathcal{V}_t denotes the set of unordered nodes in step t of Algorithm 2. Setting $\mathcal{M} = \mathcal{V}_t \setminus \{k\}$, we know that the optimal value of the problem specified in (52) is zero if and only if

$$\exists b \in \tilde{\mathcal{F}}_t : b^\top \cdot [s(z) - s^m(z)] = 0, \quad \forall z \in \mathbb{R}^n, \forall m \in \mathcal{V}_t \setminus \{k\}. \quad (172)$$

First, note that the lemma statement, $I^\pi = (I^{\pi_1}, \dots, I^{\pi_n})$ is a valid causal order, is equivalent to the statement

$$\text{de}(I^{\pi_t}) \subseteq \{I^{\pi_{t+1}}, \dots, I^{\pi_n}\}, \quad \forall t \in [n], \quad (173)$$

in which $\text{de}(i)$ denotes the descendants of node i as specified in (5). We prove the statement in (173) by induction. As an auxiliary result, we also define and prove the following statement:

$$\left[\mathbb{1}\{\mathbf{A} \cdot (\mathbf{G}^\dagger)^\top\} \right]_{\pi_t, I^{\pi_j}} = \mathbb{1}\{\mathbf{B}_{\pi_t, I^{\pi_j}}\} = \begin{cases} 0, & t > j \\ 1, & t = j \end{cases}, \quad \forall t, j \in [n]. \quad (174)$$

At the base case $t = n$, consider some $k \in [n]$. Note that $\mathcal{V}_n = I^{\mathcal{V}_n} = \{1, \dots, n\}$. Hence, $I^{\mathcal{V}_n}$ is an ancestrally closed set, based on which we can use Lemma 4 as follows. If I^k has a child in $[n] \setminus \{I^k\}$, then

$$\mathcal{R}\left(\{s - s^m : m \in \mathcal{V}_n \setminus \{k\}\}\right) = n. \quad (175)$$

Since $\tilde{\mathcal{F}}_n = \mathbb{R}^n \setminus \text{span}(\emptyset)$, (175) implies that (172) does not hold, and solving (52) does not yield a zero value. On the other hand, if I^k does not have a child in $[n] \setminus \{I^k\}$, then

$$\mathcal{R}\left(\{s - s^m : m \in \mathcal{V}_n \setminus \{k\}\}\right) = n - 1, \quad (176)$$

which implies that (172) has a unique solution b^* (up to scaling) that has zeros in all coordinates except I^k . Since b^* contains at least one non-zero element, $b_{I^k}^* \neq 0$. **Next, as the induction hypothesis**, assume that for $u \in \{t+1, \dots, n\}$, we have

$$\text{de}(I^{\pi_u}) \subseteq \{I^{\pi_{u+1}}, \dots, I^{\pi_n}\}, \quad \text{and} \quad \mathbb{1}\{\mathbf{B}_{\pi_u, I^k}\} = \begin{cases} 0, & k \in \mathcal{V}_u \setminus \{\pi_u\} \\ 1, & k = \pi_u \\ \text{free}, & \text{otherwise} \end{cases}. \quad (177)$$

We will show that $u = t$ also satisfies these conditions, and by induction, (177) will be satisfied for all $u \in [n]$, which implies that (173) and (174) are satisfied. To show this, note that $I^{\mathcal{V}_t}$ is ancestrally closed since (177) holds for all $u \in \{t+1, \dots, n\}$. This is because any $k \in I^{\mathcal{V}_t}$ cannot be a descendant of a node in $\{I^{\pi_{u+1}}, \dots, I^{\pi_n}\}$. Then, we use Lemma 4 as follows. If I^k has a child in $I^{\mathcal{V}_t}$, we have

$$\mathcal{R}\left(\{s - s^m : m \in \mathcal{V}_t \setminus \{k\}\}\right) = t. \quad (178)$$

Also note that, since $I^{\mathcal{V}_t}$ is ancestrally closed, by Lemma 1,

$$[s(Z) - s^m(Z)]_\ell = 0, \quad \forall \ell \notin I^{\mathcal{V}_t}. \quad (179)$$

Then, any vector in $\text{im}(\{s - s^m : m \in \mathcal{V}_t \setminus \{k\}\})$ can contain non-zeros only in the coordinates $I^{\mathcal{V}_t}$. Since the dimension of this image is t , and $|I^{\mathcal{V}_t}| = t$, a solution of (172) must have zeros in coordinates $I^{\mathcal{V}_t}$. However, such a vector falls into $\text{span}(\mathbf{B}_{\pi_{t+1}}^\top, \dots, \mathbf{B}_{\pi_n}^\top)$ due to the induction hypothesis that (177) holds for $u \in \{t+1, \dots, n\}$. Therefore, it is not in the feasible set $\tilde{\mathcal{F}}_t$. Hence, (172) does not hold, which means that solving (52) does not yield a zero value. Next, if I^k does not have a child in $I^{\mathcal{V}_t}$,

$$\mathcal{R}(\{s - s^m : m \in \mathcal{V}_t \setminus \{k\}\}) = t - 1. \quad (180)$$

Since $I^{\mathcal{V}_t \setminus \{k\}}$ is ancestrally closed, any vector in $\text{im}(\{s - s^m : m \in \mathcal{V}_t \setminus \{k\}\})$ can contain non-zeros only in the coordinates $I^{\mathcal{V}_t \setminus \{k\}}$, and a solution of (172) must have zeros in coordinates $I^{\mathcal{V}_t \setminus \{k\}}$. Therefore, any solution b^* to (172) satisfies that $b_\ell^* = 0$ for $\ell \in I^{\mathcal{V}_t \setminus \{k\}}$ and $b_k^* \neq 0$. Note that (172) is valid since there is a solution b^* for which

$$b_\ell^* = \begin{cases} 1 & \text{if } \ell = k, \\ 0 & \text{otherwise} \end{cases}. \quad (181)$$

Subsequently, for $\pi_t = k$, (177) is satisfied for $u = t$. Therefore, by induction, (177) is correct for all $u \in \{1, \dots, n\}$, which completes the proof of (173) and (174), and concludes the lemma.

B.3.2 PROOF OF LEMMA 6

We use the equivalency relationships in (169) and (171) to prove the statements in Lemma 6. Recall that $\mathcal{M}_{t,j}$ is defined as $\mathcal{V}_j \setminus \{\hat{\text{de}}(\pi_t) \cup \{\pi_t\}\}$ in Algorithm 3. Setting $\mathcal{M} = \mathcal{M}_{t,j}$, we know that the optimal value of the problem specified in (56) is zero if and only if

$$\exists b \in \tilde{\mathcal{F}}_t : b^\top \cdot [s(z) - s^m(z)] = 0, \quad \forall z \in \mathbb{R}^n, \forall m \in \mathcal{M}_{t,j}. \quad (182)$$

First, note that the transitive closures of two graphs are the same if and only if their transitive reductions are the same. Then, (C1) in Lemma 6 is equivalent to

$$\pi_t \in \hat{\text{pa}}_{\text{tr}}(\pi_j) \iff I^{\pi_t} \in \text{pa}_{\text{tr}}(I^{\pi_j}), \quad \forall t, j \in [n], \quad (183)$$

in which $\hat{\text{pa}}_{\text{tr}}$ and pa_{tr} denotes the parents in transitive reduction graphs $\hat{\mathcal{G}}_{\text{tr}}$ and \mathcal{G}_{tr} respectively. We also give the following statement, which we will show is equivalent to (C2) in Lemma 6.

$$\left[\mathbf{1} \{ \mathbf{A} \cdot (\mathbf{G}^\dagger)^\top \} \right]_{\pi_t, I^{\pi_j}} = \mathbf{1} \{ \mathbf{B}_{\pi_t, I^{\pi_j}} \} = \begin{cases} 0, & I^{\pi_t} \notin \text{an}(I^{\pi_j}), \\ 1, & t = j \end{cases}, \quad \forall t, j \in [n]. \quad (184)$$

We prove the desired results (183) and (184) by induction. **At the base step**, consider $t = n - 1$, and $j = n$. Then, we minimize the score variations over the set

$$\mathcal{M}_{n-1,n} = \mathcal{V}_n \setminus \{\pi_{n-1}\} = [n] \setminus \{\pi_{n-1}\}. \quad (185)$$

Since $(I^{\pi_1}, \dots, I^{\pi_n})$ is a valid causal order, the only possible path from $I^{\pi_{n-1}}$ to I^{π_n} is the possible edge between them. Note that $I^{\mathcal{V}_n}$ is an ancestrally closed set. Therefore, we can use Lemma 4 as follows. If $I^{\pi_{n-1}} \in \text{pa}(I^{\pi_n})$,

$$\mathcal{R}(\{s - s^m : m \in \mathcal{M}_{n-1,n}\}) = n. \quad (186)$$

Subsequently, (182) does not hold, which means that solving (56) does not yield a zero value. On the other hand, if $I^{\pi_{n-1}} \notin \text{pa}(I^{\pi_n})$, by Lemma 4,

$$\mathcal{R}(\{s - s^m : m \in \mathcal{M}_{n-1,n}\}) = n - 1, \quad (187)$$

which implies that (182) has a unique solution b^* (up to scaling) that has zeros in all coordinates except $I^{\pi_{n-1}}$. Next, **as the induction hypothesis**, assume that for all $v \in \{t+1, \dots, n\}$, and $j \in \{v+1, \dots, n\}$, the identified edges and minimizers satisfy

$$\pi_v \in \hat{\text{pa}}_{\text{tr}}(\pi_j) \iff I^{\pi_v} \in \text{pa}_{\text{tr}}(I^{\pi_j}), \quad \text{and} \quad \mathbb{1}\{\mathbf{B}_{\pi_v, I^{\pi_k}}\} = \begin{cases} 0, & I^{\pi_v} \notin \text{an}(I^{\pi_k}) \\ 1, & v = k \end{cases}. \quad (188)$$

We will show that $v = t$ and $j \in \{t+1, \dots, n\}$ also satisfy these conditions, and by induction, (188) will be satisfied for all $t \in [n]$ and $j \in \{t+1, \dots, n\}$, which implies that (183) and (184) are satisfied.

Now, we prove that (188) is satisfied for $v = t$ and $j \in \{t+1, \dots, n\}$ by induction as follows. **At the base step**, consider $j = t+1$. Since $\{I^{\pi_1}, \dots, I^{\pi_n}\}$ is a valid causal order, we have $I^{\pi_t} \in \text{pa}_{\text{tr}}(I^{\pi_{t+1}})$ if and only if $I^{\pi_t} \in \text{pa}(I^{\pi_{t+1}})$. Algorithm 3 has not assigned any children to π_t in $\hat{\mathcal{G}}$ yet. Hence, $\mathcal{M}_{t,t+1} = V_{t+1} \setminus \{\pi_t\}$. Since $I^{\mathcal{V}_{t+1}}$ is ancestrally closed, we use Lemma 4 as follows. If $I^{\pi_t} \in \text{pa}(I^{\pi_{t+1}})$,

$$\mathcal{R}(\{s - s^m : m \in \mathcal{M}_{t,t+1}\}) = |\mathcal{V}_{t+1}| = t+1. \quad (189)$$

Also note that, since $I^{\mathcal{V}_{t+1}}$ is ancestrally closed, by Lemma 1,

$$[s(Z) - s^m(Z)]_\ell = 0, \quad \forall \ell \notin I^{\mathcal{V}_{t+1}}. \quad (190)$$

Then, any vector in $\text{im}(\{s - s^m : m \in \mathcal{M}_{t,t+1}\})$ can contain non-zeros only in the coordinates $I^{\mathcal{V}_{t+1}}$. Since the dimension of this image is $t+1$ and $|I^{\mathcal{V}_{t+1}}| = t+1$, the solution of (182) must have zeros in coordinates $I^{\mathcal{V}_{t+1}}$. However, such a vector falls into $\text{span}(\mathbf{B}_{\pi_{t+1}}^\top, \dots, \mathbf{B}_{\pi_n}^\top)$ due to the induction hypothesis that (188) holds for $v \in \{t+1, \dots, t\}$. Therefore, it is not in the feasible set $\tilde{\mathcal{F}}_t$. Hence, (182) does not hold, which means that solving (56) does not yield a zero value. On the other hand, if $I^{\pi_t} \notin \text{pa}(I^{\pi_{t+1}})$, by Lemma 4, we have

$$\mathcal{R}(\{s - s^m : m \in \mathcal{M}_{t,t+1}\}) = t. \quad (191)$$

(191) implies that (182) has a unique solution b^* (up to scaling) that has zeros in $I^{\mathcal{M}_{t,t+1}}$ coordinates. Note that b^* must have at least one non-zero element in coordinates $I^{\mathcal{V}_t}$ to be in the feasible set $\tilde{\mathcal{F}}_t$. Since π_t is the only node in $V_t \setminus \mathcal{M}_{t,t+1}$, we have $b_{I^{\pi_t}}^* \neq 0$, which concludes the base step.

Next, **as the induction hypothesis**, assume that (188) holds for $v = t$ and $j \in \{t+1, \dots, u-1\}$ such that, if $I^{\pi_t} \in \text{pa}_{\text{tr}}(I^{\pi_j})$, then we have $\pi_t \in \hat{\text{pa}}(\pi_j)$. Note that by the induction hypothesis and using the fact that all ancestral relationships can be read off from \mathcal{G}_{tr} , we have identified all descendants of I^{π_t} in $\{I^{\pi_{t+1}}, \dots, I^{\pi_{u-1}}\}$. Then, we use Lemma 4 to prove that (188) holds for $v = t$ and $j = u$ as follows. If $I^{\pi_t} \in \text{pa}_{\text{tr}}(I^{\pi_u})$, then there is no other causal path from I^{π_t} to I^{π_u} in \mathcal{G} . Hence, we have

$$\text{de}(I^{\pi_t}) \cap \text{an}(I^{\pi_u}) = \emptyset, \quad \text{and} \quad \text{an}(I^{\pi_t}) \subseteq I^{\mathcal{M}_{t,u}}, \quad (192)$$

which implies that $I^{\mathcal{M}_{t,u}} \cup I^{\pi_t}$ is ancestrally closed. Since I^{π_t} has a children in $I^{\mathcal{M}_{t,u}}$, using Lemma 4 we have

$$\mathcal{R}(\{s - s^m : m \in \mathcal{M}_{t,u}\}) = |\mathcal{M}_{t,u}| + 1, \quad (193)$$

which implies that the solution of (182) has zeros in coordinates $I^{\mathcal{M}_{t,u}} \cup I^{\pi_t}$. However, this is not a feasible solution since such a vector falls into $\text{span}(B_{\pi_{t+1}}^\top, \dots, B_{\pi_n}^\top)$. Therefore, if $I^{\pi_t} \in \text{pa}_{\text{tr}}(I^{\pi_u})$, solving (56) does not yield a zero value and Algorithm 3 adds $\pi_t \rightarrow \pi_u$ to $\hat{\mathcal{G}}$. This completes the induction step and we have concluded that the condition (183) is satisfied for all $t \in [n]$. That is, if $I^{\pi_j} \in \text{pa}_{\text{tr}}(I^{\pi_t})$, then $\pi_j \in \hat{\text{pa}}(\pi_t)$. Next, if $I^{\pi_t} \notin \text{an}(I^{\pi_u})$, we know that $I^{\mathcal{M}_{t,u}} \cup I^{\pi_u}$ is ancestrally closed. Since I^{π_t} has no child in $I^{\mathcal{M}_{t,u}}$, using Lemma 4 we have

$$\mathcal{R}(\{s - s^m : m \in \mathcal{M}_{t,u}\}) = |\mathcal{M}_{t,u}|. \quad (194)$$

This implies that there exists a solution b^* to (182) and it satisfies $b_\ell^* = 0$ for $\ell \in I^{\mathcal{M}_{t,u}}$ and $b_{I^{\pi_t}}^* \neq 0$. This concludes that the condition (184) is satisfied for all t, j . Note that Algorithm 3 does not add an edge to $\hat{\mathcal{G}}$ in this case.

To summarize, we have shown that (i) if $I^{\pi_t} \notin \text{an}(I^{\pi_j})$, i.e., $I^{\pi_t} \notin \text{pa}_{\text{tc}}(I^{\pi_j})$, Algorithm 3 does not add the edge $\pi_t \rightarrow \pi_j$ to $\hat{\mathcal{G}}$, and (ii) if $I^{\pi_t} \in \text{pa}_{\text{tr}}(I^{\pi_j})$, the algorithm adds the edge $\pi_t \rightarrow \pi_j$ to $\hat{\mathcal{G}}$. Therefore, the transitive reductions (or closures) of \mathcal{G} and $\hat{\mathcal{G}}$ are related by permutation \mathcal{I} . Finally, note that (184) implies that

$$A \cdot (\mathbf{G}^\dagger)^\top = \mathbf{P}_{\mathcal{I}} \cdot \mathbf{U}, \quad (195)$$

for some upper triangular matrix \mathbf{U} such that its diagonal entries are non-zero and for all $i \notin \text{an}(j)$ we have $\mathbf{U}_{i,j} = 0$. Subsequently, taking the inverse transpose of both sides and substituting $\mathbf{H}^* = (\mathbf{A}^\top)^\dagger$, we obtain

$$\mathbf{H}^* \cdot G = \mathbf{P}_{\mathcal{I}} \cdot \mathbf{L}, \quad (196)$$

for some lower triangular matrix \mathbf{L} . Note that, using Lemma 15, diagonal entries of \mathbf{L} are non-zero and $j \notin \text{an}(i)$ also implies $\mathbf{L}_{i,j} = 0$. Hence, \mathbf{H}^* satisfies mixing consistency up to ancestors since

$$\hat{Z}(X; \mathbf{H}^*) = \mathbf{H}^* \cdot \mathbf{G} \cdot Z = \mathbf{P}_{\mathcal{I}} \cdot \mathbf{L} \cdot Z, \quad (197)$$

in which \mathbf{L} satisfies the properties of the matrix \mathbf{C}_{an} in Lemma 6.

B.4 Proof of Lemma 8

Recall that $\mathcal{M}_{t,j}$ is defined as $\mathcal{V}_j \setminus \{\hat{\text{ch}}(\pi_t) \cup \{\pi_t\}\}$ in Algorithm 3. Using (171), we know that solving (56) yields a zero value if and only if

$$\exists b \in \tilde{\mathcal{F}}_t : b^\top \cdot [s(z) - s^m(z)] = 0, \quad \forall z \in \mathbb{R}^n, \forall m \in \mathcal{M}_{t,j}. \quad (198)$$

Next, consider some $m \in \mathcal{M}_{t,j}$. By Lemma 1,

$$[s(Z) - s^m(Z)]_\ell = 0, \quad \forall \ell \in \overline{\text{pa}}(I^m). \quad (199)$$

This means that, for all $m \in \mathcal{M}_{t,j}$,

$$b^\top \cdot [s(z) - s^m(z)] = 0 \iff \sum_{\ell \in \overline{\text{pa}}(I^m)} b_\ell \cdot [s(z) - s^m(z)]_\ell = 0, \quad \forall z \in \mathbb{R}^n. \quad (200)$$

Next, Assumption 2 ensures that image of $(s - s^m)$ contains $|\overline{\text{pa}}(I^m)|$ linearly independent vectors. Therefore, for the right-hand side (RHS) of (200) to hold for all $m \in \mathcal{M}_{t,j}$, we must have

$$b_\ell = 0, \quad \forall \ell \in \overline{\text{pa}}(I^{\mathcal{M}_{t,j}}). \quad (201)$$

We will investigate whether such a vector b is in the feasible set $\tilde{\mathcal{F}}_t$, and prove the desired result by induction. First, note that the statement (C3) in Lemma 8 is equivalent to

$$\pi_t \in \hat{\text{pa}}(\pi_j) \iff I^{\pi_t} \in \text{pa}(I^{\pi_j}), \quad \forall t, j \in [n], \quad (202)$$

and the statement (C4) in Lemma 8 is equivalent to

$$\left[\mathbb{1}\{\mathbf{A} \cdot (\mathbf{G}^\dagger)^\top\} \right]_{\pi_t, I^{\pi_j}} = \mathbb{1}\{\mathbf{B}_{\pi_t, I^{\pi_j}}\} = \begin{cases} 0, & I^{\pi_t} \notin \text{sur}(I^{\pi_j}), \\ 1, & i = j \end{cases}, \quad \forall t, j \in [n], \quad (203)$$

except for the Markov property claim which we will prove in the end. We prove (202) and (203) by induction as follows. **At the base case**, consider $t = n - 1$ and $j = n$. Then, we minimize the score variations over the set

$$\mathcal{M}_{n-1,n} = \mathcal{V}_n \setminus \{\pi_{n-1}\} = [n] \setminus \{\pi_{n-1}\}. \quad (204)$$

If $I^{\pi_{n-1}} \in \text{pa}(I^{\pi_n})$, using Lemma 4, we have

$$\mathcal{R}(\{s - s^m : m \in \mathcal{M}_{n-1,n}\}) = n. \quad (205)$$

Subsequently, (198) does not hold, which means that solving (56) does not yield a zero value. On the other hand, if $I^{\pi_{n-1}} \notin \text{pa}(I^{\pi_n})$,

$$\mathcal{R}(\{s - s^m : m \in \mathcal{M}_{n-1,n}\}) = n - 1, \quad (206)$$

which implies that (182) has a unique solution b^* (up to scaling) that has zeros in all coordinates except $I^{\pi_{n-1}}$. In this case, since I^{π_n} is a leaf node in \mathcal{G} , we have $I^{\pi_{n-1}} \in \text{sur}(I^{\pi_n})$. Next, **as the induction hypothesis**, assume that for all $v \in \{t+1, \dots, n\}$, and $j \in \{v+1, \dots, n\}$, the identified edges and minimizers satisfy

$$\pi_v \in \hat{\text{pa}}(\pi_j) \iff I^{\pi_v} \in \text{pa}(I^{\pi_j}), \quad \text{and} \quad \mathbb{1}\{\mathbf{B}_{\pi_v, I^{\pi_k}}\} = \begin{cases} 0, & I^{\pi_v} \notin \text{sur}(I^{\pi_k}), \\ 1, & v = k \end{cases}. \quad (207)$$

(207) implies that any vector $b \in \tilde{\mathcal{F}}_t$ has at least one non-zero entry in coordinates $\{I^{\pi_1}, \dots, I^{\pi_t}\}$. Otherwise, b falls into $\text{span}(\mathbf{B}_{\pi_{t+1}}^\top, \dots, \mathbf{B}_{\pi_n}^\top)$, which is excluded from the feasible set. We will show that $v = t$ and $j \in \{t+1, \dots, n\}$ also satisfy the conditions in (207), and by induction, (207) will be satisfied for all $t \in [n]$ and $j \in \{t+1, \dots, n\}$, which implies that (202) and (203) are satisfied.

Now, we prove that (207) is satisfied for $v = t$ and $j \in \{t+1, \dots, n\}$ by induction as follows. **At the base step**, consider $j = t+1$. Algorithm 3 has not assigned any children to π_t in $\hat{\mathcal{G}}$ yet. Hence, $\mathcal{M}_{t,t+1} = \mathcal{V}_{t+1} \setminus \pi_t$. If $I^{\pi_t} \in \text{pa}(I^{\pi_{t+1}})$, we have

$$\overline{\text{pa}}(I^{\mathcal{M}_{t,t+1}}) = I^{\mathcal{V}_{t+1}}. \quad (208)$$

This means that a solution of (198) must satisfy

$$b_\ell = 0, \quad \forall \ell \in \overline{\text{pa}}(I^{\mathcal{V}_{t+1}}). \quad (209)$$

However, such a vector falls into $\text{span}(\mathbf{B}_{\pi_{t+1}}^\top, \dots, \mathbf{B}_{\pi_n}^\top)$ due to the induction hypothesis that (207) holds for $v \in \{t+1, \dots, t\}$. Therefore, it is not in the feasible set $\tilde{\mathcal{F}}_t$. Hence, (198) does not hold, which means that solving (56) does not yield a zero value and we correctly have $\pi_t \rightarrow \pi_{t+1}$ in $\hat{\mathcal{G}}$. On the other hand, if $I^{\pi_t} \notin \text{pa}(I^{t+1})$, we have

$$\overline{\text{pa}}(I^{\mathcal{M}_{t,t+1}}) = I^{\mathcal{V}_{t+1} \setminus \{\pi_t\}}. \quad (210)$$

This means that a solution of (198) exists and it satisfies

$$b_{I^{\pi_t}} \neq 0, \quad \text{and} \quad b_\ell = 0, \quad \forall \ell \in I^{\mathcal{V}_{t+1} \setminus \{\pi_t\}}. \quad (211)$$

Next, **as the induction hypothesis**, assume that (207) holds for $v = t$ and $j \in \{t+1, \dots, u-1\}$ such that, if $I^{\pi_t} \in \text{pa}(I^{\pi_j})$, then we have $\pi_t \in \hat{\text{pa}}(\pi_j)$. We determine whether $I^{\pi_t} \in \text{pa}(I^{\pi_u})$ as follows. Note that $I^{\mathcal{M}_{t,u}}$ contains $\{I^{\pi_1}, \dots, I^{\pi_{t-1}}\}$ by the definition of $\mathcal{M}_{t,u}$. If $I^{\pi_t} \in \text{pa}(I^{\pi_u})$, we have

$$I^{\pi_t} \in \overline{\text{pa}}(I^{\mathcal{M}_{t,t+1}}), \quad (212)$$

which implies that (198) does not hold. Hence, solving (56) does not yield a zero value and we correctly have $\pi_t \rightarrow \pi_u$ in $\hat{\mathcal{G}}$. On the other hand, if $I^{\pi_t} \notin \text{pa}(I^{\pi_u})$, then I^{π_t} is not contained in $\overline{\text{pa}}(I^{\mathcal{M}_{t,u}})$. Hence, a solution of (198) exists and it satisfies

$$b_{I^{\pi_t}} \neq 0, \quad \text{and} \quad b_\ell = 0, \quad \forall \ell \in I^{\mathcal{M}_{t,u}}. \quad (213)$$

Note that Algorithm 3 does not add an edge to $\hat{\mathcal{G}}$ in this case. To summarize, we have shown that (i) if $I^{\pi_t} \notin \text{pa}(I^{\pi_j})$, the algorithm does not add the edge $\pi_t \rightarrow \pi_j$ to $\hat{\mathcal{G}}$, and (ii) if $I^{\pi_t} \in \text{pa}(I^{\pi_j})$, the algorithm adds the edge $\pi_t \rightarrow \pi_j$ to $\hat{\mathcal{G}}$. Therefore, \mathcal{G} and $\hat{\mathcal{G}}$ are related through a graph isomorphism by permutation \mathcal{I} , hence (C3) in Lemma 8 is satisfied.

Finally, we prove (203) to complete the induction step. Denote the youngest non-children of π_t in $\hat{\mathcal{G}}$ by π_k . Since I^π is a valid causal order, this implies that

$$I^{\pi_t} \in \text{pa}(I^{\pi_j}), \quad \forall j \in \{k+1, \dots, n\}. \quad (214)$$

Note that \mathbf{A}_{π_t} , or equivalently \mathbf{B}_{π_t} , is finalized in the step of $j = k$ of Algorithm 3. Note that $\overline{\text{pa}}(\mathcal{M}_{t,k})$ contains all non-children of I^{π_t} in \mathcal{G} . Furthermore, if $I^{\pi_t} \in \text{pa}(I^{\pi_j})$ but $I^{\pi_t} \notin \text{sur}(I^{\pi_j})$, then there exists some $\ell \in [n]$ for which $I^{\pi_\ell} \in \text{ch}(I^{\pi_j})$ and $I^{\pi_\ell} \notin \text{ch}(I^{\pi_t})$. In this case, $I^{\pi_j} \in I^{\overline{\text{pa}}(\mathcal{M}_{t,k})}$, and we have $\mathbf{B}_{\pi_t, I^{\pi_j}} = 0$, which completes the proof of (203). Note that (203) implies

$$A \cdot (\mathbf{G}^\dagger)^\top = \mathbf{P}_{\mathcal{I}} \cdot \mathbf{U}, \quad (215)$$

for some upper triangular matrix \mathbf{U} that has non-zero diagonal entries and for all $i \notin \text{sur}(j)$ we have $\mathbf{U}_{i,j} = 0$. Subsequently, taking the inverse transpose of both sides and substituting $\mathbf{H}^* = (\mathbf{A}^\top)^\dagger$, we obtain

$$\mathbf{H}^* \cdot G = \mathbf{P}_{\mathcal{I}} \cdot \mathbf{L}, \quad (216)$$

for some lower triangular matrix \mathbf{L} . Note that, using Lemma 15, diagonal entries of \mathbf{L} are non-zero and $j \notin \text{sur}(i)$ implies $\mathbf{L}_{i,j} = 0$. Hence, \mathbf{H}^* satisfies mixing consistency up to surrounding parents since

$$\hat{Z}(X; \mathbf{H}^*) = \mathbf{H}^* \cdot \mathbf{G} \cdot Z = \mathbf{P}_{\mathcal{I}} \cdot \mathbf{L} \cdot Z, \quad (217)$$

in which \mathbf{L} satisfies the properties of \mathbf{C}_{sur} in Lemma 8.

Markov property of the mixing with surrounding parents. We investigate the properties of the mixing consistency up to surrounding parents further to prove that \hat{Z} is Markov with respect to $\hat{\mathcal{G}}$. Let ρ be the permutation that maps $\{1, \dots, n\}$ to \mathcal{I} , i.e., $I^{\rho_i} = i$ for all $i \in [n]$. Then, by pre-multiplying both sides of (217) by $\mathbf{P}_{\mathcal{I}}^\top = \mathbf{P}_\rho$, and plugging \mathbf{C}_{sur} for \mathbf{L} , we obtain

$$\mathbf{P}_\rho \cdot \hat{Z} = \mathbf{C}_{\text{sur}} \cdot Z . \quad (218)$$

Recall the following SCM specified in (6)

$$Z_i = f_i(Z_{\text{pa}(i)}, N_i) . \quad (219)$$

Since $\text{sur}(i) \subseteq \text{pa}(i)$, for each $i \in [n]$, we have

$$\hat{Z}_{\rho_i} = [\mathbf{C}_{\text{sur}}]_{i,i} \cdot Z_i + \sum_{j \in \text{sur}(i)} [\mathbf{C}_{\text{sur}}]_{i,j} Z_j \quad (220)$$

$$= [\mathbf{C}_{\text{sur}}]_{i,i} \cdot f_i(Z_{\text{pa}(i)}, N_i) + \sum_{j \in \text{sur}(i)} [\mathbf{C}_{\text{sur}}]_{i,j} \cdot Z_j , \quad (221)$$

which is a function of $Z_{\text{pa}(i)}$ and N_i . We need to specify Z_{ρ_i} in terms of $\hat{Z}_{\hat{\text{pa}}(\rho_i)}$ to prove Markov property. To prove this, it suffices to show that for any $k \in \text{pa}(i)$, Z_k is a function of $\hat{Z}_{\hat{\text{pa}}(\rho_i)}$. Using (218), we have

$$Z = \mathbf{C}_{\text{sur}}^{-1} \cdot \mathbf{P}_\rho \cdot \hat{Z} . \quad (222)$$

By Lemma 15, we know that $[\mathbf{C}_{\text{sur}}^{-1}]_{i,j} = 0$ if $i \notin \text{sur}(j)$ for distinct i and j . Subsequently, as counterpart of (220), we have

$$Z_k = [\mathbf{C}_{\text{sur}}^{-1}]_{k,k} \cdot \hat{Z}_{\rho_k} + \sum_{j \in \text{sur}(k)} [\mathbf{C}_{\text{sur}}^{-1}]_{k,j} \cdot \hat{Z}_{\rho_j} . \quad (223)$$

Since $k \in \text{pa}(i)$, we have $\rho_k \in \text{pa}(\rho_i)$ and \hat{Z}_{ρ_k} is in $\hat{Z}_{\hat{\text{pa}}(\rho_i)}$. Note that if $j \in \text{sur}(k)$, j is also in $\text{pa}(i)$. Therefore, every term in the RHS of (223) belongs to $\hat{Z}_{\hat{\text{pa}}(\rho_i)}$ and Z_k is a function of $\hat{Z}_{\hat{\text{pa}}(\rho_i)}$. Then, using (221), we know that \hat{Z}_{ρ_i} is a function of only $\hat{Z}_{\hat{\text{pa}}(\rho_i)}$ and N_i , which concludes the proof that \hat{Z} is Markov with respect to $\hat{\mathcal{G}}$.

B.5 Proof of Lemma 7

Proof of the scaling consistency. First, note that for the output of Algorithm 3, we have

$$\hat{Z}(X; \mathbf{H}^*) = \mathbf{P}_{\mathcal{I}} \cdot \mathbf{L} \cdot Z , \quad (224)$$

for some lower triangular matrix \mathbf{L} such that the diagonal entries of \mathbf{L} are non-zero and $j \notin \text{an}(i)$ implies $\mathbf{L}_{i,j} = 0$. Our goal is to find an unmixing matrix \mathbf{V} such that

$$\hat{Z}(\mathbf{V} \cdot \mathbf{H}^*) = \mathbf{V} \cdot \mathbf{P}_{\mathcal{I}} \cdot \mathbf{L} \cdot Z \quad (225)$$

satisfies the scaling consistency. To this end, our goal is to construct \mathbf{V} that satisfies

$$\mathbb{1}\{\mathbf{V} \cdot \mathbf{P}_{\mathcal{I}} \cdot \mathbf{L}\} = \mathbf{P}_{\mathcal{I}} . \quad (226)$$

Note that $\mathbf{V} = \mathbf{P}_{\mathcal{I}} \cdot \mathbf{L}^{-1} \cdot \mathbf{P}_{\mathcal{I}}^\top$ satisfies (226). Furthermore, since I^π is a valid causal order, we know that the desired matrix \mathbf{V} should have non-zero diagonal entries and satisfy $\mathbf{V}_{\pi_i, \pi_j} = 0$ for $i < j$. We will prove that Algorithm 4 achieves this solution up to scaling, and subsequently, Lemma 7 holds. For this purpose, we use the properties of hard interventions as follows. We know that, under hard interventions, in environment \mathcal{E}^m we have

$$Z_{I^m}^m \perp\!\!\!\perp Z_j^m, \quad \forall j \in \text{nd}(I^m), \quad (227)$$

in which $\text{nd}(I^m)$ denotes the set of non-descendants of I^m . Also recall that $(I^{\pi_1}, \dots, I^{\pi_n})$ is a valid causal order which implies that $\text{nd}(I^{\pi_k})$ contains $\{I^{\pi_1}, \dots, I^{\pi_{k-1}}\}$. Hence, for \mathbf{V} to satisfy $\mathbb{1}\{\mathbf{V} \cdot \mathbf{P}_{\mathcal{I}} \cdot \mathbf{L}\} = \mathbf{P}_{\mathcal{I}}$, the term $\tilde{Z} \triangleq \hat{Z}(\mathbf{V} \cdot \mathbf{H}^*)$ needs to satisfy

$$\tilde{Z}_{\pi_k}^{\pi_k} \perp\!\!\!\perp \tilde{Z}_{\pi_j}^{\pi_k}, \quad \forall j \in \{1, \dots, k-1\}. \quad (228)$$

This independence relation implies that

$$\text{Cov}(\tilde{Z}_{\pi_k}^{\pi_k}, \tilde{Z}_{\pi_j}^{\pi_k}) = 0, \quad \forall j \in [k-1]. \quad (229)$$

We leverage this property and use the covariance as a surrogate of independence. Specifically, at each step of the algorithm, we enforce the $(k-1)$ -dimensional covariance vector corresponding to node π_k and its nondescendants to be zero. In the rest of the proof, we show that this procedure eliminates mixing and achieves scaling consistency.

Since we know that our target \mathbf{V} has non-zero diagonal entries and satisfies $\mathbf{V}_{\pi_i, \pi_j} = 0$ for $i < j$, we start with the initialization $\mathbf{V} = \mathbf{I}_{n \times n}$. When learning the row vector \mathbf{V}_{π_k} , we are effectively estimating only entries $\mathbf{V}_{\pi_k, j}$ for $j \in \{\pi_1, \dots, \pi_{k-1}\}$. First, consider $k = 1$. Using the fact that I^{π_1} is a root node, the initialization $\mathbf{V} = \mathbf{I}_{n \times n}$ yields

$$[\mathbb{1}\{\mathbf{V} \cdot \mathbf{P}_{\mathcal{I}} \cdot \mathbf{L}\}]_{\pi_1, j} = \begin{cases} 1 & \text{if } j = I^{\pi_1}, \\ 0 & \text{otherwise} \end{cases}. \quad (230)$$

Next, assume that for all $\ell \in \{1, \dots, k-1\}$, we have

$$[\mathbb{1}\{\mathbf{V} \cdot \mathbf{P}_{\mathcal{I}} \cdot \mathbf{L}\}]_{\pi_\ell, j} = \begin{cases} 1 & \text{if } j = I^{\pi_\ell}, \\ 0 & \text{otherwise} \end{cases}. \quad (231)$$

We will prove that (231) also holds for $\ell = k$. Consider step k of Algorithm 4, in which we update row vector \mathbf{V}_{π_k} while keeping the previously learned row vectors $\mathbf{V}_{\pi_1}, \dots, \mathbf{V}_{\pi_{k-1}}$ fixed. Then, for any column vector $v \in \mathbb{R}^{n \times 1}$, we have

$$\text{Cov}\left(v^\top \cdot \hat{Z}^{\pi_k}, \tilde{Z}_{\pi_j}\right) = \underbrace{\mathbf{V}_{\pi_j} \cdot \mathbf{P}_{\mathcal{I}} \cdot \mathbf{L} \cdot \text{Cov}(Z^{\pi_k}) \cdot \mathbf{L}^\top \cdot \mathbf{P}_{\mathcal{I}}^\top \cdot v}_{\triangleq \mathbf{B}_j}, \quad \forall j \in \{1, \dots, k-1\}, \quad (232)$$

in which $\mathbf{B}_j \in \mathbb{R}^{1 \times n}$ is a row vector. Then, using (232) and concatenating the vectors $\{\mathbf{B}_j : j \in [k-1]\}$ to form matrix $\mathbf{B} \in \mathbb{R}^{(k-1) \times n}$, we obtain

$$\text{Cov}\left(v^\top \cdot \hat{Z}^{\pi_k}, [\tilde{Z}_{\pi_1}, \dots, \tilde{Z}_{\pi_{k-1}}]\right) = \mathbf{B} \cdot v. \quad (233)$$

We are searching for a vector v that makes $\mathbf{B} \cdot v$ a zero vector. Note that $\text{Cov}(Z^{\pi_k})$ is a full-rank matrix since causal relationships are not deterministic. Also, by construction,

$$\exists i \in [k-1] : \mathbf{V}_{\pi_i, j} \neq 0 \iff j \in \{\pi_1, \dots, \pi_{k-1}\}. \quad (234)$$

Therefore, $\mathbf{B} \in \mathbb{R}^{(k-1) \times n}$ is an unknown full-rank matrix. Note that we can obtain entries of \mathbf{B} by computing

$$\mathbf{B}_{j, \ell} = \text{Cov}(\hat{Z}_{\pi_j}^{\pi_k}, \tilde{Z}_{\pi_\ell}), \quad \forall j, \ell \in [k-1]. \quad (235)$$

This procedure corresponds to the inner for loop in Algorithm 4 for which

$$\mathbf{A}_{j, \ell} = \mathbf{B}_{j, \pi_\ell}, \quad \forall j, \ell \in [k-1]. \quad (236)$$

Then, \mathbf{A} is also a full-rank matrix, since it is a principal submatrix of the following symmetric positive semidefinite matrix

$$\mathbf{V} \cdot (\mathbf{P}_{\mathcal{I}} \cdot \mathbf{L}) \cdot \text{Cov}(Z^{\pi_k}) \cdot (\mathbf{P}_{\mathcal{I}} \cdot \mathbf{L})^\top \cdot \mathbf{V}^\top. \quad (237)$$

We also obtain π_k -th column of \mathbf{B} , denoted by b in Algorithm 4, as follows

$$b \triangleq \text{Cov}(\hat{Z}_{\pi_k}^{\pi_k}, [\tilde{Z}_{\pi_1}, \dots, \tilde{Z}_{\pi_{k-1}}]). \quad (238)$$

Recall that we are searching for a vector $v \in \mathbb{R}^{n \times 1}$ with the properties $v_{\pi_k} \neq 0$, and $v_{\pi_j} = 0$ for all $j > k$ such that $\mathbf{B} \cdot v$ becomes a zero vector. These conditions require that

$$\mathbf{B} \cdot v = [\mathbf{A} \ b] \cdot \begin{bmatrix} v_{\pi_1} \\ \vdots \\ v_{\pi_k} \end{bmatrix} = \mathbf{0}^{(k-1) \times 1}. \quad (239)$$

The identity in (239) has a unique solution up to scaling. That is, by fixing $v_{\pi_k} = 1$, we have

$$\begin{bmatrix} v_{\pi_1} \\ \vdots \\ v_{\pi_{k-1}} \end{bmatrix} = -\mathbf{A}^{-1} \cdot b. \quad (240)$$

Note that Algorithm 4 sets

$$\mathbf{V}_{\pi_k, \pi_j} = -\mathbf{A}^{-1} \cdot b = v_{\pi_j}, \quad \forall j \in [k-1]. \quad (241)$$

Hence, the algorithm has found a unique solution (up to scaling)

$$\mathbf{V}_{\pi_k} = [\mathbf{P}_{\mathcal{I}} \cdot \mathbf{L}^{-1} \cdot \mathbf{P}_{\mathcal{I}}^\top]_{\pi_k}. \quad (242)$$

Therefore, by induction, we have

$$\mathbf{V} = \mathbf{P}_{\mathcal{I}} \cdot \mathbf{L}^{-1} \cdot \mathbf{P}_{\mathcal{I}}^\top, \quad (243)$$

which satisfies $\mathbb{1}\{\mathbf{V} \cdot \mathbf{P}_{\mathcal{I}} \cdot \mathbf{L}\} = \mathbf{P}_{\mathcal{I}}$. Finally, using $\mathbb{1}\{\mathbf{V} \cdot \mathbf{P}_{\mathcal{I}} \cdot \mathbf{L}\} = \mathbf{P}_{\mathcal{I}}$ in (225), we obtain

$$\hat{Z}(\mathbf{V} \cdot \mathbf{H}^*) = \mathbf{C}_s \cdot \mathbf{P}_{\mathcal{I}} \cdot Z, \quad (244)$$

in which \mathbf{C}_s is a diagonal matrix, and the proof is complete.

Proof of the perfect DAG recovery. We show that the graph construction process in (58) achieves perfect DAG recovery as follows. First, using Lemma 2 and (244), we have

$$s_{\hat{Z}}(\hat{Z}; h) - s_{\hat{Z}}^m(\hat{Z}; h) = (\mathbf{C}_s \cdot \mathbf{P}_{\mathcal{I}})^{-\top} \cdot [s(Z) - s^m(Z)] . \quad (245)$$

Subsequently, using the fact that \mathbf{C}_s is a diagonal matrix, we obtain

$$[s_{\hat{Z}}(\hat{Z}; h) - s_{\hat{Z}}^m(\hat{Z}; h)]_i \neq 0 \iff [s(Z) - s^m(Z)]_{I^i} \neq 0 . \quad (246)$$

Then, using Lemma 1, we have

$$I^i \in \overline{\text{pa}}(I^m) \iff \mathbb{E} \left[\left| [s(Z) - s^m(Z)]_{\rho_i} \right| \right] \neq 0 \quad (247)$$

$$\iff [s_{\hat{Z}}(\hat{Z}; h) - s_{\hat{Z}}^m(\hat{Z}; h)]_i \neq 0 \quad (248)$$

$$\iff i \in \hat{\text{pa}}(m) \cup \{m\} . \quad (249)$$

This concludes the proof that $\hat{\mathcal{G}}$ and \mathcal{G} are related through a graph isomorphism by permutation \mathcal{I} , which denotes the intervention order.

B.6 Proof of Lemma 15

First, note that $\mathbf{L}_{\text{sur}} \preccurlyeq \mathbf{L}_{\text{an}}$. Hence, we start with considering a generic lower triangular matrix \mathbf{L} such that $\mathbf{I}_{n \times n} \preccurlyeq \mathbb{1}(\mathbf{L}) \preccurlyeq \mathbf{L}_{\text{an}}$. Matrix \mathbf{L} can be decomposed as

$$\mathbf{L} = \mathbf{E} \cdot (\mathbf{I}_{n \times n} + \Lambda) , \quad (250)$$

in which \mathbf{E} is a diagonal matrix and Λ is a strictly upper triangular matrix that satisfies $\mathbb{1}(\Lambda) \preccurlyeq \mathbb{1}(\mathbf{L}_{\text{an}})$. Subsequently, since \mathbf{E} is a diagonal matrix, we have

$$\mathbf{L}^{-1} = (\mathbf{I}_{n \times n} + \Lambda)^{-1} \cdot \mathbf{E}^{-1} , \quad \text{and} \quad \mathbb{1}\{\mathbf{L}^{-1}\} = \mathbb{1}\{(\mathbf{I}_{n \times n} + \Lambda)^{-1}\} . \quad (251)$$

Note that Λ is a strictly upper triangular $n \times n$ matrix, which implies that Λ^n is a zero matrix. Therefore, the inverse of $(\mathbf{I}_{n \times n} + \Lambda)$ can be expanded as

$$(\mathbf{I}_{n \times n} + \Lambda)^{-1} = \mathbf{I}_{n \times n} - \Lambda + \Lambda^2 - \cdots + (-1)^{n-1} \Lambda^{n-1} . \quad (252)$$

If $[\mathbf{I}_{n \times n} + \Lambda]_{i,j}^{-1} \neq 0$ for some $i, j \in [n]$ with $i < j$, by (252) we have $[\Lambda^k]_{i,j} \neq 0$ for some $k \in [n-1]$. Expanding matrix Λ^k yields that $[\Lambda^k]_{i,j}$ is equal to the sum of the products with k terms, i.e.,

$$[\Lambda^k]_{i,j} = \sum_{i < a_1 < \cdots < a_{k-1} < j} [\Lambda]_{i,a_1} [\Lambda]_{a_1,a_2} \cdots [\Lambda]_{a_{k-1},j} . \quad (253)$$

Therefore, if $[\Lambda^k]_{i,j} \neq 0$, there exists a sequence of entries $([\Lambda]_{i,a_1}, [\Lambda]_{a_1,a_2}, \dots, [\Lambda]_{a_{k-1},j})$ in which all terms are non-zero. Next, we prove the two cases as follows.

Case 1: Since $\mathbb{1}(\Lambda) \preccurlyeq \mathbb{1}(\mathbf{L}_{\text{an}})$, we have $[\mathbf{L}_{\text{an}}]_{i,a_1} = [\mathbf{L}_{\text{an}}]_{a_1,a_2} = \cdots = [\mathbf{L}_{\text{an}}]_{a_{k-1},j} = 1$. By the definition of \mathbf{L}_{an} , this means that

$$\overline{\text{de}}(j) \subseteq \text{de}(a_{k-1}) \subset \cdots \subset \text{de}(a_1) \subset \text{de}(i) , \quad (254)$$

which also implies that $[\mathbf{L}_{\text{an}}]_{i,j} = 1$. Therefore, we conclude that

$$[(\mathbf{I}_{n \times n} + \Lambda)^{-1}]_{i,j} \neq 0 \implies [\mathbf{L}_{\text{an}}]_{i,j} = 1 . \quad (255)$$

Hence, $\mathbf{I}_{n \times n} \preccurlyeq \mathbb{1}(\mathbf{L}^{-1}) \preccurlyeq \mathbf{L}_{\text{an}}$.

Case 2: Since $\mathbb{1}(\Lambda) \preccurlyeq \mathbb{1}(\mathbf{L}_{\text{sur}})$, we have $[\mathbf{L}_{\text{sur}}]_{i,a_1} = [\mathbf{L}_{\text{sur}}]_{a_1,a_2} = \dots = [\mathbf{L}_{\text{sur}}]_{a_{k-1},j} = 1$. By the definition of \mathbf{L}_{sur} , this means that

$$\overline{\text{ch}}(j) \subseteq \text{ch}(a_{k-1}) \subset \dots \subset \text{ch}(a_1) \subset \text{ch}(i), \quad (256)$$

which also implies $[\mathbf{L}_{\text{sur}}]_{i,j} = 1$ since $\overline{\text{ch}}(j) \subseteq \text{ch}(i)$. Therefore, we conclude that if

$$[(\mathbf{I}_{n \times n} + \Lambda)^{-1}]_{i,j} \neq 0 \implies [\mathbf{L}_{\text{sur}}]_{i,j} = 1. \quad (257)$$

Hence, $\mathbf{I}_{n \times n} \preccurlyeq \mathbb{1}(\mathbf{L}^{-1}) \preccurlyeq \mathbf{L}_{\text{sur}}$.

Appendix C. Proofs of the Results for General Transformations

In this section, we first prove identifiability in the coupled environments along with the observational environment case (Theorem 4). Then, we show that the result can be extended to coupled environments without observational environment (Theorem 5) and uncoupled environments (Theorem 6).

For convenience, we recall the following equations from the main paper. For each $h \in \mathcal{H}$ we define $\phi_h \triangleq h \circ g$. Then, $\hat{Z}(X; h)$ and Z are related as

$$\hat{Z}(X; h) = h(X) = (h \circ g)(Z) = \phi_h(Z). \quad (258)$$

Then, by setting $f = \phi_h^{-1}$, Lemma 2 yields

$$\text{between } \mathcal{E}^0 \text{ and } \mathcal{E}^m : \quad s_{\hat{Z}}(\hat{z}; h) - s_{\hat{Z}}^m(\hat{z}; h) = [J_{\phi_h}(z)]^{-\top} \cdot [s(z) - s^m(z)], \quad (259)$$

$$\text{between } \mathcal{E}^0 \text{ and } \tilde{\mathcal{E}}^m : \quad s_{\hat{Z}}(\hat{z}; h) - \tilde{s}_{\hat{Z}}^m(\hat{z}; h) = [J_{\phi_h}(z)]^{-\top} \cdot [s(z) - \tilde{s}^m(z)], \quad (260)$$

$$\text{between } \mathcal{E}^m \text{ and } \tilde{\mathcal{E}}^m : \quad s_{\hat{Z}}^m(\hat{z}; h) - \tilde{s}_{\hat{Z}}^m(\hat{z}; h) = [J_{\phi_h}(z)]^{-\top} \cdot [s^m(z) - \tilde{s}^m(z)]. \quad (261)$$

C.1 Proof of Lemma 11

The crucial component of our proofs for general transformations is Lemma 11 which states that the number of variations between the score estimates $s_{\hat{Z}}^m(\hat{z}; h)$ and $\tilde{s}_{\hat{Z}}^m(\hat{z}; h)$ cannot be less than the number of variations under the true encoder g^{-1} , that is $n = \|\mathbf{D}_t\|_0$. First, we provide the following linear algebraic property.

Proposition 3 *If $\mathbf{A} \in \mathbb{R}^{n \times n}$ is a full-rank matrix, then there exists a permutation matrix \mathbf{P} such that the diagonal entries of $\mathbf{P} \cdot \mathbf{A}$ are non-zero.*

Proof: Denote the set of all permutations of $[n]$ by \mathcal{S}_n . From Leibniz formula for matrix determinants, we have

$$\det(\mathbf{A}) = \sum_{\pi \in \mathcal{S}_n} \text{sign}(\pi) \cdot \prod_{i=1}^n \mathbf{A}_{i,\pi_i} \quad (262)$$

where $\text{sign}(\pi)$ for a permutation π of $[n]$ is $+1$ and -1 for even and odd permutations, respectively. \mathbf{A} is invertible if and only if $\det(\mathbf{A}) \neq 0$, which implies that

$$\exists \pi \in \mathcal{S}_n : \text{sign}(\pi) \cdot \prod_{i=1}^n \mathbf{A}_{i,\pi_i} \neq 0. \quad (263)$$

By the definition of \mathbf{P}_π , we have $[\mathbf{P}_\pi \cdot \mathbf{A}]_{i,i} = \mathbf{A}_{i,\pi_i}$. Then, all diagonal entries of $\mathbf{P} \cdot \mathbf{A}$ are non-zero. \square

Recall the definition of score change matrix $\mathbf{D}_t(h)$ in (64). Using (261), we can write entries of $\mathbf{D}_t(h)$ equivalently as

$$[\mathbf{D}_t(h)]_{i,m} = \mathbb{E} \left[\left| [J_{\phi_h}^{-\top}(Z)]_i \cdot [s^m(Z) - \tilde{s}^m(Z)] \right| \right], \quad \forall i, m \in [n]. \quad (264)$$

Since $\phi_h = h \circ g$ is a diffeomorphism, $[J_{\phi_h}^{-\top}(z)]$ is full-rank for all $(h, z) \in \mathcal{H} \times \mathbb{R}^n$. Using Proposition 3, for all (h, z) , there exists a permutation $\pi(h, z)$ of $[n]$ with permutation matrix $\mathbf{P}_1(h, z)$ such that

$$[\mathbf{P}_1(h, z) \cdot J_{\phi_h}^{-\top}(z)]_{i,i} \neq 0, \quad \forall i \in [n], \quad \text{where } \mathbf{P}_1(h, z) \triangleq \mathbf{P}_{\pi(h, z)}. \quad (265)$$

Next, recall that interventional discrepancy between q and \tilde{q} means that, for each $i \in [n]$, there exists a null set $\mathcal{T}_i \subset \mathbb{R}$ such that $[s^{\rho_i}(z)]_i \neq [\tilde{s}^{\rho_i}(z)]_i$ for all $z_i \in \mathcal{K} \setminus \mathcal{T}_i$ (regardless of the value of other coordinates of z). Then, there exists a null set $\mathcal{T} \subset \mathbb{R}^n$ such that $[s^{\rho_i}(z)]_i \neq [\tilde{s}^{\rho_i}(z)]_i$ for all $i \in [n]$ for all $z \in \mathbb{R}^n \setminus \mathcal{T}$. We denote this set $\mathbb{R}^n \setminus \mathcal{T}$ by \mathcal{Z} as follows:

$$\mathcal{Z} \triangleq \{z \in \mathbb{R}^n : [s^{\rho_i}(z)]_i \neq [\tilde{s}^{\rho_i}(z)]_i, \quad \forall i \in [n]\}. \quad (266)$$

Then, for all $z \in \mathcal{Z}$, $h \in \mathcal{H}$, and $i \in [n]$, we have

$$[\mathbf{D}_t(h)]_{\pi_i(h, z), \rho_i} = \mathbb{E} \left[\left| [J_{\phi_h}^{-\top}(Z)]_{\pi_i(h, z)} \cdot [s^{\rho_i}(Z) - \tilde{s}^{\rho_i}(Z)] \right| \right] \quad (267)$$

$$= \mathbb{E} \left[\left| [J_{\phi_h}^{-\top}(Z)]_{\pi_i(h, z), i} \cdot [s^{\rho_i}(Z) - \tilde{s}^{\rho_i}(Z)]_i \right| \right], \quad (268)$$

in which $\pi_i(h, z)$ denotes the i -th element of the permutation $\pi(h, z)$. By the definition of $\pi(h, z)$, for any $z \in \mathcal{Z}$, we know that $[J_{\phi_h}^{-\top}(z)]_{\pi_i(h, z), i} \neq 0$. Furthermore, by the definition of \mathcal{Z} , we have $[s^{\rho_i}(z) - \tilde{s}^{\rho_i}(z)]_i \neq 0$ for $z \in \mathcal{Z}$. Then, we have $[\mathbf{D}_t(h)]_{\pi_i(h, z), \rho_i} \neq 0$, which implies

$$\mathbb{1}\{\mathbf{D}_t(h)\} \succcurlyeq \mathbf{P}_1^\top(h, z) \cdot \mathbf{P}_\rho, \quad \forall h \in \mathcal{H}, \quad \forall z \in \mathcal{Z}. \quad (269)$$

Therefore, $\|\mathbf{D}_t(h)\|_0 \geq \|\mathbf{P}_\rho\|_0 = n$ for any $h \in \mathcal{H}$, and the proof is concluded since we have $\mathbb{1}\{\mathbf{D}_t\} = \mathbf{P}_\rho$.

C.2 Proof of Theorem 4

First, we investigate the perfect recovery of latent variables.

Recovering the latent variables. We recover the latent variables using only the coupled interventional environments $\{(\mathcal{E}^m, \tilde{\mathcal{E}}^m) : m \in [n]\}$. Let ρ be the permutation that maps $\{1, \dots, n\}$ to \mathcal{I} , i.e., $I^{\rho_i} = i$ for all $i \in [n]$ and \mathbf{P}_ρ to denote the permutation matrix that corresponds to ρ , i.e.,

$$[\mathbf{P}_\rho]_{i,m} = \begin{cases} 1, & m = \rho_i, \\ 0, & \text{else.} \end{cases} \quad (270)$$

Since we consider coupled atomic interventions, the only varying causal mechanism between \mathcal{E}^{ρ_i} and $\tilde{\mathcal{E}}^{\rho_i}$ is that of the intervened node in $I^{\rho_i} = \tilde{I}^{\rho_i} = i$. Then, by Lemma 1(iii), we have

$$\mathbb{E} \left[\left| [s^m(Z) - \tilde{s}^m(Z)]_k \right| \right] \neq 0 \iff k = i. \quad (271)$$

We recall the definition of true score change matrix \mathbf{D}_t in (67) with entries for all $i, m \in [n]$,

$$[\mathbf{D}_t]_{i,m} \triangleq \mathbb{E} \left[\left| [s^m(Z) - \tilde{s}^m(Z)]_i \right| \right]. \quad (272)$$

Then, using (271), we have

$$\mathbb{1}\{\mathbf{D}_t\} = \mathbf{P}_\rho = \mathbf{P}_\mathcal{I}^\top. \quad (273)$$

Therefore, the lower bound for ℓ_0 norm in Lemma 11 is achieved if and only if $\mathbb{1}\{\mathbf{D}_t(h)\} = \mathbf{P}_\rho$, which is an unknown permutation matrix. Since the only diagonal permutation matrix is $\mathbf{I}_{n \times n}$, the solution set of the constrained optimization problem in (70) is given by

$$\mathcal{H}_1 \triangleq \{h \in \mathcal{H} : \mathbb{1}\{\mathbf{D}_t(h)\} = \mathbf{I}_{n \times n}\}. \quad (274)$$

Next, consider some fixed solution $h^* \in \mathcal{H}_1$. Due to (269), we have

$$\mathbb{1}\{\mathbf{D}_t(h^*)\} = \mathbf{I}_{n \times n} \succcurlyeq \mathbf{P}_1^\top(h^*, z) \cdot \mathbf{P}_\rho, \quad (275)$$

which implies that we must have $\mathbf{P}_1(h^*, z) = \mathbf{P}_\rho$ for all $z \in \mathcal{Z}$. Then, $\pi_i(h^*, z) = \rho_i$ for all $i \in [n]$. We will show that for all $i \neq j$, we have

$$[J_{\phi_{h^*}}^{-1}(z)]_{j,\rho_i} = 0, \quad \forall z \in \mathbb{R}^n \quad (276)$$

To show (276), first consider $i \neq j$, which implies $[\mathbf{D}_t(h^*)]_{\rho_i, \rho_j} = 0$ since $\mathbb{1}\{\mathbf{D}_t(h^*)\} = \mathbf{I}_{n \times n}$. Then, using (264), $\mathbb{1}\{\mathbf{D}_t(h^*)\} = \mathbf{I}_{n \times n}$ and Lemma 1(i), we have

$$[\mathbf{D}_t(h^*)]_{\rho_i, \rho_j} = \mathbb{E} \left[\left| [J_{\phi_{h^*}}^{-1}(Z)]_{\rho_i} \cdot [s^{\rho_j}(Z) - \tilde{s}^{\rho_j}(Z)] \right| \right] \quad (277)$$

$$= \mathbb{E} \left[\left| [J_{\phi_{h^*}}^{-1}(Z)]_{j,\rho_i} \cdot [s^{\rho_j}(Z) - \tilde{s}^{\rho_j}(Z)]_j \right| \right] \quad (278)$$

$$= 0. \quad (279)$$

Note that $[s^{\rho_j}(z) - \tilde{s}^{\rho_j}(z)]_j \neq 0$ for all $z \in \mathcal{Z}$. Hence, if $[J_{\phi_{h^*}}^{-1}(z)]_{j,\rho_i}$ is non-zero over a non-zero-measure set within \mathcal{Z} , then $[\mathbf{D}_t(h^*)]_{\rho_i, \rho_j}$ would not be zero. Therefore, $[J_{\phi_{h^*}}^{-1}(z)]_{j,\rho_i} = 0$ on a set of measure 1. Since $J_{\phi_{h^*}}^{-1}$ is a continuous function, this implies that

$$[J_{\phi_{h^*}}^{-1}(z)]_{j,\rho_i} = 0, \quad z \in \mathbb{R}^n. \quad (280)$$

To see this, suppose that $[J_{\phi_{h^*}}^{-1}(z^*)]_{j,\rho_i} > 0$ for some $z^* \in \mathcal{Z}$. Due to continuity, there exists an open set including z^* for which $[J_{\phi_{h^*}}^{-1}(z^*)]_{j,\rho_i} > 0$, and since open sets have non-zero measure, we reach a contradiction. Therefore, if $i \neq j$, $[J_{\phi_{h^*}}^{-1}(z)]_{j,\rho_i} = 0$ for all $z \in \mathbb{R}^n$. Since $J_{\phi_{h^*}}^{-1}(z)$ must be full-rank for all $z \in \mathbb{R}^n$, we have

$$[J_{\phi_{h^*}}^{-1}(z)]_{i,\rho_i} \neq 0, \quad \forall z \in \mathbb{R}^n, \forall i \in [n]. \quad (281)$$

Then, for any $h^* \in \mathcal{H}_1$, $[\hat{Z}(X; h^*)]_{\rho_i} = [\phi_{h^*}(Z)]_{\rho_i}$ is a function of only Z_i , and we have

$$[\hat{Z}(X; h^*)]_{\rho_i} = \phi_{h^*}(Z_i), \quad \forall i \in [n], \quad (282)$$

which concludes the proof.

Recovering the latent graph Consider the selected solution $h^* \in \mathcal{H}_1$. We construct the graph $\hat{\mathcal{G}}$ as follows. We create n nodes and assign the non-zero coordinates of ρ_j -th column of $\mathbf{D}(h^*)$ as the parents of node ρ_j in $\hat{\mathcal{G}}$, i.e.,

$$\hat{\text{pa}}(\rho_j) \triangleq \left\{ \rho_i \neq \rho_j : [\mathbf{D}(h^*)]_{\rho_i, \rho_j} \neq 0 \right\}, \quad \forall j \in [n]. \quad (283)$$

Using (65) and (259), we have

$$\hat{\text{pa}}(\rho_j) \stackrel{(65)}{=} \left\{ \rho_i \neq \rho_j : \mathbb{E} \left[\left| [s_{\hat{Z}}(\hat{Z}; h^*) - \tilde{s}_{\hat{Z}}^{\rho_j}(\hat{Z}; h^*)]_{\rho_i} \right| \right] \neq 0 \right\} \quad (284)$$

$$\stackrel{(259)}{=} \left\{ \rho_i \neq \rho_j : \mathbb{E} \left[\left| [J_{\phi_{h^*}}^{-\top}(Z)]_{\rho_i} \cdot [s(Z) - \tilde{s}^{\rho_j}(Z)] \right| \right] \neq 0 \right\} \quad (285)$$

$$= \left\{ \rho_i \neq \rho_j : \mathbb{E} \left[\left| [J_{\phi_{h^*}}^{-\top}(Z)]_{\rho_i, i} \cdot [s(Z) - \tilde{s}^{\rho_j}(Z)]_i \right| \right] \neq 0 \right\}. \quad (286)$$

Since $[J_{\phi_{h^*}}^{-\top}(z)]_{\rho_i, i} \neq 0$ for all $z \in \mathbb{R}^n$, we have

$$\hat{\text{pa}}(\rho_j) = \left\{ \rho_i \neq \rho_j : \mathbb{E} \left[\left| [s(Z) - \tilde{s}^{\rho_j}(Z)]_i \right| \right] \neq 0 \right\}. \quad (287)$$

From Lemma 1(i), $\mathbb{E} \left[\left| [s(Z) - \tilde{s}^{\rho_j}(Z)]_i \right| \right] \neq 0$ if and only if $i \in \overline{\text{pa}}(j)$. Therefore, (283) implies that $\rho_i \in \hat{\text{pa}}(\rho_j)$ if and only if $i \in \text{pa}(j)$, which shows that \mathcal{G} and $\hat{\mathcal{G}}$ are related through a graph isomorphism by permutation ρ , which was defined as \mathcal{I}^{-1} .

C.3 Proof of Theorem 5

In the proof of Theorem 4, we showed that coupled hard interventions (without using observational environment) are sufficient for recovering the latent variables. Then, in this proof, we just focus on recovering the latent graph. Specifically, we will show that if p (pdf of Z) is adjacency-faithful to \mathcal{G} and the latent causal model is an additive noise model, then we can recover \mathcal{G} without having access to observational environment \mathcal{E}^0 . By Lemma 1(iv), true latent score changes across $\{\mathcal{E}^{\rho_i}, \tilde{\mathcal{E}}^{\rho_j}\}$ gives us $\overline{\text{pa}}(i, j)$ for $i \neq j$. First, we use the perfect latent recovery result to show that Lemma 1(iv) also applies to estimated latent score changes. Specifically, using (261) and $\mathbb{1}\{J_{\phi_{h^*}}^{-1}\} = \mathbf{P}_\rho$, we have

$$[s_{\hat{Z}}^{\rho_i}(\hat{Z}; h^*) - \tilde{s}_{\hat{Z}}^{\rho_j}(\hat{Z}; h^*)]_{\rho_k} = [J_{\phi_{h^*}}^{-\top}(z)]_{\rho_k} \cdot [s^{\rho_i}(z) - \tilde{s}^{\rho_j}(z)] \quad (288)$$

$$= [J_{\phi_{h^*}}^{-\top}(z)]_{\rho_k, k} \cdot [s^{\rho_i}(z) - \tilde{s}^{\rho_j}(z)]_k. \quad (289)$$

Recall that we have found $[J_{\phi_{h^*}}^{-\top}(z)]_{\rho_k, k} \neq 0$ for all $z \in \mathbb{R}^n$ in (281). Then, we have

$$\mathbb{E} \left[\left| [s_{\hat{Z}}^{\rho_i}(\hat{Z}; h^*) - \tilde{s}_{\hat{Z}}^{\rho_j}(\hat{Z}; h^*)]_{\rho_k} \right| \right] \neq 0 \iff \mathbb{E} \left[\left| [s^{\rho_i}(Z) - \tilde{s}^{\rho_j}(Z)]_k \right| \right] \neq 0. \quad (290)$$

Hence, by Lemma 1(iv),

$$\mathbb{E} \left[\left| [s_{\hat{Z}}^{\rho_i}(\hat{Z}; h^*) - \tilde{s}_{\hat{Z}}^{\rho_j}(\hat{Z}; h^*)]_{\rho_k} \right| \right] \neq 0 \iff k \in \overline{\text{pa}}(i, j). \quad (291)$$

Let us denote the graph \mathcal{G}_ρ that is related to \mathcal{G} by permutation ρ , i.e., $i \in \text{pa}(j)$ if and only if $\rho_i \in \text{pa}_\rho(\rho_j)$ for which $\text{pa}_\rho(\rho_j)$ denotes the parents of node ρ_j in \mathcal{G}_ρ . Using (291), we have

$$\mathbb{E} \left[\left| [s_{\hat{Z}}^{\rho_i}(\hat{Z}; h^*) - \tilde{s}_{\hat{Z}}^{\rho_j}(\hat{Z}; h^*)]_{\rho_k} \right| \right] \neq 0 \iff \rho_k \in \overline{\text{pa}}_\rho(\rho_i, \rho_j). \quad (292)$$

In the rest of the proof, we will show how to obtain $\{\text{pa}_\rho(i) : i \in [n]\}$ using $\{\overline{\text{pa}}_\rho(i, j) : i, j \in [n], i \neq j\}$. Since \mathcal{G}_ρ is a graph isomorphism of \mathcal{G} , this problem is equivalent to obtaining $\{\text{pa}(i) : i \in [n]\}$ using $\{\overline{\text{pa}}(i, j) : i, j \in [n], i \neq j\}$. Note that \hat{Z}_i (which corresponds to node i in \mathcal{G}_ρ) is intervened in environments \mathcal{E}^i and $\tilde{\mathcal{E}}^i$. We denote the set of root nodes by

$$\mathcal{K} \triangleq \{i \in [n] : \text{pa}(i) = \emptyset\}, \quad (293)$$

and also define

$$\mathcal{B}_i \triangleq \bigcap_{j \neq i} \overline{\text{pa}}(i, j), \quad \forall i \in [n], \quad \text{and} \quad \mathcal{B} \triangleq \{i : |\mathcal{B}_i| = 1\}. \quad (294)$$

Note that $\overline{\text{pa}}(i) \subseteq \mathcal{B}_i$. Hence, $|\mathcal{B}_i| = 1$ implies that i is a root node. We investigate the graph recovery in three cases.

1. $|\mathcal{B}| \geq 3$: For any node $i \in [n]$, we have

$$\overline{\text{pa}}(i) \subseteq \mathcal{B}_i \subseteq \bigcap_{j \in \mathcal{K} \setminus \{i\}} \overline{\text{pa}}(i, j) = \overline{\text{pa}}(i) \cup \left\{ \bigcap_{j \in \mathcal{K} \setminus \{i\}} \{j\} \right\} = \overline{\text{pa}}(i). \quad (295)$$

Note that, the last equality is due to $\bigcap_{j \in \mathcal{K} \setminus \{i\}} \{j\} = \emptyset$ since there are at least two root nodes excluding i . Then, $\mathcal{B}_i = \overline{\text{pa}}(i)$ for all $i \in [n]$ and we are done.

2. $|\mathcal{B}| = 2$: The two nodes in \mathcal{B} are root nodes. If there were at least three root nodes, we would have at least three nodes in \mathcal{B} . Hence, the two nodes in \mathcal{B} are the only root nodes. Subsequently, every $i \notin \mathcal{B}$ is also not in \mathcal{K} and we have

$$\overline{\text{pa}}(i) \subseteq \mathcal{B}_i \subseteq \bigcap_{j \in \mathcal{K}} \overline{\text{pa}}(i, j) = \overline{\text{pa}}(i) \cup \left\{ \bigcap_{j \in \mathcal{K}} \{j\} \right\} = \overline{\text{pa}}(i). \quad (296)$$

Hence, $\mathcal{B}_i = \overline{\text{pa}}(i)$ for every non-root node i and we already have the two root nodes in \mathcal{B} , which completes the graph recovery.

3. $|\mathcal{B}| \leq 1$: First, consider all (i, j) pairs such that $|\overline{\text{pa}}(i, j)| = 2$. For such an (i, j) pair, at least one of the nodes is a root node, otherwise $\overline{\text{pa}}(i, j)$ would contain a third node. Using these pairs, we identify all root nodes as follows. Note that a hard intervention on node i makes Z_i independent of all of its non-descendants, and all conditional independence relations are preserved under element-wise diffeomorphisms such as ϕ_{h^*} . Then, using the adjacency-faithfulness assumption, we infer that

- if $\hat{Z}_i \perp\!\!\!\perp \hat{Z}_j$ in \mathcal{E}^i and $\hat{Z}_i \perp\!\!\!\perp \hat{Z}_j$ in $\tilde{\mathcal{E}}^j$, then both i and j are root nodes.
- if $\hat{Z}_i \not\perp\!\!\!\perp \hat{Z}_j$ in \mathcal{E}^i , then $i \rightarrow j$ and i is a root node.

- if $\hat{Z}_i \not\perp\!\!\!\perp \hat{Z}_j$ in $\tilde{\mathcal{E}}^j$, then $j \rightarrow i$ and j is a root node.

This implies that by using at most two independence tests, we can determine whether i and j nodes are root nodes. Hence, by at most n independence tests, we identify all root nodes. We also know that there are at most two root nodes. If we have two root nodes, then $\mathcal{B}_i = \overline{\text{pa}}(i)$ for all non-root nodes, and the graph is recovered. If we have only one root node i , then for any $j \neq i$ we have

$$\overline{\text{pa}}(j) \subseteq \mathcal{B}_j \subseteq \overline{\text{pa}}(i, j) = \overline{\text{pa}}(j) \cup \{i\}. \quad (297)$$

Finally, if $\hat{Z}_j \perp\!\!\!\perp \hat{Z}_i \mid \{\hat{Z}_\ell : \ell \in \mathcal{B}_j \setminus \{i\}\}$ in $\tilde{\mathcal{E}}^j$, we have $i \notin \overline{\text{pa}}(j)$ due to adjacency-faithfulness. Otherwise, we conclude that $i \in \overline{\text{pa}}(j)$. Hence, an additional $(n - 1)$ conditional independence tests ensure the recovery of all $\overline{\text{pa}}(j)$ sets, and the graph recovery is complete.

C.4 Proof of Lemma 12

We will prove it by contradiction. Suppose that h^* is a solution to the optimization problem \mathcal{P}_2 specified in (71). Using the fact that $[J_{\phi_{h^*}}^{-\top}(z)]$ is full-rank for all $z \in \mathbb{R}^n$, and the score difference vector $[s^{\rho_i}(z) - \tilde{s}^{\rho_i}(z)]$ is not identically zero, (264) and Proposition 2 imply that $\mathbf{D}_t(h^*)$ does not have any zero columns. Subsequently, $\|\mathbf{D}_t(h^*)\|_0 \geq n$, and since $\mathbf{D}_t(h^*)$ is diagonal, we have $\mathbb{1}\{\mathbf{D}_t(h^*)\} = \mathbf{I}_{n \times n}$. We use $J^* \triangleq J_{\phi_{h^*}}^{-\top}$ as shorthand. If $\rho_i = \tilde{\rho}_i$ for some $i \in [n]$, using $\mathbf{D}_t(h^*) = \mathbf{I}_{n \times n}$ and Lemma 1(iii), for $j \neq i$, we have

$$0 = [\mathbf{D}_t(h^*)]_{\rho_j, \rho_i} \quad (298)$$

$$= \mathbb{E} \left[\left| [J^*(Z)]_{\rho_j} \cdot [s^{\rho_i}(Z) - \tilde{s}^{\rho_i}(Z)] \right| \right] \quad (299)$$

$$= \mathbb{E} \left[\left| [J^*(Z)]_{\rho_j, i} \cdot [s^{\rho_i}(Z) - \tilde{s}^{\rho_i}(Z)]_i \right| \right]. \quad (300)$$

Recall that, by interventional discrepancy between q and \tilde{q} , we have $[s^{\rho_i}(z) - \tilde{s}^{\rho_i}(z)]_i \neq 0$ except for a null set. Then, (298) implies that we have $[J^*(z)]_{\rho_j, i} = 0$ except for a null set. Since J^* is continuous, this implies that $[J^*(z)]_{\rho_j, i} = 0$ for all $z \in \mathbb{R}^n$. Furthermore, since $J^*(z)$ is invertible for all z , none of its columns can be a zero vector. Hence, for all $z \in \mathbb{R}^n$, $[J^*(z)]_{\rho_j, i} \neq 0$. To summarize, if $\rho_i = \tilde{\rho}_i$, we have

$$\forall z \in \mathbb{R}^n \quad [J^*(z)]_{j, i} \neq 0 \iff j = \rho_i. \quad (301)$$

Now, consider the set of *mismatched nodes*

$$\mathcal{A} \triangleq \{i \in [n] : \rho_i \neq \tilde{\rho}_i\}. \quad (302)$$

Let $a \in \mathcal{A}$ be a non-descendant of all the other nodes in \mathcal{A} . There exist nodes $b, c \in \mathcal{A}$, not necessarily distinct, such that

$$\rho_a = \tilde{\rho}_b, \quad \text{and} \quad \rho_c = \tilde{\rho}_a. \quad (303)$$

In four steps, we will show that $\mathbf{D}(h^*)_{\rho_a, \rho_c} \neq 0$ and $\mathbf{D}(h^*)_{\rho_c, \rho_a} \neq 0$, which violates the constraint $\mathbb{1}\{\mathbf{D}(h)\} \odot \mathbb{1}\{\mathbf{D}^\top(h)\} = \mathbf{I}_{n \times n}$ and will conclude the proof by contradiction. Before giving the

steps, we provide the following argument which we repeatedly use in the rest of the proof. For any continuous function $f : \mathbb{R}^n \rightarrow \mathbb{R}$, we have

$$\mathbb{E}[|f(Z)|] \neq 0 \iff \mathbb{E}\left[|f(Z) \cdot [s(Z) - s^{\rho_a}(Z)]_a|\right] \neq 0, \quad (304)$$

$$\text{and } \mathbb{E}[|f(Z)|] \neq 0 \iff \mathbb{E}\left[|f(Z) \cdot [s(Z) - \tilde{s}^{\rho_c}(Z)]_a|\right] \neq 0. \quad (305)$$

First, suppose that $\mathbb{E}[|f(Z)|] \neq 0$. Then, there exists an open set $\Psi \subseteq \mathbb{R}^n$ for which $f(z) \neq 0$ for all $z \in \Psi$. Due to interventional discrepancy between p and q , there exists an open set within Ψ for which $[s^{\rho_a}(Z) - s(Z)]_a \neq 0$. This implies that

$$\mathbb{E}\left[|f(Z) \cdot [s(Z) - s^{\rho_a}(Z)]_a|\right] \neq 0. \quad (306)$$

For the other direction, suppose that $\mathbb{E}[|f(Z) \cdot [s^{\rho_a}(Z) - s(Z)]_a|] \neq 0$, which implies that there exists an open set Ψ for which both $f(z)$ and $[s^{\rho_a}(z) - s(z)]_a$ are non-zero. Then, $\mathbb{E}[|f(Z)|] \neq 0$, and we have (304). Similarly, due to $\rho_c = \tilde{\rho}_a$ and interventional discrepancy between p_a and \tilde{q}_a , we obtain (305).

Step 1: Show that $\mathbb{E}[|[J^*(Z)]_{\rho_a,a}|] \neq 0$. First, using (264) and Lemma 1(i), we have

$$[\mathbf{D}(h^*)]_{\rho_a, \rho_a} = \mathbb{E}\left[|[J^*(Z)]_{\rho_a} \cdot [s(Z) - s^{\rho_a}(Z)]_a|\right] \quad (307)$$

$$= \mathbb{E}\left[\left| \sum_{j \in \overline{\text{pa}}(a)} [J^*(Z)]_{\rho_a, j} \cdot [s(Z) - s^{\rho_a}(Z)]_j \right| \right]. \quad (308)$$

Note that $\overline{\text{pa}}(a) \cap \mathcal{A} = \{a\}$ since a is non-descendant of the other nodes in \mathcal{A} . Consider $j \in \text{pa}(a)$, which implies that $j \notin \mathcal{A}$ and $\rho_j = \tilde{\rho}_j$. By (301), we have $[J^*(Z)]_{\rho_a, j} = 0$. Then, (308) becomes

$$[\mathbf{D}(h^*)]_{\rho_a, \rho_a} = \mathbb{E}\left[|[J^*(Z)]_{\rho_a, a} \cdot [s(Z) - s^{\rho_a}(Z)]_a|\right] \neq 0, \quad (309)$$

since diagonal entries of $\mathbf{D}(h^*)$ are non-zero due to the last constraint in (71). Then, (304) implies that $\mathbb{E}[|[J^*(Z)]_{\rho_a, a}|] \neq 0$.

Step 2: Show that $[\tilde{\mathbf{D}}(h^*)]_{\rho_a, \rho_c} \neq 0$. Next, we use $\rho_c = \tilde{\rho}_a$ and Lemma 1(i) to obtain

$$[\tilde{\mathbf{D}}(h^*)]_{\rho_a, \rho_c} = \mathbb{E}\left[|[J^*(Z)]_{\rho_a} \cdot [s(Z) - \tilde{s}^{\rho_c}(Z)]_c|\right] \quad (310)$$

$$= \mathbb{E}\left[\left| \sum_{j \in \overline{\text{pa}}(a)} [J^*(Z)]_{\rho_a, j} \cdot [s(Z) - \tilde{s}^{\rho_c}(Z)]_j \right| \right] \quad (311)$$

$$= \mathbb{E}\left[|[J^*(Z)]_{\rho_a, a} \cdot [s(Z) - \tilde{s}^{\rho_c}(Z)]_a|\right]. \quad (312)$$

Using (305) and Step 1 result, we have $[\tilde{\mathbf{D}}(h^*)]_{\rho_a, \rho_c} \neq 0$.

Step 3: Show that $\mathbb{E}\left[\left| [J^*(Z)]_{\rho_c, a} \right| \right] \neq 0$. Using (264) and Lemma 1(i), we have

$$[\tilde{\mathbf{D}}(h^*)]_{\rho_c, \rho_c} = \mathbb{E}\left[\left| [J^*(Z)]_{\rho_c} \cdot [s(Z) - \tilde{s}^{\rho_c}(Z)] \right| \right] \quad (313)$$

$$= \mathbb{E}\left[\left| \sum_{j \in \overline{\text{pa}}(a)} [J^*(Z)]_{\rho_c, j} \cdot [s(Z) - \tilde{s}^{\rho_c}(Z)]_j \right| \right] \quad (314)$$

$$= \mathbb{E}\left[\left| [J^*(Z)]_{\rho_c, a} \cdot [s(Z) - \tilde{s}^{\rho_c}(Z)]_a \right| \right]. \quad (315)$$

Since $\mathbb{1}\{\mathbf{D}(h^*)\} = \mathbb{1}\{\tilde{\mathbf{D}}(h^*)\}$, the diagonal entry $[\tilde{\mathbf{D}}(h^*)]_{\rho_c, \rho_c}$ is non-zero. Then, using (305) we have $\mathbb{E}\left[\left| [J^*(Z)]_{\rho_c, a} \right| \right] \neq 0$.

Step 4: Show that $[\mathbf{D}(h^*)]_{\rho_c, \rho_a} \neq 0$. Next, we use $\rho_c = \tilde{\rho}_a$ and Lemma 1(i) to obtain

$$[\tilde{\mathbf{D}}(h^*)]_{\rho_c, \rho_a} = \mathbb{E}\left[\left| [J^*(Z)]_{\rho_c} \cdot [s(Z) - s^{\rho_a}(Z)] \right| \right] \quad (316)$$

$$= \mathbb{E}\left[\left| \sum_{j \in \overline{\text{pa}}(a)} [J^*(Z)]_{\rho_c, j} \cdot [s(Z) - s^{\rho_a}(Z)]_j \right| \right] \quad (317)$$

$$= \mathbb{E}\left[\left| [J^*(Z)]_{\rho_c, a} \cdot [s(Z) - s^{\rho_a}(Z)]_a \right| \right]. \quad (318)$$

Using (304) and Step 3 result, we have $[\mathbf{D}(h^*)]_{\rho_c, \rho_a} \neq 0$.

However, using the constraint $\mathbb{1}\{\mathbf{D}(h^*)\} = \mathbb{1}\{\tilde{\mathbf{D}}(h^*)\}$, we have $[\mathbf{D}(h^*)]_{\rho_a, \rho_c} \neq 0$. Then, $[\mathbf{D}(h^*) \odot \mathbf{D}^\top(h^*)]_{\rho_a, \rho_c} \neq 0$, which violates the last constraint in (71). Therefore, if the coupling is incorrect, optimization problem \mathcal{P}_2 has no feasible solution.

C.5 Proof of Lemma 13

We consider the true encoder g^{-1} under the permutation ρ^{-1} , that is $h = \rho^{-1} \circ g^{-1}$, and show that it is a solution to \mathcal{P}_2 specified in (71). First, note that $\phi_h = \rho^{-1} \circ g^{-1} \circ g = \rho^{-1}$, which is just a permutation. Hence, $J_{\phi_h}^{-\top}$ becomes the permutation matrix \mathbf{P}_ρ^\top . Then, for all $i, m \in [n]$ we have

$$[\mathbf{D}_t(h)]_{\rho_i, m} = \mathbb{E}\left[\left| [\mathbf{P}_\rho^\top]_{\rho_i} \cdot [s^m(Z) - \tilde{s}^m(Z)] \right| \right] = \mathbb{E}\left[\left| [s^m(Z) - \tilde{s}^m(Z)]_i \right| \right]. \quad (319)$$

Then, by Lemma 1(i), we have $[\mathbf{D}_t(h)]_{\rho_i, m} \neq 0$ if and only if $i = I^m$, which means $m = \rho_i$ and $\mathbf{D}_t(h)$ is a diagonal matrix. Hence, h satisfies the first constraint. Next, consider $\mathbf{D}(h)$. For all $i, j \in [n]$, we have

$$[\mathbf{D}_t(h)]_{\rho_i, \rho_j} = \mathbb{E}\left[\left| [\mathbf{P}_\rho^\top]_{\rho_i} \cdot [s(Z) - s^{\rho_j}(Z)] \right| \right] = \mathbb{E}\left[\left| [s^{\rho_j}(Z) - \tilde{s}^{\rho_j}(Z)]_i \right| \right]. \quad (320)$$

By Lemma 1(i), we have $[\mathbf{D}(h)]_{\rho_i, \rho_j} \neq 0$ if and only if $i = \overline{\text{pa}}(j)$. Since $\rho = \tilde{\rho}$, similarly, we have $[\tilde{\mathbf{D}}(h_\rho)]_{\rho_i, \rho_j} \neq 0$ if and only if $i \in \overline{\text{pa}}(j)$. Therefore, we have $\mathbb{1}\{\mathbf{D}(h)\} = \mathbb{1}\{\tilde{\mathbf{D}}(h)\}$, $\mathbf{D}(h)$ has full diagonal and it does not have non-zero values in symmetric entries. Hence, h satisfies the second and third constraints. Therefore, h is a solution to \mathcal{P}_2 since it satisfies all constraints and the diagonal matrix $\mathbf{D}_t(h)$ has $\|\mathbf{D}_t(h)\|_0 = n$, which is the lower bound established.

C.6 Proof of Theorem 6

Recall that $\tilde{\mathcal{I}} = \{\tilde{I}^1, \dots, \tilde{I}^n\}$ is the permutation of intervened nodes in $\tilde{\mathcal{E}}$, so coupling π considered in (71) is just equal to $\tilde{\mathcal{I}}$. Similarly to the definition of ρ for \mathcal{I} in the proof of Theorem 4, let $\tilde{\rho}$ be the permutation that maps $\{1, \dots, n\}$ to $\tilde{\mathcal{I}}$, i.e., $I^{\tilde{\rho}_i} = i$ for all $i \in [n]$. Then, $\mathbf{P}_{\tilde{\rho}}$ denotes the permutation matrix for the intervention order of the environments $\{\tilde{\mathcal{E}}^1, \dots, \tilde{\mathcal{E}}^n\}$, i.e.,

$$[\mathbf{P}_{\tilde{\rho}}]_{i,j} = \begin{cases} 1, & j = \tilde{\rho}_i, \\ 0, & \text{else.} \end{cases} \quad (321)$$

Lemma 12 shows that if the coupling is incorrect, i.e., $\pi \neq \mathcal{I}$ or equivalently $\rho \neq \tilde{\rho}$, the optimization problem in (71) does not have a feasible solution. Next, Lemma 13 shows that if the coupling is correct, i.e., $\rho = \tilde{\rho}$, there exists a solution to \mathcal{P}_2 . Lemmas 12 and 13 collectively prove identifiability as follows. We can search over the permutations of $[n]$ until \mathcal{P}_2 admits a solution h^* . By Lemma 12, the existence of this solution means that coupling is correct. Note that when the coupling is correct, the constraint set of \mathcal{P}_1 is a subset of the constraints in \mathcal{P}_2 . Furthermore, the minimum value of $\|\mathbf{D}_t(h)\|_0$ is lower bounded by n (Lemma 11), which is achieved by the solution h^* (Lemma 13). Hence, h^* is also a solution to \mathcal{P}_1 , and by Theorem 4, it satisfies perfect recovery of the latent DAG and the latent variables.

Appendix D. Analysis of the Assumptions

D.1 Analysis of Assumption 1

In this subsection, we prove Lemma 9 statement, i.e., Assumption 1 is satisfied for additive noise models under hard interventions, as follows.

Score decomposition. Consider a hard interventional environment \mathcal{E}^m and let $I^m = i$ be the intervened node. Following (4) and (16), the latent scores $s(z)$ and $s^m(z)$ are decomposed as

$$s(z) = \nabla_z \log p_i(z_i | z_{\text{pa}(i)}) + \sum_{j \neq i} \nabla_z \log p_j(z_j | z_{\text{pa}(j)}), \quad (322)$$

$$\text{and } s^m(z) = \nabla_z \log q_i(z_i) + \sum_{j \neq i} \nabla_z \log p_j(z_j | z_{\text{pa}(j)}). \quad (323)$$

Hence, $s(z)$ and $s^m(z)$ differ in only the causal mechanism of node i . Subsequently, we have

$$s(z) - s^m(z) = \nabla_z \log p_i(z_i | z_{\text{pa}(i)}) - \nabla_z \log q_i(z_i). \quad (324)$$

Focusing on the relevant two entries of the score difference, intervened node i and a parent $k \in \text{pa}(i)$,

$$\begin{bmatrix} [s - s^m]_k \\ [s - s^m]_i \end{bmatrix} = \begin{bmatrix} [\nabla_z \log p(z_i | z_{\text{pa}(i)})]_k \\ [\nabla_z \log p(z_i | z_{\text{pa}(i)})]_i - [\nabla_z \log q(z_i)]_i \end{bmatrix}. \quad (325)$$

Additive noise model. The additive noise model for node i is given by

$$Z_i = f_i(Z_{\text{pa}(i)}) + N_i, \quad (326)$$

as specified in (7). When node i is hard intervened, Z_i is generated according to

$$Z_i = \bar{N}_i, \quad (327)$$

in which \bar{N}_i denotes the exogenous noise term for the interventional model. Then, denoting the pdfs of N_i and \bar{N}_i by p_N and q_N , respectively, (326) and (327) imply that

$$p_i(z_i | z_{\text{pa}(i)}) = p_N(z_i - f_i(z_{\text{pa}(i)})), \quad \text{and} \quad q_i(z_i) = q_N(z_i). \quad (328)$$

Denote the score functions associated with p_N and q_N by

$$r_p(u) \triangleq \frac{d}{du} \log p_N(u) = \frac{p'_N(u)}{p_N(u)}, \quad \text{and} \quad r_q(u) \triangleq \frac{d}{du} \log q_N(u) = \frac{q'_N(u)}{q_N(u)}. \quad (329)$$

Define n_i and \bar{n}_i as the realizations of N_i and \bar{N}_i when $Z_i = z_i$ and $Z_{\text{pa}(i)} = z_{\text{pa}(i)}$. Then, we have $\bar{n}_i = n_i + f_i(z_{\text{pa}(i)})$. Using (328) and (329), we can express (325) as

$$\begin{bmatrix} [s - s^m]_k \\ [s - s^m]_i \end{bmatrix} = \begin{bmatrix} -\frac{\partial f_i(z_{\text{pa}(i)})}{\partial z_k} \cdot r_p(n_i) \\ r_p(n_i) - r_q(n_i + f_i(z_{\text{pa}(i)})) \end{bmatrix}. \quad (330)$$

Proof by contradiction. We will prove the desired result by contradiction. Assume that

$$\mathcal{R} \left(\begin{bmatrix} [s - s^m]_k \\ [s - s^m]_i \end{bmatrix} \right) < 2, \quad (331)$$

which implies that there exists a constant $\kappa \in \mathbb{R}$ such that

$$\kappa \cdot [s(z) - s^m(z)]_i = [s(z) - s^m(z)]_k, \quad \forall z \in \mathbb{R}^n. \quad (332)$$

Then, using (330), we have

$$\kappa \cdot \frac{\partial f_i(z_{\text{pa}(i)})}{\partial z_k} + 1 = \frac{r_q(n_i + f_i(z_{\text{pa}(i)}))}{r_p(n_i)}. \quad (333)$$

We scrutinize (333) in two cases.

Case 1: $\frac{\partial f_i(z_{\text{pa}(i)})}{\partial z_k}$ is constant. In this case, let $\eta = \frac{\partial f_i(z_{\text{pa}(i)})}{\partial z_k}$ for some $\eta \in \mathbb{R}$ for all $z_{\text{pa}(i)} \in \mathbb{R}^{|\text{pa}(i)|}$. Then, the RHS of (333) is also constant for all $z_{\text{pa}(i)} \in \mathbb{R}^{|\text{pa}(i)|}$ and $n_i \in \mathbb{R}$. Fix a realization $n_i = n_i^*$ and note that $f_i(z_{\text{pa}(i)})$ needs to be constant, denoted by δ^* , for all $z_{\text{pa}(i)} \in \mathbb{R}^{|\text{pa}(i)|}$. However, this implies that $\frac{\partial f_i(z_{\text{pa}(i)})}{\partial z_k} = 0$, and we have $r_q(n_i + \delta^*) = r_p(n_i)$ for all $n_i \in \mathbb{R}$. This implies that $p_N(n_i) = \eta^* q_N(n_i + \delta^*)$ for some constant η^* . Since p_N and q_N are pdfs, the only choice is $\eta^* = 1$ and $p_N(n_i) = q_N(n_i + \delta^*)$, then $p_i(z_i | z_{\text{pa}(i)}) = q_i(z_i)$, which contradicts the premise that an intervention changes the causal mechanism of the target node i .

Case 2: $\frac{\partial f_i(z_{\text{pa}(i)})}{\partial z_k}$ is not constant. In this case, note that LHS of (333) is not a function of n_i . Then, taking the derivative of both sides with respect to n_i and rearranging, we obtain

$$\frac{r'_p(n_i)}{r_p(n_i)} = \frac{r'_q(n_i + f_i(z_{\text{pa}(i)}))}{r_q(n_i + f_i(z_{\text{pa}(i)}))}, \quad \forall (n_i, z_{\text{pa}(i)}) \in \mathbb{R} \times \mathbb{R}^{|\text{pa}(i)|}. \quad (334)$$

Next, consider a fixed realization $n_i = n_i^*$, and denote the value of LHS by α . Since $f_i(z_{\text{pa}(i)})$ is continuous and not constant, its image contains an open interval $\Theta \subseteq \mathbb{R}$. Denoting $u \triangleq f_i(z_{\text{pa}(i)})$, we have

$$\alpha = \frac{r'_q(n_i^* + u)}{r_q(n_i^* + u)}, \quad \forall u \in \Theta. \quad (335)$$

The only solution to this equality is that $r_q(n_i^* + u)$ is an exponential function, $r_q(u) = k_1 \exp(\alpha u)$ over interval $u \in \Theta$. Since r_q is an analytic function that equals to an exponential function over an interval, it is exponential over entire \mathbb{R} . This implies that the pdf $q_N(u)$ is of the form $q_N(u) = k_2 \exp((k_1/\alpha) \exp(\alpha u))$. However, this cannot be a valid pdf since its integral over \mathbb{R} diverges. Then, (331) cannot be true and we have

$$\mathcal{R} \left(\begin{bmatrix} [s - s^m]_k \\ [s - s^m]_i \end{bmatrix} \right) = 2, \quad \text{where } i = I_m. \quad (336)$$

D.2 Analysis of Assumption 2

In this section, we establish the necessary and sufficient conditions under which Assumption 2 holds for additive models. Furthermore, we show that a large class of non-linear models in the latent space satisfy these conditions, including the two-layer neural networks. We have focused on such NNs since they effectively approximate continuous functions (Cybenko, 1989). Readily, the necessary and sufficient conditions can be investigated for other choices of non-linear functions.

D.2.1 INTERPRETING ASSUMPTION 2

The implication of Assumption 2 is that the effect of an intervention is not lost in any linear combination of the varying coordinates of the scores. To formalize this, for each node $i \in [n]$, we define

$$\mathcal{C}_i \triangleq \{c \in \mathbb{R}^n : \exists j \in \overline{\text{pa}}(i) \text{ such that } c_j \neq 0\}, \quad (337)$$

and provide the following equivalent condition which will simplify the subsequent analysis.

Assumption 3 Consider an atomic environment set \mathcal{E} . Then, for all $c \in \mathcal{C}_\ell$, we have

$$\mathbb{E} \left[\left| c^\top \cdot [s(Z) - s^m(Z)] \right| \right] \neq 0, \quad \text{where } \ell = I^m. \quad (338)$$

Lemma 16 Assumption 2 and Assumption 3 are equivalent.

Proof: First, note that for a random variable X , $\mathbb{E}[|X|] = 0$ if and only if $\mathbb{E}[X^2] = 0$ if and only if $X = 0$ almost surely. Consider environment \mathcal{E}^m and let $I^m = \ell$. Then, (338) holds if and only if

$$\mathbb{E}\left[\left(c^\top \cdot [s(Z) - s^m(Z)]\right)^2\right] \neq 0. \quad (339)$$

Next, note that $\mathcal{R}(s - s^m)$ is equal to the rank of the covariance matrix

$$\mathbf{E}^m \triangleq \mathbb{E}\left[\left[s(Z) - s^m(Z)\right] \cdot \left[s(Z) - s^m(Z)\right]^\top\right]. \quad (340)$$

By Lemma 1, the only nonzero entries of \mathbf{E}^m lie in the submatrix with row and columns indices $\overline{\text{pa}}(i)$. Since \mathbf{E}^m is a covariance matrix, it is symmetric and positive-semidefinite. Then, there exists a matrix \mathbf{F}^m such that $\mathbf{E}^m = [\mathbf{F}^m]^\top \cdot \mathbf{F}^m$ and j -th column of \mathbf{F}^m is a zero vector for all $j \notin \overline{\text{pa}}(i)$. Then, for any $c \in \mathbb{R}^n$, $\mathbf{F}^m \cdot c$ is a linear combination of the nonzero columns of \mathbf{F}^m with the coefficients $\{c_j : j \in \overline{\text{pa}}(i)\}$. Subsequently, we have

$$\mathbf{F}^m \cdot c \neq \mathbf{0}, \quad \forall c \in \mathcal{C}_i \iff \mathbf{E}^m \cdot c \neq \mathbf{0}, \quad \forall c \in \mathcal{C}_i \iff \text{rank}(\mathbf{E}^m) = |\overline{\text{pa}}(i)|, \quad (341)$$

which concludes the proof of Lemma 16.

Necessary and sufficient conditions. Consider the additive noise model for node i

$$Z_i = f_i(Z_{\text{pa}(i)}) + N_i, \quad (342)$$

as specified in (7). When node i is soft intervened, Z_i is generated according to

$$Z_i = \bar{f}_i(Z_{\text{pa}(i)}) + \bar{N}_i, \quad (343)$$

in which \bar{f}_i and \bar{N}_i specify the interventional mechanism for node i . The following lemma characterizes the necessary and sufficient conditions under which Assumption 3 is satisfied. In this subsection, we use φ as the shorthand for $z_{\text{pa}(i)}$.

Lemma 17 *For each node $i \in [n]$ consider the following two set of equations for $c \in \mathbb{R}^n$:*

$$\begin{cases} c_i - c^\top \cdot \nabla_z f_i(\varphi) = 0 \\ c_i - c^\top \cdot \nabla_z \bar{f}_i(\varphi) = 0 \end{cases}, \quad \forall \varphi \in \mathbb{R}^{|\overline{\text{pa}}(i)|}. \quad (344)$$

Assumption 3 holds if and only if the only all solutions c to (344) satisfy $c \notin \mathcal{C}_i$, or based on (337), equivalently

$$\forall j \in \overline{\text{pa}}(i) : \quad c_j = 0. \quad (345)$$

Proof: See Appendix D.2.2.

To provide some intuition about the conditions in Lemma 17, we consider a node $i \in [n]$ and discuss the conditions in the context of a few examples. Note that by sweeping $\varphi \in \mathbb{R}^{|\overline{\text{pa}}(i)|}$ we generate a continuum of linear equations of the form:

$$c_i - c^\top \cdot \nabla_z f_i(\varphi) = 0, \quad \text{and} \quad c_i - c^\top \cdot \nabla_z \bar{f}_i(\varphi) = 0. \quad (346)$$

Note that for all $j \notin \text{pa}(i)$ we have $[\nabla_z f_i(\varphi)]_j = [\nabla_z \bar{f}_i(\varphi)]_j = 0$. Hence, in finding the solutions to (346) only the coordinates $\{j \in \overline{\text{pa}}(i)\}$ of c are relevant. Let us define

$$u(\varphi) \triangleq \nabla_\varphi f_i(\varphi), \quad \text{and} \quad \bar{u}(\varphi) \triangleq \nabla_\varphi \bar{f}_i(\varphi), \quad (347)$$

which are the gradients of f_i and \bar{f}_i by considering only the coordinates of z in $\{j \in \text{pa}(i)\}$. Accordingly, we also define b by concatenating only the coordinates of c with their indices in $\{j \in \text{pa}(i)\}$. Next, consider w distinct choices of φ and denote them by $\{\varphi^t \in \mathbb{R}^{|\text{pa}(i)|} : t \in [w]\}$. By concatenating the two equations in (347) specialized to these realizations, we get the following linear system with $2w$ equations and $|\text{pa}(i)| + 1$ unknown variables.

$$\underbrace{\begin{bmatrix} [u(\varphi^1)]^\top & -1 \\ [\bar{u}(\varphi^1)]^\top & -1 \\ \vdots & \vdots \\ [u(\varphi^w)]^\top & -1 \\ [\bar{u}(\varphi^w)]^\top & -1 \end{bmatrix}}_{\triangleq \mathbf{V} \in \mathbb{R}^{2w \times (|\text{pa}(i)|+1)}} \begin{bmatrix} b \\ c_i \end{bmatrix} = \mathbf{0}_{2w}. \quad (348)$$

When \mathbf{V} is full-rank, i.e., $\text{rank}(\mathbf{V}) = |\text{pa}(i)| + 1$, the system has only the trivial solutions $c_i = 0$ and $b = \mathbf{0}$. Then, we make the following observations.

1. If f_i and \bar{f}_i are linear functions, the vector spaces generated by u and \bar{u} have dimensions 1. Subsequently, we always have $\text{rank}(\mathbf{V}) \leq 2$, rendering an underdetermined system when $|\text{pa}(i)| \geq 2$. Hence, when the maximum degree of \mathcal{G} is at least 2, a linear causal model does not satisfy Assumption 3.
2. If f_i and \bar{f}_i are quadratic with full-rank matrices, i.e., $f_i(\varphi) = \varphi^\top \mathbf{A} \varphi$ and $\bar{f}_i(\varphi) = \varphi^\top \bar{\mathbf{A}} \varphi$ where $\text{rank}(\mathbf{A}) = \text{rank}(\bar{\mathbf{A}}) = |\text{pa}(i)|$, there is a choice of $w \geq |\text{pa}(i)| + 1$ and realizations $\{\varphi^t \in \mathbb{R}^{|\text{pa}(i)|} : t \in [w]\}$ for which $\text{rank}(\mathbf{V}) = |\text{pa}(i)| + 1$ and the system in (346) admits only the trivial solutions $a_i = 0$ and $b = \mathbf{0}$. Hence, quadratic causal models satisfy Assumption 2.
3. If f_i and \bar{f}_i are two-layer NNs with a sufficiently large number of hidden neurons, they also render a fully determined system, and as a result, they satisfy Assumption 3.

We investigate the last example in detail as follows. Assume that f_i and \bar{f}_i are two-layer NNs with $|\text{pa}(i)|$ inputs, w_i and \bar{w}_i hidden nodes, respectively, and with sigmoid activation functions. Denote the weight matrices between input and hidden layers in f_i and \bar{f}_i by $\mathbf{W}^i \in \mathbb{R}^{w_i \times |\text{pa}(i)|}$ and $\bar{\mathbf{W}}^i \in \mathbb{R}^{\bar{w}_i \times |\text{pa}(i)|}$, respectively. Furthermore, define $\nu \in \mathbb{R}^{w_i}$ and $\bar{\nu} \in \mathbb{R}^{\bar{w}_i}$ as the weights between the hidden layer and output in f_i and \bar{f}_i , respectively. Finally, define ν_0 and $\bar{\nu}_0$ as the bias terms. Hence, we have

$$f_i(\varphi) = \nu^\top \cdot \sigma(\mathbf{W}^i \cdot \varphi) + \nu_0 = \sum_{j=1}^{w_i} \nu_j \cdot \sigma(\mathbf{W}_j^i \cdot \varphi) + \nu_0, \quad (349)$$

$$\text{and} \quad \bar{f}_i(\varphi) = \bar{\nu}^\top \cdot \sigma(\bar{\mathbf{W}}^i \cdot \varphi) + \bar{\nu}_0 = \sum_{j=1}^{\bar{w}_i} \bar{\nu}_j \cdot \sigma(\bar{\mathbf{W}}_j^i \cdot \varphi) + \bar{\nu}_0, \quad (350)$$

in which activation function σ is applied element-wise.

Lemma 10 Consider NNs f_i and \bar{f}_i specified in (349) and (350). If for all $i \in [n]$ we have

$$\max\{\text{rank}(\mathbf{W}^i), \text{rank}(\bar{\mathbf{W}}^i)\} = |\text{pa}(i)|, \quad (351)$$

then Assumption 3 holds.

Proof: See Appendix D.2.3.

D.2.2 PROOF OF LEMMA 17

We show that for each node $i \in [n]$, the condition

$$\mathbb{E}\left[\left|c^\top \cdot [s(Z) - s^m(Z)]\right|\right] \neq 0, \quad \forall c \in \mathcal{C}_i, \quad (352)$$

holds if and only if the following continuum of equations admit their solutions c in $\mathbb{R}^n \setminus \mathcal{C}_i$.

$$\begin{cases} c_i - c^\top \cdot \nabla_z f_i(\varphi) = 0 \\ c_i - c^\top \cdot \nabla_z \bar{f}_i(\varphi) = 0 \end{cases}, \quad \forall \varphi \in \mathbb{R}^{|\text{pa}(i)|}, \quad (353)$$

in which shorthand φ is used for $z_{\text{pa}(i)}$. Let \mathcal{E}^m be the environment in which node i is intervened. We first note that the condition in (352) can be equivalently stated as follows. Using (19), for all $c \in \mathcal{C}_i$ we have

$$\mathbb{E}\left[\left|c^\top \cdot [\nabla_z \log p_i(Z_i | Z_{\text{pa}(i)}) - \nabla_z \log q_i(Z_i | Z_{\text{pa}(i)})]\right|\right] \neq 0. \quad (354)$$

This can be readily verified by noting that

$$c^\top \cdot [s(z) - s^m(z)] \stackrel{(18),(19)}{=} c^\top \cdot [\nabla_z \log p(z_i | z_{\text{pa}(i)}) - \nabla_z \log q_i(z_i | z_{\text{pa}(i)})]. \quad (355)$$

Also, using Proposition 2, (354) is equivalent to

$$\forall c \in \mathcal{C}_i, \quad \exists z : \quad c^\top \cdot \nabla_z \log p_i(z_i | z_{\text{pa}(i)}) \neq c^\top \cdot \nabla_z \log q_i(z_i | z_{\text{pa}(i)}). \quad (356)$$

The additive noise model for node i is given by

$$Z_i = f_i(Z_{\text{pa}(i)}) + N_i, \quad (357)$$

as specified in (7). When node i is soft intervened, Z_i is generated according to

$$Z_i = \bar{f}_i(Z_{\text{pa}(i)}) + \bar{N}_i, \quad (358)$$

in which \bar{f}_i and \bar{N}_i specify the interventional mechanism for node i . Then, denoting the pdfs of N_i and \bar{N}_i by p_N and q_N , respectively, (357) and (358) imply that

$$p_i(z_i | z_{\text{pa}(i)}) = p_N(z_i - f_i(z_{\text{pa}(i)})), \quad \text{and} \quad q_i(z_i | z_{\text{pa}(i)}) = q_N(z_i - \bar{f}_i(z_{\text{pa}(i)})). \quad (359)$$

Denote the score functions associated with p_N and q_N by

$$r_p(u) \triangleq \frac{d}{du} \log p_N(u) = \frac{p'_N(u)}{p_N(u)}, \quad \text{and} \quad r_q(u) \triangleq \frac{d}{du} \log q_N(u) = \frac{q'_N(u)}{q_N(u)}. \quad (360)$$

Define n_i and \bar{n}_i as the realizations of N_i and \bar{N}_i when $Z_i = z_i$ and $Z_{\text{pa}(i)} = z_{\text{pa}(i)}$. By defining $\delta(z_{\text{pa}(i)}) \triangleq f_i(z_{\text{pa}(i)}) - \bar{f}_i(z_{\text{pa}(i)})$, we have $\bar{n}_i = n_i + \delta(z_{\text{pa}(i)})$. Using (360) and (359), we can express the relevant entries of $\nabla_z \log p_i(z_i | z_{\text{pa}(i)})$ and $\nabla_z \log q_i(z_i | z_{\text{pa}(i)})$ as

$$[\nabla_z \log p(z_i | z_{\text{pa}(i)})]_j = \begin{cases} r_p(n_i), & j = i, \\ -\frac{\partial f_i(z_{\text{pa}(i)})}{\partial z_j} r_p(n_i), & j \in \text{pa}(i), \\ 0, & j \notin \overline{\text{pa}}(i), \end{cases} \quad (361)$$

$$\text{and} \quad [\nabla_z \log q_i(z_i | z_{\text{pa}(i)})]_j = \begin{cases} r_q(\bar{n}_i), & j = i, \\ -\frac{\partial \bar{f}_i(z_{\text{pa}(i)})}{\partial z_j} r_q(\bar{n}_i), & j \in \text{pa}(i), \\ 0, & j \notin \overline{\text{pa}}(i). \end{cases} \quad (362)$$

By substituting (361)–(362) in (356) and rearranging the terms, the statement in (356) becomes equivalent to following statement. For all $c \in \mathcal{C}_i$, there exist $n_i \in \mathbb{R}$ and $z_{\text{pa}(i)} \in \mathbb{R}^{|\text{pa}(i)|}$ such that

$$r_p(n_i) \cdot \left(c_i - \sum_{j \in \text{pa}(i)} c_j \cdot \frac{\partial f_i(z_{\text{pa}(i)})}{\partial z_j} \right) \neq r_q(n_i + \delta(z_{\text{pa}(i)})) \cdot \left(c_i - \sum_{j \in \text{pa}(i)} c_j \cdot \frac{\partial \bar{f}_i(z_{\text{pa}(i)})}{\partial z_j} \right), \quad (363)$$

which by using the shorthand φ for $z_{\text{pa}(i)}$ can be compactly presented as follows. For all $c \in \mathcal{C}_i$, there exists $n_i \in \mathbb{R}$ and $\varphi \in \mathbb{R}^{|\text{pa}(i)|}$ such that

$$r_p(n_i) \cdot [c_i - c^\top \cdot \nabla_z f_i(\varphi)] \neq r_q(n_i + \delta(\varphi)) \cdot [c_i - c^\top \cdot \nabla_z \bar{f}_i(\varphi)]. \quad (364)$$

Hence, Assumption 3 is equivalent to the statement in (364), which we use for the rest of the proof.

Sufficient condition. We show that if (353) admit solutions c only in $\mathbb{R}^n \setminus \mathcal{C}_i$, then the statement in (364) holds. By contradiction, assume that there exists $c^* \in \mathcal{C}_i$ such that for all $n_i \in \mathbb{R}$ and $\varphi \in \mathbb{R}^{|\text{pa}(i)|}$,

$$r_p(n_i) \cdot [c_i^* - (c^*)^\top \cdot \nabla_z f_i(\varphi)] = r_q(n_i + \delta(\varphi)) \cdot [c_i^* - (c^*)^\top \cdot \nabla_z \bar{f}_i(\varphi)]. \quad (365)$$

We show that $c^* \in \mathcal{C}_i$ is also a solution to (353), contradicting the premise. In order to show that $c^* \in \mathcal{C}_i$ is also a solution to (353), suppose, by contradiction, that (365) holds, and there exists $\varphi^* \in \mathbb{R}^{|\text{pa}(i)|}$ corresponding to which

$$(c^*)^\top \cdot \nabla_z \bar{f}_i(\varphi^*) - c_i^* \neq 0. \quad (366)$$

Note that f_i is a continuously differentiable function and also a function of z_j for all $j \in \text{pa}(i)$. Hence, there exists an open set $\Phi \subseteq \mathbb{R}^{|\text{pa}(i)|}$ for φ for which $(c^*)^\top \cdot \nabla_z f_i(\varphi^*) - c_i^*$ is non-zero everywhere in Φ . Likewise, r_p cannot constantly be zero over all possible intervals Ω . This is because

otherwise, it would have to necessarily be a constant zero function (since it is analytic), which is an invalid score function. Hence, there exists an open interval $\Omega \subseteq \mathbb{R}$ over which $r_p(n_i)$ is non-zero for all $n_i \in \Omega$. Subsequently, the left-hand side of (365) is non-zero over the Cartesian product $(n_i, \varphi) \in \Omega \times \Phi$. This means that if (365) is true, then both functions on its right-hand side must be also non-zero over $\Omega \times \Phi$. Hence, by rearranging the terms in (365) we have

$$\frac{r_q(n_i + \delta(\varphi))}{r_p(n_i)} = \frac{c_i^* - (c^*)^\top \cdot \nabla_z f_i(\varphi)}{c_i^* - (c^*)^\top \cdot \nabla_z \bar{f}_i(\varphi)}, \quad \forall (n_i, \varphi) \in \Omega \times \Phi. \quad (367)$$

In two steps, we show that (367) cannot be valid.

Step 1. First, we show that function δ cannot be a constant over Φ (interval specified above). Suppose the contrary and assume that $\delta(\varphi) = \delta^*$ for all $\varphi \in \Phi$. Hence, the gradient of δ is zero. Using the definition of δ , this implies that

$$\nabla_z f_i(\varphi) = \nabla_z \bar{f}_i(\varphi), \quad \forall \varphi \in \Phi. \quad (368)$$

Then, by leveraging (367), we conclude that $r_p(n_i) = r_q(n_i + \delta^*)$ for all $n_i \in \Omega$. Since $r_p(n_i)$ and $r_q(n_i + \delta^*)$ are analytic functions that agree on an open interval of \mathbb{R} , they are equal for all $n_i \in \mathbb{R}$ as well. This implies that $p_N(n_i) = \eta \cdot q_N(n_i + \delta^*)$ for some constant η . Since p_N and q_N are pdfs, the only choice is $\eta = 1$ and $p_N(n_i) = q_N(n_i + \delta^*)$, then $p_i(z_i | z_{\text{pa}(i)}) = q_i(z_i | z_{\text{pa}(i)})$, which contradicts the premise.

Step 2. Finally, we will show that (367) cannot be true when δ is not a constant function over Φ . Note that the right-hand side of (367) is not a function of n_i . Then, taking the derivative of both sides with respect to n_i and rearranging, we obtain

$$\frac{r'_p(n_i)}{r_p(n_i)} = \frac{r'_q(n_i + \delta(\varphi))}{r_q(n_i + \delta(\varphi))}, \quad \forall (n_i, \varphi) \in \Omega \times \Phi. \quad (369)$$

Next, consider a fixed realization $n_i = n_i^*$, and denote the value of LHS by α . Since δ is continuous and not constant over Φ , its image contains an open interval $\Theta \subseteq \mathbb{R}$. Denoting $u \triangleq \delta(\varphi)$, we get

$$\alpha = \frac{r'_q(n_i^* + u)}{r_q(n_i^* + u)}, \quad \forall u \in \Theta. \quad (370)$$

The only solution to this equality is that $r_q(n_i^* + u)$ is an exponential function, $r_q(u) = k_1 \exp(\alpha u)$ over interval $u \in \Theta$. Since r_q is an analytic function that equals to an exponential function over an interval, it is exponential over entire \mathbb{R} . This implies that the pdf $q_N(u)$ is of the form $q_N(u) = k_2 \exp((k_1/\alpha) \exp(\alpha u))$. However, this cannot be a valid pdf since its integral over \mathbb{R} diverges. Hence, (367) is not true, and the premise that there exists $c^* \in \mathcal{C}_i$ and $\varphi \in \mathbb{R}^{|\text{pa}(i)|}$ corresponding to which (366) holds is invalid, concluding that for all $\varphi \in \mathbb{R}^{|\text{pa}(i)|}$ we have $c^{\top} \cdot \nabla_z \bar{f}_i(\varphi) = c_i$. Proving the counterpart identity $c^{\top} \cdot \nabla_z f_i(\varphi) = c_i$ follows similarly. Therefore, (365) implies

$$\begin{cases} c_i^* - (c^*)^\top \cdot \nabla_z f_i(\varphi) = 0 \\ c_i^* - (c^*)^\top \cdot \nabla_z \bar{f}_i(\varphi) = 0 \end{cases}, \quad \forall \varphi \in \mathbb{R}^{|\text{pa}(i)|}, \quad (371)$$

which means that we have found a solution to (353) that is not in $\mathbb{R}^n \setminus \mathcal{C}_i$, contradicting the premise.

Necessary condition. Assume that Assumption 3, and equivalently, the statement in (364) holds but (353) has a solution c^* in \mathcal{C}_i . Hence,

$$c_i^* - (c^*)^\top \cdot \nabla_z f_i(\varphi) = c_i^* - (c^*)^\top \cdot \nabla_z \bar{f}_i(\varphi) = 0, \quad \forall \varphi \in \mathbb{R}^{|\text{pa}(i)|}. \quad (372)$$

Then, multiplying left side by $r_p(n_i)$ and right side by $r_q(n_i + \delta(\varphi))$, we obtain that for all $n_i \in \mathbb{R}$ and $\varphi \in \mathbb{R}^{|\text{pa}(i)|}$

$$r_p(n_i) \cdot [c_i^* - (c^*)^\top \cdot \nabla_z f_i(\varphi)] = r_q(n_i + \delta(\varphi)) \cdot [c_i^* - (c^*)^\top \cdot \nabla_z \bar{f}_i(\varphi)] = 0, \quad (373)$$

which implies that for all $c \in \mathcal{C}_i$, $n_i \in \mathbb{R}$ and $\varphi \in \mathbb{R}^{|\text{pa}(i)|}$

$$r_p(n_i) \cdot [c_i - c^\top \cdot \nabla_z f_i(\varphi)] = r_q(n_i + \delta(\varphi)) \cdot [c_i - c^\top \cdot \nabla_z \bar{f}_i(\varphi)]. \quad (374)$$

This contradicts Assumption 3. Hence, the proof is complete.

D.2.3 PROOF OF LEMMA 10

Approach. We will use the same argument as at the beginning of the proof of Lemma 17. Specifically, we will show that for any node i and two-layer NNs f_i and \bar{f}_i with weight matrices \mathbf{W}^i and $\bar{\mathbf{W}}^i$, the following continuum of equations admit their solutions c in $\mathbb{R}^n \setminus \mathcal{C}_i$.

$$\begin{cases} c_i - c^\top \cdot \nabla_z \bar{f}_i(\varphi) = 0 \\ c_i - c^\top \cdot \nabla_z f_i(\varphi) = 0 \end{cases}, \quad \forall \varphi \in \mathbb{R}^{|\text{pa}(i)|}, \quad (375)$$

in which shorthand φ is used for $z_{\text{pa}(i)}$. Hence, by invoking Lemma 17, Assumption 3 holds.

Definitions. Define $d_i \triangleq |\text{pa}(i)|$. Since $\max\{\text{rank}(\mathbf{W}^i), \text{rank}(\bar{\mathbf{W}}^i)\} = d_i$, without loss of generality, suppose that $\mathbf{W}^i \in \mathbb{R}^{w_i \times d_i}$ has rank d_i . The rest of the proof follows similarly for the case of $\text{rank}(\bar{\mathbf{W}}^i) = d_i$. We use shorthand $\{\mathbf{W}, w\}$ for $\{\mathbf{W}^i, w_i\}$ when it is obvious from context.

Parameterization. Note that f_i can be represented by different parameterizations, some containing more hidden nodes than others. Without loss of generality, let w be the fewest number of nodes that can represent f_i . This implies that the entries of ν are non-zero. Otherwise, if $\nu_i = 0$, we can remove i -th hidden node and still have the same f_i . Similarly, the rows of \mathbf{W} are distinct. Otherwise, if there exist rows $\mathbf{W}_i = \mathbf{W}_j$ for distinct $i, j \in [w]$, removing j -th hidden node and using $(\nu_i + \nu_j)$ in place of ν_i results the same function as f_i with $(w - 1)$ hidden nodes. Similarly, we have $\mathbf{W}_i \neq \mathbf{0}$ for all $i \in [w]$. Otherwise, we have

$$\nu_i \cdot \sigma(\mathbf{W}_i \cdot \varphi) + \nu_0 = (\nu_0 + \frac{\nu_i}{2}), \quad (376)$$

and by removing i -th hidden node and using $(\nu_0 + \frac{\nu_i}{2})$ instead of ν_0 , we reach the same function as f_i with $(w - 1)$ hidden nodes. Finally, we have $\mathbf{W}_i + \mathbf{W}_j \neq \mathbf{0}$. Otherwise, we have

$$\nu_i \cdot \sigma(\mathbf{W}_i \cdot \varphi) + \nu_j \sigma(\mathbf{W}_j \cdot \varphi) + \nu_0 = (\nu_i - \nu_j) \cdot \sigma(\mathbf{W}_i \cdot \varphi) + (\nu_0 + \nu_j), \quad (377)$$

and by removing j -th hidden node and using $(\nu_i - \nu_j)$ instead of ν_i and $(\nu_0 + \nu_j)$ instead of ν_0 , we reach the same function as f_i with $(w - 1)$ hidden nodes. In summary, we have

$$\mathbf{W}_i \neq \mathbf{0}, \quad \nu_i \neq 0, \quad \forall i \in [w], \quad \text{and} \quad \mathbf{W}_i \pm \mathbf{W}_j \neq \mathbf{0}, \quad \forall i, j \in [w] : i \neq j. \quad (378)$$

We will show that there does not exist $c \in \mathcal{C}_i$ such that $c^\top \cdot \nabla_z f_i(\varphi) = c_i$ for all $\varphi \in \mathbb{R}^{d_i}$. Assume the contrary, and assume there exists $c^* \in \mathcal{C}_i$ such that

$$(c^*)^\top \cdot \nabla_z f_i(\varphi) = c_i^* , \quad \forall \varphi \in \mathbb{R}^{d_i} . \quad (379)$$

This is equivalent to showing that there exists non-zero $b^* \in \mathbb{R}^{d_i}$ such that

$$(b^*)^\top \cdot \nabla_\varphi f_i(\varphi) = c_i^* , \quad \forall \varphi \in \mathbb{R}^{d_i} . \quad (380)$$

Based on (349), the gradient of $f_i(\varphi)$ is

$$\nabla_\varphi f_i(\varphi) = \mathbf{W}^\top \cdot \text{diag}(\nu) \cdot \dot{\sigma}(W \cdot \varphi) , \quad (381)$$

where $\text{diag}(\nu)$ is the diagonal matrix with ν as its diagonal elements, and $\dot{\sigma}$ is the derivative of the sigmoid function, applied element-wise to its argument. Hence, based on (379), the contradiction premise is equivalent to having a non-zero $b^* \in \mathbb{R}^{d_i}$ such that

$$[\dot{\sigma}(W \cdot \varphi)]^\top \cdot \text{diag}(\nu) \cdot \mathbf{W} \cdot b^* = c_i , \quad \forall \varphi \in \mathbb{R}^{d_i} . \quad (382)$$

We note that since \mathbf{W} is full-rank and ν_i is non-zero for all $i \in [w]$, the matrix $\text{diag}(\nu) \cdot \mathbf{W}$ is full-rank as well and it has a trivial null space. Subsequently, $b^* \in \mathbb{R}^{d_i}$ is non-zero if and only if $(\text{diag}(\nu) \cdot \mathbf{W} \cdot b^*) \in \mathbb{R}^w$ is non-zero. We will use the following lemma to show that (382) cannot be true. This establishes that the contradiction premise is not correct, and completes the proof.

Lemma 18 *Let $u \in \mathbb{R}^p$ have non-zero entries with distinct absolute values, i.e., $u_i \neq 0$ and $|u_i| \neq |u_j|$ for all $i \neq j$, and $a \in \mathbb{R}$ be a constant. Then, for every non-zero vector $c \in \mathbb{R}^p$, there exists $\alpha \in \mathbb{R}$ such that $[\dot{\sigma}(\alpha u)]^\top \cdot c \neq a$.*

Proof: See Appendix D.2.4.

Let us define $\xi \triangleq \mathbf{W} \cdot \varphi$. We will show that there exists $\varphi^* \in \mathbb{R}^{d_i}$ such that $\xi = \mathbf{W} \cdot \varphi^*$ satisfies the conditions in Lemma 18. Then, using Lemma 18 with the choice of $u = \mathbf{W} \cdot \varphi^*$, $d = \text{diag}(\nu) \cdot \mathbf{W} \cdot b^*$, and $a = c_i$, we find that there exists $\alpha \in \mathbb{R}$ such that

$$[\dot{\sigma}(\alpha \cdot \mathbf{W} \cdot \varphi^*)]^\top \cdot \text{diag}(\nu) \cdot \mathbf{W} \cdot b^* \neq c_i . \quad (383)$$

Hence, (382) is false since it is violated for $\varphi = \alpha \varphi^*$ and the proof is completed. We show the existence of such φ^* as follows. We first construct the set of φ values for which conditions of Lemma 18 on w are *not* satisfied. The set in question is the union of the following cases: (i) $\xi_i = \mathbf{W}_i \cdot \varphi = 0$ for some $i \in [w]$, (ii) $|\xi_i| = |\xi_j|$ for some distinct $i, j \in [w]$, or equivalently, $(\mathbf{W}_i \pm \mathbf{W}_j)\varphi = 0$. Note that $\mathbf{W}_i \neq \mathbf{0}$ and $\mathbf{W}_i \pm \mathbf{W}_j \neq \mathbf{0}$ by (378). For a non-zero vector $y \in \mathbb{R}^{d_i}$, the set $\{\varphi \in \mathbb{R}^{d_i} : y^\top \varphi = 0\}$ is a $(d_i - 1)$ -dimensional subspace of \mathbb{R}^{d_i} . Then, there is w number of $(d_i - 1)$ -dimensional subspaces that fall under case (i), and $w(w - 1)$ number of $(d_i - 1)$ -dimensional subspaces that fall under case (ii). Therefore, there are w^2 lower-dimensional subspaces for which the conditions of Lemma 18 do not hold. However, \mathbb{R}^{d_i} cannot be covered by a finite number of lower-dimensional subspaces of itself. Therefore, there exists $\varphi^* \in \mathbb{R}^{d_i}$ such that $\xi = \mathbf{W} \cdot \varphi^*$ satisfies the conditions of Lemma 18, and the proof is completed.

D.2.4 PROOF OF LEMMA 18

Assume the contrary and suppose that there exists a non-zero d and a for a given u . Define the function $g_u(\alpha) \triangleq c^\top \cdot \dot{\sigma}(\alpha u)$. Note that

$$\dot{\sigma}(x) = \frac{1}{1 + e^{-x} + e^x} \quad (384)$$

is an even analytic function, and its Taylor series expansion at 0 has the domain of convergence $\{x \in \mathbb{R} : |x| < \frac{\pi}{2}\}$. Thus, for all $\alpha \in (-\frac{\pi}{2 \max_i |u_i|}, \frac{\pi}{2 \max_i |u_i|})$,

$$a = g_u(\alpha) = \sum_{j=1}^p c_j \cdot \dot{\sigma}(\alpha u_j) = \sum_{i=0}^{\infty} \gamma_i \sum_{j=1}^p c_j (\alpha u_j)^{2i} = \sum_{i=0}^{\infty} (\gamma_i \sum_{j=1}^p c_j u_j^{2i}) \alpha^{2i}. \quad (385)$$

Note that $g_u(\alpha)$ is a constant function of $\alpha \in (-\frac{\pi}{2 \max_i |u_i|}, \frac{\pi}{2 \max_i |u_i|})$. Thus, its Taylor coefficients, i.e., $(\gamma_i \sum_{j=1}^p c_j u_j^{2i})$, are zero for all $i \in \mathbb{N}^+$. However, the coefficients of even powers in Taylor expansion of $\dot{\sigma}$, i.e., γ_i 's, are non-zero (Weisstein, 2002). Therefore, we have $\sum_{i=1}^p (c_j u_j^{2i}) = 0$ for all $i \in \mathbb{N}^+$. Next, construct the following system of linear equations,

$$\begin{bmatrix} u_1^2 & u_1^4 & \dots & u_1^{2w} \\ \vdots & \vdots & \dots & \vdots \\ u_p^2 & u_p^4 & \dots & u_p^{2w} \end{bmatrix} \begin{bmatrix} c_1 \\ \vdots \\ c_p \end{bmatrix} = \mathbf{0}. \quad (386)$$

This is equivalent to

$$\text{diag}([u_1^2, \dots, u_p^2]^\top) \cdot \underbrace{\begin{bmatrix} 1 & u_1^2 & \dots & u_1^{2(p-1)} \\ \vdots & \vdots & \dots & \vdots \\ 1 & u_p^2 & \dots & u_p^{2(p-1)} \end{bmatrix}}_{\text{Vandermonde}} \cdot \begin{bmatrix} c_1 \\ \vdots \\ c_p \end{bmatrix} = \mathbf{0}. \quad (387)$$

Note that the Vandermonde matrix in (387) has determinant $\prod_{1 \leq i \leq j < p} (u_i^2 - u_j^2)$, which is non-zero since $|u_i| \neq |u_j|$ for $i \neq j$. Multiplying an invertible matrix with a diagonal invertible matrix generates another invertible matrix, and c must be a zero vector which is a contradiction. Hence, there does not exist such c for which $c^\top \cdot \dot{\sigma}(\alpha u)$ is constant for every $\alpha \in \mathbb{R}$.

D.3 Assumptions of (Zhang et al., 2023)

We clarify that Assumption 2 of Zhang et al. (2023), which is referred to as “linear interventional faithfulness”, *requires* nonlinear SCMs. Subsequently, both of their main results (Theorem 1 and Theorem 2) require this assumption. First, note that Zhang et al. (2023, p.6) implicitly explain that their results are for nonlinear SCMs: “*In general, we show in Appendix B that a large class of non-linear SCMs and soft interventions satisfy this assumption.*” Next, we show that this assumption is violated for linear additive noise models as follows. First, we quote their assumption:

Linear interventional faithfulness (Zhang et al., 2023, Assumption 2): Intervention I on node i satisfies linear interventional faithfulness if for every $j \in \text{ch}(i) \cup \{i\}$ such that $\text{pa}(j) \cap \text{de}(i) = \emptyset$, it holds that $\mathbb{P}(Z_j + C^\top Z_S) \neq \mathbb{P}^I(Z_j + C^\top Z_S)$ for all constant vectors $C \in \mathbb{R}^{|S|}$ where $S = [n] \setminus \text{de}(i)$.

Linear SCMs violate linear interventional faithfulness. Next, we show that linear SCMs violate the above linear interventional faithfulness assumption. Consider an intervention on node i , and let $j \in \text{ch}(i)$ such that $\text{pa}(i) \cap \text{de}(i) = \emptyset$. Let

$$Z_j = \mathbf{w}^\top Z_{\text{pa}(j)} + \epsilon_j, \quad (388)$$

where $\mathbf{w} \in \mathbb{R}^{|\text{pa}(j)|}$ denotes the weight vector. Note that we have $\text{pa}(j) \subseteq S = [p] \setminus \text{de}(i)$ since $\text{pa}(i) \cap \text{de}(i) = \emptyset$. Consider vector $C \in \mathbb{R}^{|S|}$ such that $C_{\text{pa}(j)} = -\mathbf{W}$ and $C_{S \setminus \text{pa}(j)} = \mathbf{0}$ where $C_{\text{pa}(j)}$ denotes the entries corresponding to nodes in $\text{pa}(j)$. Then, we have

$$Z_j + C^\top Z_S = \epsilon_j, \quad (389)$$

which remains invariant after an intervention on node i and yields $\mathbb{P}(Z_j + C^\top Z_S) = \mathbb{P}^I(Z_j + C^\top Z_S)$. Therefore, linear SCMs violate linear interventional faithfulness.

Appendix E. Empirical Evaluations: Details and Additional Results

E.1 Implementation Details of LSCALE-I Algorithm

Score function of the linear Gaussian model. For a Gaussian random vector $Y \sim \mathcal{N}(\mu, \Sigma)$, the score function of Y is given by

$$s_Y(y) = -\Sigma^{-1} \cdot (y - \mu). \quad (390)$$

Using the linear model specified in (84), in environment \mathcal{E}^0 ,

$$Z = (\mathbf{I}_n - \mathbf{A})^{-1} \cdot N_i. \quad (391)$$

Since N_i is a zero mean Gaussian random vector and $(\mathbf{I}_n - \mathbf{A})^{-1}$ is a full rank matrix, Z is a zero mean Gaussian random vector. Hence,

$$s(z) = -[\text{Cov}(Z)]^{-1} \cdot z. \quad (392)$$

Note that the covariance of Z has the following form

$$\text{Cov}(Z) = (\mathbf{I}_n - \mathbf{A})^{-1} \cdot \text{diag}([\sigma_1^2, \dots, \sigma_n^2]^\top) \cdot ((\mathbf{I}_n - \mathbf{A})^{-1})^\top. \quad (393)$$

Similarly, the score function of Z in \mathcal{E}^m is given by

$$s^m(z) = -[\text{Cov}(Z^m)]^{-1} \cdot z, \quad \forall m \in [n], \quad (394)$$

in which Z^m denotes the latent variables Z in environment \mathcal{E}^m . Finally, by setting $f = \mathbf{G}$, Corollary 1 specifies the score differences of X in terms of Z under different environment pairs as

$$s_X(x) - s_X^m(x) = (\mathbf{G}^\dagger)^\top \cdot [s(z) - s^m(z)]. \quad (395)$$

Score estimation for a linear Gaussian model. For all environments $\mathcal{E}^m \in \mathcal{E}$, given n_s i.i.d. samples of X , we first compute the sample covariance matrix denoted by $\hat{\Sigma}^m$. Then, we compute the sample precision matrix as

$$\hat{\Theta}^m \triangleq (\hat{\Sigma}^m)^\dagger, \quad (396)$$

which leads to the score function estimate given by

$$\hat{s}_X^m(x) \triangleq -\hat{\Theta}^m \cdot x. \quad (397)$$

Preprocessing: Dimensionality reduction. Since $X = \mathbf{G} \cdot Z$, we can compute $\text{im}(\mathbf{G})$ using n random samples of X almost surely. Specifically, $\text{im}(\mathbf{G})$ equals the column space of the sample covariance matrix of n samples of X . In LSCALE-I, as a preprocessing step, we compute this subspace and express samples of X and s_X in this basis. This procedure effectively reduces the dimension of X and s_X from d to n . Then, we perform steps of LSCALE-I using this n dimensional observed data. Next, we solve the optimization problems in (52) of Algorithm 2 and (56) of Algorithm 3 by investigating certain null spaces as follows.

Implementation of Algorithm 2 (Step L2). For each $t \in [n]$ and $k \in \mathcal{V}_t$, we consider the set of $a \in \text{im}(\mathbf{G})$ which results in $c = 0$ in (52)

$$\text{null}(\mathcal{V}_{t,k}) \triangleq \left\{ a \in \text{im}(\mathbf{G}) : \sum_{m \in \mathcal{V}_t \setminus \{k\}} \mathbb{E} \left[\left| a^\top \cdot [s_X(X) - s_X^m(X)] \right| \right] = 0 \right\}, \quad (398)$$

which we will shortly show that is a null space. In Algorithm 2, we check whether $\text{null}(\mathcal{V}_{t,k})$ intersects with the feasible set

$$\mathcal{F}_t = \text{im}(\mathbf{G}) \setminus \text{span}(\mathbf{A}_{\pi_{t+1}}^\top, \dots, \mathbf{A}_{\pi_n}^\top). \quad (399)$$

Using Proposition 2, we can write $\text{null}(\mathcal{V}_{t,k})$ as

$$\text{null}(\mathcal{V}_{t,k}) = \left\{ a \in \text{im}(\mathbf{G}) : \forall m \in \mathcal{V}_t \setminus \{k\} \quad a^\top \cdot \text{Cor}(s_X(X) - s_X^m(X)) \cdot a = 0 \right\} \quad (400)$$

$$= \left\{ a \in \text{im}(\mathbf{G}) : a^\top \cdot \left(\sum_{m \in \mathcal{V}_t \setminus \{k\}} \text{Cor}(s_X(X) - s_X^m(X)) \right) \cdot a = 0 \right\}, \quad (401)$$

where $\text{Cor}(Y) \triangleq \mathbb{E}(Y \cdot Y^\top)$ denotes the correlation matrix of a random vector Y . By noting that $\text{Cor}(s_X(X) - s_X^m(X))$ is a symmetric matrix for all $m \in [n]$, (401) shows that $\text{null}(\mathcal{V}_{t,k})$ is a null space. Specifically,

$$\text{null}(\mathcal{V}_{t,k}) = \text{im}(\mathbf{G}) \cap \text{null} \left(\sum_{m \in \mathcal{V}_t \setminus \{k\}} \text{Cor}(s_X(X) - s_X^m(X)) \right). \quad (402)$$

The optimization problem in (52) has solution $c = 0$ if and only if $\mathcal{F}_t \cap \text{null}(\mathcal{V}_{t,k})$ is not empty. Then, using (399) and (402), (52) has solution $c = 0$ if and only if

$$\text{null}(\mathcal{V}_{t,k}) = \text{im}(\mathbf{G}) \cap \text{null} \left(\sum_{m \in \mathcal{V}_t \setminus \{k\}} \text{Cor}(s_X(X) - s_X^m(X)) \right) \not\subseteq \text{span}(\mathbf{A}_{\pi_{t+1}}^\top, \dots, \mathbf{A}_{\pi_n}^\top). \quad (403)$$

Note that both the left and right-hand sides of this relation are subspaces of \mathbb{R}^d . Therefore, (403) holds if and only if

$$\dim \left(\text{null}(\mathcal{V}_{t,k}) \cap (\text{span}(\mathbf{A}_{\pi_{t+1}}^\top, \dots, \mathbf{A}_{\pi_n}^\top))^\perp \right) \neq 0. \quad (404)$$

Table 10: LSCALE-I for a linear causal model with **one hard** intervention per node ($n = 8$).

n	d	n_s	perfect scores			noisy scores		
			MCC	$\ell(Z, \hat{Z})$	$\text{SHD}(\mathcal{G}, \hat{\mathcal{G}})$	MCC	$\ell(Z, \hat{Z})$	$\text{SHD}(\mathcal{G}, \hat{\mathcal{G}})$
8	8	5000	1.00 ± 0.00	0.02 ± 0.00	1.36 ± 0.16	1.00 ± 0.00	0.04 ± 0.00	4.55 ± 0.23
8	25	5000	1.00 ± 0.00	0.02 ± 0.00	1.35 ± 0.13	1.00 ± 0.00	0.04 ± 0.00	4.72 ± 0.27
8	100	5000	1.00 ± 0.00	0.02 ± 0.00	1.35 ± 0.15	1.00 ± 0.00	0.04 ± 0.00	4.80 ± 0.23
8	8	10000	1.00 ± 0.00	0.01 ± 0.00	1.19 ± 0.14	1.00 ± 0.00	0.03 ± 0.00	2.45 ± 0.18
8	25	10000	1.00 ± 0.00	0.01 ± 0.00	1.11 ± 0.13	1.00 ± 0.00	0.03 ± 0.00	2.68 ± 0.19
8	100	10000	1.00 ± 0.00	0.01 ± 0.00	0.87 ± 0.11	1.00 ± 0.00	0.03 ± 0.00	2.53 ± 0.20
8	8	50000	1.00 ± 0.00	0.01 ± 0.00	0.23 ± 0.08	1.00 ± 0.00	0.01 ± 0.00	0.66 ± 0.10
8	25	50000	1.00 ± 0.00	0.01 ± 0.00	0.15 ± 0.06	1.00 ± 0.00	0.01 ± 0.00	0.58 ± 0.10
8	100	50000	1.00 ± 0.00	0.01 ± 0.00	0.18 ± 0.06	1.00 ± 0.00	0.01 ± 0.00	0.47 ± 0.09

Implementation of Algorithm 3 (Step L3). First, we define

$$\text{null}(\mathcal{M}_{t,j}) \triangleq \left\{ a \in \text{im}(\mathbf{G}) : \sum_{m \in \mathcal{M}_{t,j}} \mathbb{E} \left[\left| a^\top \cdot [s_X(X) - s_X^m(X)] \right| \right] = 0 \right\}. \quad (405)$$

Using the same arguments as for Algorithm 2, we have

$$\text{null}(\mathcal{M}_{t,j}) = \text{im}(\mathbf{G}) \cap \text{null} \left(\sum_{m \in \mathcal{M}_{t,j}} \text{Cor}(s_X(X) - s_X^m(X)) \right), \quad (406)$$

which is a subspace of \mathbb{R}^d . Then, the optimization problem (56) has solution $c = 0$ if and only if

$$\mathcal{F}_t \cap \text{null}(\mathcal{V}_{t,k}) \neq \emptyset \quad (407)$$

$$\iff \text{null}(\mathcal{V}_{t,k}) \not\subseteq \text{span}(\mathbf{A}_{\pi_{t+1}}^\top, \dots, \mathbf{A}_{\pi_n}^\top) \quad (408)$$

$$\iff \dim \left(\text{null}(\mathcal{M}_{t,j}) \cap (\text{span}(\mathbf{A}_{\pi_{t+1}}^\top, \dots, \mathbf{A}_{\pi_n}^\top))^\perp \right) \neq 0. \quad (409)$$

E.2 Additional Results for LSCALE-I

In this section, we extend the simulation settings in Section 7.1 and investigate the performance of LSCALE-I under a larger graph size and quadratic latent causal models.

Increasing latent dimension n . We repeat the experiments in Section 7.1 for $n = 8$ and report the results for hard and soft interventions in Tables 10 and 11. The main observations are similar to those from Tables 3 and 4. Specifically, LSCALE-I achieves close to perfect performance using perfect scores for both hard and soft intervention settings. For the case of noisy scores, given enough samples, LSCALE-I demonstrates strong performance at recovering both Z and \mathcal{G} . We note that the overall performance under $n = 5$ variables is slightly stronger than that of under $n = 8$ variables, which is expected due to the increasing problem complexity with n .

Quadratic latent causal models. Next, we replace the linear latent model in Section 7.1 with a quadratic latent model specified in (85). Section 7.1 already reports the results for soft interventions (Table 5. Here, we report the results of hard interventions on quadratic latent models. Table 12

Table 11: LSCALE-I for a linear causal model with **one soft** intervention per node ($n = 8$).

n	d	n_s	perfect scores			noisy scores		
			MCC	$\ell_{\text{an}}(Z, \hat{Z})$	$\text{SHD}(\mathcal{G}_{\text{tc}}, \hat{\mathcal{G}}_{\text{tc}})$	MCC	$\ell_{\text{an}}(Z, \hat{Z})$	$\text{SHD}(\mathcal{G}_{\text{tc}}, \hat{\mathcal{G}}_{\text{tc}})$
8	8	5000	0.87 ± 0.01	0.00 ± 0.00	0.00 ± 0.00	0.79 ± 0.01	3.44 ± 0.28	5.34 ± 0.37
8	25	5000	0.88 ± 0.01	0.00 ± 0.00	0.00 ± 0.00	0.80 ± 0.01	2.55 ± 0.22	4.50 ± 0.30
8	100	5000	0.88 ± 0.01	0.00 ± 0.00	0.00 ± 0.00	0.80 ± 0.01	3.01 ± 0.24	4.82 ± 0.32
8	8	10000	0.89 ± 0.01	0.00 ± 0.00	0.00 ± 0.00	0.79 ± 0.01	1.92 ± 0.22	3.17 ± 0.29
8	25	10000	0.88 ± 0.01	0.00 ± 0.00	0.00 ± 0.00	0.80 ± 0.01	2.15 ± 0.23	3.40 ± 0.29
8	100	10000	0.88 ± 0.01	0.00 ± 0.00	0.00 ± 0.00	0.80 ± 0.01	2.28 ± 0.25	3.63 ± 0.32
8	8	50000	0.89 ± 0.01	0.00 ± 0.00	0.00 ± 0.00	0.83 ± 0.01	0.30 ± 0.08	0.42 ± 0.11
8	25	50000	0.92 ± 0.01	0.00 ± 0.00	0.00 ± 0.00	0.83 ± 0.01	0.18 ± 0.07	0.25 ± 0.10
8	100	50000	0.88 ± 0.01	0.00 ± 0.00	0.00 ± 0.00	0.82 ± 0.01	0.23 ± 0.07	0.33 ± 0.10

Table 12: LSCALE-I for a quadratic causal model with **one hard** intervention per node ($n = 5$).

n	d	n_s	perfect scores			noisy scores		
			MCC	$\ell(Z, \hat{Z})$	$\text{SHD}(\mathcal{G}, \hat{\mathcal{G}})$	MCC	$\ell(Z, \hat{Z})$	$\text{SHD}(\mathcal{G}, \hat{\mathcal{G}})$
5	5	5000	1.00 ± 0.00	0.01 ± 0.00	0.10 ± 0.03	0.98 ± 0.00	0.15 ± 0.01	6.41 ± 0.25
5	25	5000	1.00 ± 0.00	0.01 ± 0.00	0.09 ± 0.03	0.99 ± 0.00	0.10 ± 0.01	6.05 ± 0.23
5	100	5000	1.00 ± 0.00	0.01 ± 0.00	0.22 ± 0.04	0.99 ± 0.00	0.10 ± 0.01	6.01 ± 0.24
5	5	10000	1.00 ± 0.00	0.01 ± 0.00	0.14 ± 0.04	0.99 ± 0.00	0.08 ± 0.00	5.81 ± 0.25
5	25	10000	1.00 ± 0.00	0.01 ± 0.00	0.15 ± 0.04	0.99 ± 0.00	0.07 ± 0.00	5.30 ± 0.24
5	100	10000	1.00 ± 0.00	0.01 ± 0.00	0.23 ± 0.04	0.99 ± 0.00	0.07 ± 0.00	5.48 ± 0.22
5	5	50000	1.00 ± 0.00	0.01 ± 0.00	0.17 ± 0.04	1.00 ± 0.00	0.06 ± 0.00	4.88 ± 0.21
5	25	50000	1.00 ± 0.00	0.01 ± 0.00	0.24 ± 0.05	1.00 ± 0.00	0.06 ± 0.00	4.45 ± 0.29
5	100	50000	1.00 ± 0.00	0.01 ± 0.00	0.16 ± 0.04	1.00 ± 0.00	0.06 ± 0.00	4.77 ± 0.22

shows that by using perfect scores, LSCALE-I performs nearly perfectly. This result agrees with our observations in the linear causal model setting in Tables 3 and 10. Furthermore, even under noisy scores, the latent variable recovery is close to being perfect, demonstrated by MCC of 0.99. On the other hand, the graph recovery suffers more from the noisy score estimates. This observation is further scrutinized in Section 7.4.

E.3 Implementation Details of GSCALE-I Algorithm

We perform experiments for the coupled interventions setting, and solve the following optimization problem in Step G2 of GSCALE-I,

$$\min_h \|\mathbf{D}_t(h) - \mathbf{I}_{n \times n}\|_{1,1} + \lambda \mathbb{E} \left[\|h^{-1}(h(X)) - X\|_2^2 \right]. \quad (410)$$

where $\lambda > 0$ is a regularization parameter to ensure injectivity. In the following, first, we show why this problem is equivalent to solving (70). Then, we describe the computation of the ground truth score differences for X and discuss other implementation details.

Solving (410) implies solving (70) We prove this equivalence by showing that the minimum value of the objective function in (410) is zero, and that this value can only be achieved by the minimizers

of the optimization problem in (70). For $\lambda > 0$, the value function in (410) is nonnegative. Therefore, if a value of 0 can be achieved, it is the minimum of this function. Note that the reconstruction term is zero if and only if h is a valid encoder, i.e., $h \in \mathcal{H}$. Next, we construct a class of candidate encoders that render the score difference loss term (the first term) in (410) zero, thus achieving the minimum. In (273), we have shown that the latent score change matrix, equivalently, $\mathbf{D}_t(g^{-1})$, has a specific support:

$$\mathbb{1}\{\mathbf{D}_t(g^{-1})\} = \mathbf{P}_{\mathcal{I}}^\top. \quad (411)$$

Using the score transformation rule (39), this implies that permuting the entries of Z , i.e., output of g^{-1} , by the intervention order \mathcal{I} yields

$$\mathbb{1}\{\mathbf{D}_t(\mathcal{I} \circ g^{-1})\} = \mathbf{P}_{\mathcal{I}} \cdot \mathbb{1}\{\mathbf{D}_t(g^{-1})\} = \mathbf{P}_{\mathcal{I}} \cdot \mathbf{P}_{\mathcal{I}}^\top = \mathbf{I}_{n \times n}. \quad (412)$$

Next, note that if we element-wise scale the output of $\mathcal{I} \circ g^{-1}$ by a diagonal matrix \mathbf{S} , the scores transform via

$$\mathbf{D}_t(\mathbf{S} \circ \mathcal{I} \circ g^{-1}) = \mathbf{S}^{-1} \cdot \mathbf{D}_t(\mathcal{I} \circ g^{-1}). \quad (413)$$

Therefore, by selecting $\mathbf{S} = \mathbf{D}_t(\mathcal{I} \circ g^{-1})$, and $h = \mathbf{S} \circ \mathcal{I} \circ g^{-1}$, we ensure that the matrix $\mathbf{D}_t(h)$ is exactly equal to $\mathbf{I}_{n \times n}$, which means it is a minimizer of (410). Note that unless $h \in \mathcal{H}$ and $\mathbf{D}_t = \mathbf{I}_{n \times n}$, the loss function in (410) will not be minimized, i.e., zero. It is impossible for a non-diagonal \mathbf{D}_t matrix to satisfy this. The set of $h \in \mathcal{H}$ that yield diagonal $\mathbf{D}_t(h)$ is exactly the solution set of (70). Therefore, we have proven that solutions to (410) are necessarily solutions to (70), which concludes the proof.

Score function of the quadratic model. Following (16), score functions s^m and \tilde{s}^m are decomposed as follows.

$$s^m(z) = \nabla_z \log q_\ell(z_\ell) + \sum_{i \neq \ell} \nabla_z \log p_i(z_i \mid z_{\text{pa}(i)}), \quad (414)$$

$$\text{and } \tilde{s}^m(z) = \nabla_z \log \tilde{q}_\ell(z_\ell) + \sum_{i \neq \ell} \nabla_z \log p_i(z_i \mid z_{\text{pa}(i)}). \quad (415)$$

For additive noise models, the terms in (414) and (415) have closed-form expressions. Specifically, using (112) and denoting the score functions of the noise terms $\{N_i : i \in [n]\}$ by $\{r_i : i \in [n]\}$, we have

$$[s(z)]_i = r_i(n_i) - \sum_{j \in \text{ch}(i)} \frac{\partial f_i(z_{\text{pa}(j)})}{\partial z_i} \cdot r_j(n_j). \quad (416)$$

Recall that we consider a quadratic latent model in Section 7.2 with

$$f_i(z_{\text{pa}(i)}) = \sqrt{z_{\text{pa}(i)}^\top \cdot \mathbf{A}_i \cdot z_{\text{pa}(i)}}, \quad \text{and } N_i \sim \mathcal{N}(0, \sigma_i^2), \quad (417)$$

which implies

$$\frac{\partial f_j(z_{\text{pa}(j)})}{\partial z_i} = \frac{[\mathbf{A}_j]_i \cdot z_{\text{pa}(j)}}{\sqrt{z_{\text{pa}(j)}^\top \cdot \mathbf{A}_j \cdot z_{\text{pa}(j)}}}, \quad \text{and } r_i(n_i) = -\frac{n_i}{\sigma_i^2}, \quad \forall i \in [n]. \quad (418)$$

Components of the score functions s^m and \tilde{s}^m can be computed similarly. Subsequently, using Corollary 1 of Lemma 2, we can compute the score differences of observed variables as follows.

$$s_X(x) - s_X^m(x) = \left[[J_g(z)]^\dagger \right]^\top \cdot [s(z) - s^m(z)], \quad (419)$$

$$s_X(x) - \tilde{s}_X^m(x) = \left[[J_g(z)]^\dagger \right]^\top \cdot [s(z) - \tilde{s}^m(z)], \quad (420)$$

$$s_X^m(x) - \tilde{s}_X^m(x) = \left[[J_g(z)]^\dagger \right]^\top \cdot [s^m(z) - \tilde{s}^m(z)]. \quad (421)$$

Implementation steps. We use n_s samples from the observational environment to compute empirical expectations. Since encoder h is parameterized by \mathbf{H} , we use gradient descent to learn this matrix. To do so, we minimize the loss described above in (410). We denote the final parameter estimate by \mathbf{H}^* and the encoder parameterized by \mathbf{H}^* by h^* .

In the simulation results reported in Section 7.2, we set $\lambda = 1$ and solve (410) using RMSprop optimizer with learning rate 10^{-3} for 3×10^4 steps for $n = 5$ and 4×10^4 steps for $n = 8$. We also use early stopping when the training converges before the maximum number of steps. Recall that the latent graph estimate $\hat{\mathcal{G}}$ is constructed using $\mathbb{1}\{\mathbf{D}(h^*)\}$. We use a threshold $\lambda_{\mathcal{G}}$ to obtain the graph from the upper triangular part of $\mathbf{D}(h^*)$ as follows.

$$\hat{\text{pa}}(i) = \{j : j < i \text{ and } [\mathbf{D}(h^*)]_{j,i} \geq \lambda_{\mathcal{G}}\}, \quad \forall i \in [n]. \quad (422)$$

We set $\lambda_{\mathcal{G}} = 0.1$ for $n = 5$ and $\lambda_{\mathcal{G}} = 0.2$ for $n = 8$.

E.4 Additional Results for GSCALE-I

Increasing latent dimension n . We repeat the experiments in Section 7.2 for $n = 8$ and report the results in Table 13. The main observations are similar to those from Table 6. Specifically, recovery of the latent variables is close to perfect, indicated by MCC of 0.95. We note that \mathcal{G} with $n = 8$ nodes and density 0.5 has an expected number of 14 edges. Hence, having an average SHD of approximately 1.5 indicates a strong graph recovery. When using noisy scores though, we observe a significant decrease in the performance, similar to that in Table 6. Still, we note that MCC did not change too much from $n = 5$ case (approximately 0.75) to $n = 8$ case (approximately 0.70).

Table 13: GSCALE-I for a quadratic causal model with **two coupled hard** interventions per node ($n = 8$) when using $n_s = 500$ samples. Noisy scores are obtained using SSM-VR with $n_{\text{score}} = 30000$ samples.

n	d	perfect scores			noisy scores		
		MCC	$\ell(Z, \hat{Z})$	$\text{SHD}(\mathcal{G}, \hat{\mathcal{G}})$	MCC	$\ell(Z, \hat{Z})$	$\text{SHD}(\mathcal{G}, \hat{\mathcal{G}})$
8	8	0.95 ± 0.01	0.18 ± 0.02	1.82 ± 0.29	0.64 ± 0.01	0.82 ± 0.10	11.9 ± 0.97
8	25	0.97 ± 0.01	0.22 ± 0.03	1.40 ± 0.28	0.67 ± 0.74	0.68 ± 0.06	10.2 ± 0.66
8	100	0.95 ± 0.01	0.24 ± 0.01	1.50 ± 0.27	0.71 ± 0.01	0.72 ± 0.04	12.9 ± 0.44